UNIVERSITY OF CALIFORNIA,
IRVINE

Host Interneurons Mediate Cortical Plasticity Reactivated by Embryonic Inhibitory Cell Transplantation

DISSERTATION

submitted in partial satisfaction of the requirements
for the degree of

DOCTOR OF PHILOSOPHY

in Biological Sciences

by

XiaoTing Zheng

Dissertation Committee:
Associate Professor Sunil P. Gandhi, Chair
Professor Ron Frostig
Professor Xiangmin Xu

2020

DEDICATION

To

my family and friends

for their love and encouragement

TABLE OF CONTENTS

LIST OF FIGURES

LIST OF TABLES

ACKNOWLEDGEMENTS

I am very grateful for my advisor Dr. Sunil Gandhi's guidance and support in the past 6 years. I have been truly inspired by his genuine enthusiasm for knowledge and truth. As a graduate student, sometimes I felt comfortable by just focusing on my own little area of science. But I thank Dr. Gandhi for always helping and challenging me to see the bigger picture. I loved the science and the techniques that I learned from the Gandhi lab, but the most valuable lesson I learned from Dr. Gandhi is how to face challenges without fear. There were plenty of opportunities to fail in grad school, but Dr. Gandhi has never failed to support me and cheer me on until I also learned to believe in my own ability to achieve.

I am also grateful for my thesis committee members Dr. Ron Frostig and Dr. Xu. Thank you for your valuable time and feedback. In addition to being on my committee, Dr. Xu has also been a valuable collaborator. Thank you, Dr. Xu, for always being supportive and generous with your time and lab resources.

I would also like to extend special thanks to all of the members of the Gandhi lab and collaborators in the Xu lab. Particularly, Kirstie has provided tremendous help not only to my project but also valuable friendship throughout the years. I also appreciate Dr. Carey Huh's support, generosity with her time, and enthusiasm for science. Also, thank you, Carey, for showing me how to find reasons to celebrate in life! My research project would not be possible without Jack! Thank you for maintaining the code and fulfilling our constant demands! A special thanks to Dr. Steven Grieco from Dr. Xu's lab. Thank you for always providing insightful and thoughtful comments on my projects.

I am especially grateful to my family and friends. Thank you for listening, encouraging, and walking alongside me during my PhD journey. Your support means the world to me!

Lastly, I would like to acknowledge the co-authors' contributions to the manuscript based on this dissertation. I thank Dario Figueroa-Velez for generating the initial Ca^{2+} imaging results, Kirstie Salinas for performing majority of the surgeries on adult transplant recipients, Taylor Nakayama for performing whole brain clearing and light-sheet imaging, Xiaoxiao Lin for performing rabies virus injections, and Dr. Gandhi and Dr. Xu for supervising the project. This work was funded by two multi-PI grants from the US National Eye Institute to Dr. Gandhi and Dr. Xu, NRSAs to XiaoTing Zheng and Dario Figueroa, and a NSF GRFP fellowship to Kirstie Salinas.

VITA

XiaoTing Zheng

2013	B.A. in Neurobiology and Behavior; Psychology
	Wesleyan University, Middletown, CT
2014	M.A. in Neurobiology and Behavior,
	Wesleyan University, Middletown, CT
2017	M.S. in Biological Sciences,
	University of California, Irvine
2020	Ph.D. in Biological Sciences,
	University of California, Irvine

FIELD OF STUDY

Neurobiology and Behavior

PUBLICATIONS

Zheng XT, Salinas, KJ, Figueroa Velez DX, Nakayama T, Lin X, Xu X, and Gandhi SP. (2020) Host Interneurons Mediate Cortical Plasticity Reactivated by Embryonic Inhibitory Cell Transplantation. **Submitted and in revision.**

Grieco SF, Qiao X, **Zheng XT**, Liu Y, Chen L, Zhang H, Gavornik J, Lai C, Gandhi SP, Holmes TC, Xu X. (2020). Subanesthetic ketamine reactivates adult cortical plasticity to restore vision from amblyopia. *Current Biology.* In press, accepted 7/01/2020.

Sun Y, Ikrar T, Davis MF, Gong N, **Zheng X**, Luo ZD, Lai C, Mei L, Holmes T, Gandhi SP, Xu X. (2016) Neuregulin-1(NRG1)/ErbB4 signaling in parvalbumin interneurons regulates visual cortical plasticity. *Neuron*, 92(1): 160–173.

Zheng XT and Gandhi SP. (2016) Healing Pains of the Past Using Neuronal Transplantation. *Neuron*, 92(6): 1157-1159.

Henderson K, Gupta J, Tagliatela S, Litvina E, **Zheng XT**, Van Zandt M, Woods N, Grund E, Lin D, Royston S, Yanagawa Y, Aaron G, and Naegele JR. (2014) Long-Term Seizure Suppression and Optogenetic Analysis of Synaptic Connectivity in Epileptic Mice with Hippocampal Grafts of GABAergic Interneurons. *Journal of Neuroscience*, 34(40):13492–13504.

ABSTRACT OF THE DISSERTATION

Host Interneurons Mediate Cortical Plasticity Reactivated by Embryonic Inhibitory Cell Transplantation

by

XiaoTing Zheng

Doctor of Philosophy in Biological Sciences

University of California, Irvine, 2020

Professor Sunil P. Gandhi, Chair

The adult brain lacks sensitivity to changes in the sensory environment found in the juvenile brain. The transplantation of embryonic interneurons has been shown to restore juvenile plasticity to the adult host visual cortex. We show that the transplanted PV interneurons mature, disperse and synaptically integrate into the host brain. However, it is unclear how the integration of transplanted cells re-sensitizes the host brain to visual deprivation. It is not known whether transplanted interneurons directly mediate the renewed cortical plasticity or whether these cells act indirectly by modifying the host interneuron circuitry. Here we find that the transplant-induced reorganization of host circuits is specifically mediated by a developmental signaling pathway Neuregulin (NRG1)/ErbB4 in host parvalbumin (PV) interneurons. It has been shown that during development, NRG1/ErbB4 regulates the excitatory inputs onto PV interneurons. NRG1/ErbB4-mediated loss of excitatory synapses on PV interneurons is necessary for deprivation-induced cortical plasticity in development. Here we show that in transplant recipients, brief visual deprivation reduces the visual activity of host PV interneurons but

has negligible effects on the responses of transplanted PV interneurons. Exogenous NRG1 both prevents the deprivation-induced reduction in the visual responses of host PV interneurons and blocks the transplant-induced reorganization of the host circuit. Furthermore, transplantation fails to induce plasticity in recipients that have ErbB4 receptors knocked out specifically in PV interneurons. Altogether, our results indicate that transplanted embryonic interneurons reactivate cortical plasticity by rejuvenating a developmentally restricted signaling pathway in host PV interneurons.

CHAPTER 1: INTRODUCTION

1.1 Overview

Experience-dependent cortical reorganization declines as animals mature. Limited potential for neural plasticity prevents the brain from recovering from injuries or deficits in adulthood. Numerous studies have demonstrated the ability of inhibitory neuron transplantation to induce a second critical period for juvenile-like plasticity and restore brain function in mature animals (Davis et al., 2015; Hunt et al., 2013; Southwell et al., 2010; Yang et al., 2016; Zhu et al., 2019). However, the mechanism behind these remarkable effects remains elusive. It may be that transplanted cells replace the function of aged or dysfunctional host interneurons. Alternately, it may be that transplanted cells modify host interneurons to create a new critical period for synaptic plasticity.

In juvenile development, neuregulin1 (NRG1)/ErbB4 signaling within parvalbumin (PV) interneurons is involved in initiating cortical plasticity. A brief monocular deprivation (MD) rapidly reduces NRG1/ErbB4-mediated excitatory inputs onto PV interneurons which, in turn, leads to a reduction in PV interneuron responses. Reduction in PV inhibition allows subsequent expression of ocular dominance (OD) plasticity of the excitatory neurons. Whether a similar mechanism is involved in the transplant induced cortical plasticity is not known. The main objectives for this thesis are to investigate (1) how the activity of transplant interneurons regulates cortical plasticity in the transplant recipients; and (2) whether NRG1/ErbB4 signaling is involved.

In the following sections, I will provide a detailed background on ocular dominance plasticity in the mouse visual cortex, potential mechanisms for both developmental and

transplant-induced cortical plasticity, and specific questions that will be answered by this thesis.

1.2 Ocular Dominance Plasticity As a Model For Experience-Dependent Cortical Reorganization

In early life development, neural circuits are molded by animals' experience. Critical period is a restricted window in development in which the neural circuits are highly sensitive to the sensory inputs or experience of the individuals. Well-known examples include the critical periods for language and motor skill acquisition in humans, song learning in songbirds, and imprinting in geese. In the laboratories, the critical period for the development of binocular vision is a widely used model for understanding the mechanisms underlying experience-dependent reorganization of the neural circuits. Although the initial discoveries were made in larger mammals such as rabbits and kittens (Hubel and Wiesel 1970; Wiesel and Hubel 1963), rodent models have become more extensively used because of their shorter life span and the availability of the transgenic lines.

Studies using intrinsic optical imaging and single-cell recording have provided insight into how experience shapes the inputs from the eyes to the primary visual cortex (Frenkel and Bear, 2004; Gordon and Stryker, 1996). In mice, the peak of the critical period for the development of binocular vision is around postnatal day 28 – 32, during which brief visual manipulation can have long-lasting effects on the eye-specific cortical responses. A higher proportion of neurons in the binocular zone of the mouse primary visual cortex (V1) responds to the inputs from the contralateral eye. With brief MD to the contralateral eye,

cortical responses driven by that eye decrease and shift the bias towards the ipsilateral open eye (Gordon and Stryker, 1996; Sato and Stryker 2008). This cortical reorganization is called ocular dominance (OD) plasticity.

The cortex's sensitivity to visual manipulation declines as the animals age. Even though plasticity can still be induced in older animals (>P100), longer term of MD is required (Lehmann and Löwel, 2008). The effects on the contralateral deprived and ipsilateral open eye responses are also different from that observed in juveniles. Using intrinsic signal optical imaging, Sato and Stryker (2008) shows that during juvenile critical period, four days of MD suppresses the responses through the deprived eye, while there is little effect on the response amplitude through the open eye. In adult animals, not only is a longer period of MD (>7 days as opposed to 3-4 days in juvenile) required to produce OD plasticity, but the plasticity is also mainly driven by the potentiation of the ipsilateral eye input. Even after seven days of MD, there is no observable effect on the response amplitude of the deprived eye.

1.3 Maturation of GABAergic Inhibition Gates the Onset of the Critical Period

The maturation of GABAergic interneurons gates the onset of the juvenile critical period for the development of binocular vision (Fagiolini and Hensch, 2000; Hensch, 2005; Hensch et al., 1998; Huang et al., 1999). One of the earliest supporting pieces of evidence came from the studies performed in mice with overexpression of brain-derived neurotrophic factor (BDNF; Huang et al., 1999). These mice showed accelerated maturation of inhibitory neurons and a precocious onset of critical period for OD plasticity. In contrast, disruption in

GABA synthesis and transmission as in GAD65 KO mice results in a delayed critical period. (Hensch et al., 1998). GABAergic interneurons are a heterogeneous population of neurons that exhibit distinct electrophysiological, neurochemical and morphological profiles (Tremblay et al. 2016). To identify the specific cell types, Fagiolini et al. (2004) genetically mutate GABAA receptor subunits to demonstrate that GABAA α1-subunit but not α2-subunit knock-in mutants exhibit a deficit in ocular dominance plasticity. The α1-subunit containing GABAA receptors are concentrated at the soma of the postsynaptic neurons, where they receive inhibitory inputs mainly from fast-spiking parvalbumin (PV)-positive basket cells (Fagiolini et al., 2004). On the other hand, GABAA receptors containing α2-subunit are concentrated on the initial axon segments of the principal cells, where fast-spiking chandelier cells make their synaptic contacts. This cell-type specific role of fast-spiking, basket PV cells in determining the onset of critical period has been confirmed by the subsequent studies (Heimel et al., 2011; Hensch, 2005; Levelt & Hübener, 2012).

While maturation of inhibition is necessary for initiating the critical period for cortical plasticity during early development, the continual increase of inhibition eventually closes the critical period. Several studies have tested this hypothesis by directly suppressing GABAergic transmission in post critical period animals, either pharmacologically (Harauzov et al., 2010) or chemogenetically with DREADDs (Kuhlman et al., 2013). They show that these manipulations can reactivate OD plasticity in the adult cortex. Interestingly, studies in which rodents are raised in an enriched environment (EE) show that EE also reactivates cortical plasticity in the adult cortex by reducing the intracortical inhibition (Sale et al., 2007; Sale et al., 2010). Altogether, these results indicate that the critical period is strictly regulated by the level of cortical inhibition. Onset of the juvenile critical period depends on the maturation of

GABAergic inhibition, but the critical period closes and plasticity declines as the inhibition continues to increase.

1.4 The Role of GABAergic Interneurons in Regulating OD Plasticity

It is not clear, however, how GABAergic interneurons contribute to the expression of experience-dependent OD plasticity once the critical period is initiated. Using *in vivo* single-cell recording and Ca^{2+} imaging, previous studies examine the direct effect of MD on the responses of excitatory and inhibitory interneurons in the binocular V1 (Gandhi et al., 2008; Kameyama et al., 2010; Kuhlman et al., 2013; Yazaki-Sugiyama et al., 2009). Due to the variation in experimental designs and transgenic mouse lines used, there are still major discrepancies in the findings. However, the consensus of these major studies is that (1) the responses of the interneurons, including PV interneurons, in the visual cortex can be directly modulated by visual deprivation; (2) ocular dominance shift of interneurons mirrors that of the excitatory neurons, though the time scales of the shift for these two cell types are still debatable. Like the excitatory neurons, interneuron responses start out contralaterally biased (Gandhi et al., 2008; Kameyama et al., 2010; Kuhlman et al., 2013). After 4-7 days of MD, the responses of interneurons seem to match that of the excitatory neurons. At this point, their responses are significantly more binocular than before MD due to a significant reduction in contralateral responses but also slight increase in ipsilateral responses (Gandhi et al., 2008; Kameyama et al., 2010; Yazaki-Sugiyama et al., 2009).

Out of these four studies, only Kuhlman et al. (2013) examines the initial changes in cell-type specific responses induced by MD. The study shows a rapid reduction in PV interneuron responses that happens within the first 24-hour of MD. This reduction in PV

interneuron responses is mainly caused by the reduction of layer 4 and layer 5 excitatory inputs onto these PV interneurons. A subsequent study by Sun et al. (2016) definitively confirms that the rapid and transient reduction in PV interneuron activity is necessary for the subsequent OD plasticity. These two studies were the first to demonstrate the role of PV interneuron activity in cortical reorganization.

Although earlier studies mainly focused on the role of PV interneurons in ocular dominance plasticity, recent studies have started to investigate the other subtypes of GABAergic interneurons, namely somatostatin (SOM)- and vasoactive intestinal polypeptide (VIP)-positive interneurons. The interest in SOM interneurons came from the observation that during development, even a brief MD (Oray et al., 2004) can induce structural reorganization of the dendritic spines of excitatory pyramidal neurons in the visual cortex. These spines are where excitatory neurons make synapses, and also where the dendrite-targeting SOM interneurons terminate their axons. This initial study on the structural reorganization sparked interest in the functional implication of dendritic plasticity.

To understand how the development of SOM interneurons influences the onset of the critical period for OD plasticity, Lazarus and Huang (2011) presents the first comparison of the maturation profiles of PV and SOM inhibition. They find that while the electrophysiological properties of PV interneurons mature and plateau along with the onset of the critical period, the excitability of SOM interneurons continues to increase until the peak of the critical period. These findings confirm the previous results that the onset of the critical period coincides with the maturation of PV interneurons (Hensch et al., 2005). Additionally, these results strongly suggest that SOM-provided dendritic inhibition may be

crucial for regulating plasticity after the onset of the critical period. How SOM interneuron activity is affected by visual experience and whether this change in activity contributes to OD plasticity is not known. Because of their postsynaptic contacts on the dendritic shafts of excitatory neurons, SOM interneurons may be in a good position to directly orchestrate the competition of excitatory synapses.

Over the past fifty years since the initial discovery of ocular dominance columns and ocular dominance plasticity by Hubel and Wiesel, we have learned much more about the cellular and molecular basis and regulators for the onset of critical period. There is no doubt that the maturation of GABAergic interneurons is important for the onset of the critical period for ocular dominance plasticity. Moreover, studies suggest that GABAergic interneurons do not merely set up the machinery for cortical plasticity, but they also directly participate in the expression of plasticity. However, we are only starting to understand the mechanisms underlying interneuron-mediated cortical plasticity.

1.5 Molecular Mechanisms Underlying Visual Cortical Plasticity: the Role of Neuregulin1/ErbB4 Signaling

Previous reviews have discussed the interneuron-mediated mechanisms underlying ocular dominance plasticity (Bavelier et al., 2010; Heimel et al., 2011; Levelt and Hübener, 2012; Sale et al., 2010). In this section, I will focus on Neuregulin1/ErbB4-mediated circuit disinhibitory mechanism. Even though circuit disinhibition has been extensively studied in the context of learning and memory (Letzkus et al., 2015), we have only recently begun to understand its role in cortical plasticity. Using *in vivo* electrophysiological recording,

Kuhlman et al. (2013) shows that the firing rate of PV interneurons reduces immediately after one day of MD. Excitatory neurons, in turn, increase in their firing rate. This rapid reduction in cortical inhibition is necessary for the subsequent competition of eye-specific inputs and OD shift. When the PV-mediated disinhibition of excitatory neurons is blocked pharmacologically, OD plasticity does not occur (Sun et al., 2016).

Performing circuit mapping analysis (Kuhlman et al., 2013; Sun et al., 2016), it is further confirmed that the reduction in PV interneuron responses is mainly due to the reduction in the layers 4 and 5 excitatory inputs onto these cells. What are the candidate molecules that regulate the excitatory inputs onto PV interneurons? Here, we will focus on the role of neuregulin1 (NRG1)/ErbB4 signaling pathway.

NRG1 binds to receptor tyrosine kinases called ErbB4 receptors and together they regulate many different stages of circuit assembly, from early embryonic brain development (Flames et al., 2004; Mei and Nave, 2004; Yau et al., 2003) to later activity-dependent circuit organization (Mei and Nave, 2014). Here we will focus on the role of NRG1/ErbB4 signaling in circuit plasticity in postnatal development. Inactive pro-NRG1 is a transmembrane protein. Upon activation, the N-terminal that contains the EGF-like signaling domain of type I and type II NRG1 is cleaved and become soluble proteins. They can then bind to the ErbB4 receptors on the same cells that release NRG1 (e.g. autocrine) or the receptors on other cells (e.g. paracrine; Falls, 2003). In contrast, type III NRG1 remains on the cell membrane and requires cell-to-cell contact to activate ErbB4 receptors. In this manuscript, we do not differentiate the types of NRG1. In the cortex, NRG1 is expressed in multiple cell types,

including both excitatory and inhibitory neurons as well as glial cells (Liu et al., 2011). The subcellular localization depends on the NRG1 isoforms (Vullhorst et al., 2017).

ErbB4 receptors are expressed predominantly but not exclusively by PV interneurons in the visual cortex (Batista-Brito et al., 2017; Mei and Nave, 2014; Sun et al., 2016; Vullhorst et al., 2009). Although majority of studies find that ErbB4 receptors are localized to the excitatory synapses on the cell bodies and dendrites of PV interneurons (Buonanno and Fischbach, 2001; Garcia et al., 2000; Huang et al., 2000), others suggest that they may also be present at the axon terminals of PV interneurons (Fazzari et al., 2010; Woo et al., 2007).

NRG1 and ErbB4 expressions in the cortex are developmentally regulated (Grieco et al., 2020; Liu et al., 2011). Both NRG1 and ErbB4 expressions have been detected in interneurons as early as embryonic development during which they are involved in survival, maturation and migration of interneuron progenitors (Liu et al., 2011; Mei and Nave, 2014). In the postnatal visual cortex, ErbB4 expression in PV interneurons stays relatively stable (Grieco et al., 2020; Sun et al., 2016). In contrast, NRG1 expression level in PV interneurons peaks during the critical period around P26-P28 and gradually decreases and stabilizes in adulthood (Grieco et al., 2020; Sun et al., 2016). On the other hand, NRG1 and ErbB4 expressions in excitatory neurons are stable in postnatal visual cortex.

The level of NRG1 in PV interneurons is also activity dependent. Both short-term and long-term MD during development reduce the level of NRG1 in PV interneurons, but have very little effect on NRG1 level in excitatory cells (Grieco et al., 2020; Sun et al., 2016). The overall expression of ErbB4 does not change after MD (Grieco et al., 2020; Sun et al., 2016),

but the phosphorylated ErbB4 expression is reduced (Sun et al., 2016), in agreement with the reduced NRG1 binding.

In the visual cortex, NRG1/ErbB4 signaling regulates the excitatory synapses onto PV interneurons (Gu et al., 2016; Sun et al., 2016). During the juvenile critical period, one day MD rapidly decreases the level of PV interneuron activity in layer 2/3 binocular visual cortex (Kuhlman et al., 2013; Sun et al., 2016). Using laser-scanning photostimulation (LSPS) via glutamate uncaging, Sun et al. (2016) confirms that the reduction in PV interneuron responses is mainly due to the loss of excitatory inputs from L4 and L5. At the molecular level, it is mediated by the reduction in the level of NRG1 within PV interneurons (Sun et al., 2016). The reduction of PV interneuron responses can be rescued with exogenous NRG1. The downstream signaling of NRG1 depends on binding of ErbB4 receptor on PV interneurons, because in the presence of ErbB4 inhibitor, exogenous NRG1 fails to restore excitatory inputs onto PV interneurons after MD. Furthermore, exogenous NRG1 shows no effect on mini-excitatory postsynaptic current amplitude in PV cells in PV-cre;ErbB4 knock-out mutant mice. It has been proposed that soluble NRG1 can produce autocrine as well as paracrine signals (Falls, 2003). Since the NRG1 level within PV interneuron is activity dependent, it is possible that in the visual cortex, NRG1 acts through an autocrine loop. One can imagine that PV interneurons produce NRG1 and transport to the membrane, the transmembrane pro-NRG1 (inactive form) is then cleaved when the PV interneurons are stimulated by the presynaptic excitatory inputs, and the soluble extracellular domain of NRG1 (active form) binds to the ErbB4 receptors on PV interneurons to further potentiate excitatory inputs. However, this hypothesis has to be further tested.

The canonical forward signaling pathway of NRG1/ErbB4 is the subject of many reviews (Mei and Xiong, 2008; Mei and Nave, 2014). NRG1 binding of ErbB4 receptors induces dimerization of the receptors and activates the ErbB4 kinase domain, resulting in phosphorylation of the intracellular domains. The phosphorylation activates the downstream kinase pathway, including protein kinase C (PKC) pathway, which subsequently results in protein synthesis (Mei and Xiong, 2008; Sun et al., 2016). Specifically blocking the activity of PKC in PV interneurons, Sun et al. (2016) shows that exogenous NRG1 fails to prevent the reduction in PV interneuron activity after MD. PKC-dependent protein synthesis may be linked to AMPA receptor production and trafficking (Mei and Xiong, 2008; Sun et al. 2016) because blocking the AMPA receptor insertion prevents NRG1-mediated increase in PV interneuron activity. Taken together, these results suggest that protein synthesis is needed for NRG1/ErbB4-mediated potentiation of excitatory synapses in PV interneurons.

1.6 Interneuron Transplantation Reactivates a New Critical Period for Ocular Dominance Plasticity in Adult Mouse Visual Cortex

Mature mammalian brains have a limited potential for regeneration and repair. Dentate gyrus and olfactory bulb are the only two regions in the adult brain where new neurons are generated throughout animal's life. It is well accepted that there are no newborn cells in the adult cortex. This limitation of the adult brain makes it difficult for the brain to recover itself from injuries or neurological disorders which is characterized a substantial loss of neurons. The initial attempt for cell-based therapy came from epilepsy research. In temporal lobe epilepsy, there is a loss of GABAergic interneurons in the hilus of

hippocampus. The excitatory cells become more excitable with less local inhibition. Therefore, it seemed reasonable to transplant GABAergic inhibitory interneurons to the seizure focal site to restore inhibition. Even though the normal adult brains have limited capacity for regenerating new cells, these transplanted embryonic interneurons readily integrated into the host tissue and suppressed seizures. Since the initial studies in epilepsy, labs across the world have adopted interneuron transplantation to treat a number of neurological disorders, including traumatic brain injuries, autism spectrum disorders and schizophrenia. Interneuron transplantation is not only used to treat diseased brains, but our lab and others have demonstrated that these embryonic interneurons can reactivate a new critical period for plasticity in the adult brain. Even though these show that maturation of the transplanted interneurons regulates the timing of the second critical period, the mechanisms underlying the reactivated cortical plasticity are not well understood.

Considering that reduction of intracortical inhibition can reactivate cortical plasticity, at first it may seem counterintuitive that interneuron transplantation can induce OD plasticity in the adult brain. These findings imply that cortical plasticity may be reactivated by changes in the host inhibitory circuitry, not simply the reduction in the level of cortical inhibition.

1.6.1 Origins of subtypes of GABAergic interneurons

Majority of the initial studies in the field have focused on the maturation and differentiation of transplanted interneurons. Taken from region in the embryonic forebrain, ganglionic eminence, these embryonic interneurons have demonstrated great potential for migration in the host brain. They can spread to up to 2 mm from the site of injection (Davis

et al., 2015; Zhu et al., 2019). This probably has to do the fact these cells have to migrate all the way to distant brains like cortex and hippocampus in the normal developing brain. What makes these cells so useful is their ability to differentiate into subtypes of GABAergic interneurons. There are three regions in the ganglionic eminence, and each region gives rise to different subtypes of interneurons (Wonders and Anderson, 2006). Somatostatin and PV interneurons are generated in the medial ganglionic eminence (MGE), while caudal ganglionic eminence (CGE) gives rise to majority of interneurons that express vasoactive intestinal peptide (VIP). On the other hand, lateral ganglionic eminence (LGE) gives rise to majority of interneurons that migrate to the olfactory bulb. Much of the early research in the interneuron transplantation field was devoted to the characterization of the transplanted interneurons, and they found that transplanted interneurons retain the ability to differentiate into different GABAergic interneuron subtypes, although the host environment also plays a role in determining the final proportion of each cell types. In order for the transplanted cells to exert therapeutic effects on the host brains, they must be integrated into the host circuit. So far, *in vitro* electrophysiology recordings have provided evidence that these cells exhibited electrophysiological properties that mostly resemble the normal interneurons (Larimer et al. 2017). Pair-recording experiments suggest that these cells are receiving proper inputs and forming connections with the host cells (Larimer et al., 2017; Southwell et al., 2010).

1.6.2 Therapeutic potentials of interneuron transplantation

It is still not clear, however, how these transplanted interneurons modify the host circuit and ameliorate the effects caused by normal aging or injuries. In the case of epilepsy and other neurological disorders that are characterized by loss of interneurons, where there

is a loss of specific subtypes of cells, it makes sense to think that transplanted cells simply replace the lost interneurons and suppress seizures by forming a healthy local inhibitory circuit that controls the firing of the host excitatory cells. This hypothesis is further supported by the studies on critical period. Numerous studies have demonstrated that critical period started when the transplanted interneuron reach their developmental critical period for ocular dominance plasticity (Davis et al., 2015; Priya et al., 2019; Southwell et al., 2010). Therefore, it seems that transplanted cells form a young circuit that recapitulate the developmental process. They create a new critical period plasticity when they reach certain maturation state in the adult host brain.

There is loss of GABAergic interneurons in the hilus of hippocampus in patients with temporal lobe epilepsy. Studies using GABAergic interneurons derived from embryonic stem cells or induced pluripotent stem cells as well as from the medial ganglionic eminence of mouse embryos all demonstrate that GABAergic interneuron transplantation suppresses seizures in mouse models of temporal lobe epilepsy (Hunt et al., 2013; Henderson et al., 2014; Upadhya et al., 2019). Hunt et al. 2013 also demonstrates that interneuron transplantation rescues cognitive deficits in epileptic mice. A recent study directly demonstrates the causal link of synaptic integration and seizure suppression using chemogenetic manipulations (Upadhya et al., 2019). Seizure suppression is reduced when the transplanted cells are silenced using DREADDs, providing evidence that the activity of transplanted interneurons is necessary for seizure suppression.

Traumatic brain injury is another disorder marked by an irreversible loss of inhibitory interneurons in the hippocampus. While interneuron transplantation does not

modify the lesion in the host hippocampus, it improves animals' cognitive abilities (Zhu et al., 2019). The study demonstrates that the transplanted interneurons mature, differentiate into PV and SST interneurons and synaptically integrate into the host circuit and form inhibitory synapses onto the host cells in the hippocampus. Zhu et al. (2019) uses DREADD to manipulate the activity of transplanted interneurons and shows that silencing the activity of transplanted interneurons prevents the improvement in cognitive ability in transplant recipients, further supporting the idea that the activity of transplanted interneurons is necessary for disease amelioration.

At least one study seems to challenge the idea that transplanted interneurons simply replace the function of the lost cells in the host brain. In an Alzheimer's mouse model, in which the expression of Nav1.1 in the host cells is abolished, transplantation of wildtype MGE cells fails to rescue the cognitive and behavioral deficits (Martinez-Losa et al., 2018). Instead, overexpression of Nav1.1 in transplanted MGE cells is needed to rescue cognitive deficits in the mutant mice and restores gamma oscillation during behavioral tasks. Altogether, these studies suggest that the disease-modifying effect of MGE transplant partially depends on the state of the host circuit. When the host circuit is perturbed beyond a certain point, wildtype MGE cells are not sufficient to compensate for the deficit.

1.6.3 Potential mechanisms for visual cortical plasticity

In addition to recovering brain functions in disease models, interneuron transplantation can reactivate a second critical period in healthy adult cortex (Davis et al., 2015). The effect is specific to interneurons from MGE because cells from CGE and LGE do not reactivate plasticity (Davis et al., 2015; Larimer et al. 2016). Moreover, transplanted

interneurons reactivate the second critical period at the time when these cells would have reached their developmental critical period, specifically at 33 – 35 days after transplantation (DAT; Davis et al., 2015; Priya et al., 2019; Southwell et al., 2010). As during the juvenile critical period, beyond this reactivated critical period the plasticity in the host brain becomes limited again. In the amygdala, transplanted reactivated critical period for fear erasure occurs two weeks after transplantation (Yang et al., 2016). These findings suggest that the timing of critical period may be different for different neural circuits. Moreover, the timing of the second critical period may depend on the maturation state of the transplanted interneurons.

Two recent studies examine the direct role of transplant interneurons in ocular dominance plasticity during the reactivated critical period. Vesicular GABA transporter (VGAT) in normal GABAergic interneurons helps to package the neurotransmitters into vesicles. Disrupting the function of VGAT directly affects GABA transmission. Harvesting and transplanting MGE cells from VGAT KO mutant embryos, Priya et al. (2019) shows that even though these cells mature and disperse, they fail to induce ocular dominance plasticity. This result suggests the importance of transplant interneuron activity in inducing OD plasticity. One caveat with the study is that the transplanted interneurons from VGAT mutant embryos seem developmentally immature and develop abnormally. It is possible that the transplanted cells fail to integrate. A subsequent study uses optogenetics to manipulate the activity of transplanted interneurons and finds that the activity of transplanted interneurons is not needed for the expression of OD plasticity once it has been triggered (Hoseini et al., 2019). Altogether, these results suggest the activity of transplanted interneurons is required

for the onset of the critical period, but it may not be necessary for the expression of OD plasticity.

Recent studies challenge the idea that the activity of transplanted interneurons alone dictates the timing of the reactivated critical period. As mentioned above, in host animals with mutated Nav1.1, wildtype MGE cells are not sufficient to correct the behavioral deficits in those animals (Martinez-Losa et al., 2018). This result suggests that the host brain may partially influence the disease-modifying effect of the transplanted interneurons. Yang et al. (2016) demonstrates that transplantation of MGE cells in the amygdala facilitates fear erasure in adult mice. However, the reactivated critical period in the transplant recipient occurs earlier (14DAT equivalent to P7) than observed in normal developing animals (P16-23). Furthermore, they show that during the reactivated critical period for fear erasure, there is a significant reduction in the expression of PNN in the host PV interneurons. In fact, the level of PNN in the host PV interneurons of the P49 adult recipients is equivalent to the level in a P21 mouse. Yang et al. (2016) provides the first direct evidence that interneuron transplantation exerts its effect by rejuvenating the host PV interneurons.

1.7 Hypothesis and Significance

Previous studies from our lab and others show that interneuron transplantation can reactivate a new critical period in the postnatal cortex (Davis et al., 2015; Larimer et al., 2016; Priya et al., 2019; Southwell et al., 2010; Tang et al., 2014). The timing of the second critical period parallels the maturation of the transplanted interneurons, reminiscent of the juvenile critical period. Hoseini et al. (2019) manipulates the activity of transplanted

interneurons after four days of MD to show that transplanted interneuron activity is not involved in the expression of OD plasticity. In future studies, the manipulation can be done in the first day of MD to determine if transplanted PV interneuron activity plays a role in the initiation of transplant-induced cortical plasticity. Furthermore, Yang et al. (2016) is the first study that examines the role of a specific subtype of GABAergic interneurons in transplant-reactivated plasticity in the amygdala. In contrast, the visual cortex and hippocampus transplantation studies have not yet examined cell-type specific mechanisms in transplant-reactivated plasticity.

In development, NRG1/ErbB4 signaling in PV interneurons mediates the initial disinhibition of the excitatory circuit which subsequently results in OD plasticity. We hypothesize that NRG1/ErbB4 within transplanted PV interneurons may act similarly in transplant recipients during the reactivated critical period.

Using *in vivo* time-lapse Ca^{2+} imaging, intrinsic signal optical imaging and pharmacological manipulation, this thesis aims to determine whether the same developmental processes underlying developmental OD plasticity are involved in transplant-induced plasticity, namely: (a) whether MD reduces transplanted PV interneuron activity; (b) whether the reduction in transplanted PV interneuron activity is mediated by NRG1/ErbB4 signaling; and (c) whether the reduction in transplanted PV interneuron activity is necessary for transplant-induced plasticity.

This thesis provides the first cellular-resolution, *in vivo* Ca^{2+} imaging results on a cell-type specific mechanism underlying reactivated cortical plasticity in transplant recipients. Our findings here show that interneuron transplantation reactivates a molecular signaling

pathway, which is normally restricted to juvenile development, within the adult host PV interneurons. The remaining question is how interneuron transplantation rejuvenates the host PV interneurons. Perhaps our study will inspire others to pursue the molecules that mediate the rejuvenation of host inhibitory neurons.

1.8 Outline

Chapter 2 provides detailed methods used in this thesis. Chapter 3 characterizes the maturation of transplanted PV interneurons and provides evidence that these cells integrate into the host circuit. Chapter 4 investigates the effect of MD on transplanted as well as host PV interneurons, and tests whether NRG1/ErbB4 plays a role in regulating the responses of PV interneurons and subsequent OD plasticity. Chapter 5 presents a general discussion of the findings.

CHAPTER 2: METHODS

2.1 Resource Table

REAGENT or RESOURCE	SOURCE	IDENTIFIER
Antibodies		
Mouse anti-Parvalbumin	Sigma	P3088
Chicken anti-GFP	Aves	GFP-1010
Rabbit anti-GABA	Sigma	2052
Goat anti-Mouse Alexa 647	Invitrogen	A21240
Goat anti-Chicken Alexa 488	Invitrogen	A11039
Goat anti-Rabbit Alexa 647	Invitrogen	A21245
Bacterial and Virus Strains		
AAV1-GCaMP6s virus		
synapsin-driven AAV1-GCaMP6s virus		
EnvA-SADΔG-DsRed rabies	Sun et al., 2019	N/A
pAAV-Ef1a-DIO-H2B-GFP-2A-oG-WPRE-hGH	Addgene	74289
Chemicals, Peptides, and Recombinant Proteins		
Leibovitz's L-15 medium	Gibco	21083027
DNAse	Roche	0471672800
Rimadyl	Zoetis	141-199
Chlorprothixene	Sigma	C1671
Recombinant Human NRG1-beta 1	Roche	396-HB
Experimental Models: Organisms/Strains		
B6;129P2-*Pvalb*$^{tm1(cre)Arbr}$/J	The Jackson Laboratory	008069
B6;129S6-Gt(ROSA)*26Sor*$^{tm14(CAG-tdTomato)Hze}$/J	The Jackson Laboratory	007914
STOCK Slc32a1$^{tm2(cre)Lowl}$/J	The Jackson Laboratory	028862
C57BL/6J	The Jackson Laboratory	000664
LSL-R26$^{TVA-lacZ}$	Seidler et al., 2008	N/A
PV-cre;ErbB4$^{flx/flx}$	Long et al., 2003	N/A
CD1	Charles River Laboratories	482
Software and Algorithms		
Custom-written Python scripts		
Matlab Psychophysics Toolbox extensions		
Prism 8.00	GraphPad	
ImageJ		
LAS X image processing software	Leica	https://www.leica-microsystems.com

2.2 Experimental Models and Subjects

All protocols and procedures followed the guidelines of the Animal Care and Use Committee at the University of California, Irvine. The following mouse lines were used in this study: B6;129P2-*Pvalb*$^{tm1(cre)Arbr/}$J (PV-cre), B6;129S6-Gt(ROSA)*26Sor*$^{tm14(CAG-tdTomato)Hze/}$J (Ai14, JAX 007914), STOCK Slc32a1$^{tm2(cre)Lowl}$/J (Vgat-ires-cre, JAX 028862), C57BL/6J (JAX 000664), and LSL-R26$^{TVA\text{-}lacZ}$ (Rosa-TVA) (Seidler et al., 2008). To visualize either parvalbumin (PV) interneurons or all GABAergic interneurons, PV-cre or VGAT-cre homozygous mice, respectively, were crossed with cre-dependent red fluorescent Ai14 reporter mice. The embryonic donor tissue used for transplantation was generated either by crossing VGAT-tdTomato or PV-tdTomato homozygous males with C57BL/6J or CD1 wildtype females, or by crossing PV-cre or VGAT-cre homozygous mice with Ai14 homozygous mice. To remove ErbB4 specifically from PV interneurons, the mice homozygous for loxP-flanked (flx) ErbB4 alleles (Long et al., 2003) were first crossed with PV-cre homozygous mice. The resulting PV-Cre$^{+/-}$, ErbB4$^{flx/+}$ mice were crossed with each other to generate PV-cre$^{+/+}$; ErbB4$^{flx/flx}$ mice, which were used as adult transplant recipients in some of the experiments. To selectively express TVA receptors (avian retroviral receptor, tumor virus A in PV cells, Rosa-TVA homozygous mice were crossed with PV-cre homozygous animals. For retrograde tracing of transplanted PV cells, we transplanted PV-cre;TVA embryonic tissue into wildtype adult mice. This approach restricts the initial infection of rabies virus to transplanted TVA-expressing PV cells. Refer to Table 1 for more details on the experimental groups for each experiment.

2.3 Interneuron Transplantation in Adult Visual Cortex

The procedure was previously described (Davis et al., 2015). Embryonic days (E) 13.5-14 embryos from timed breeding were used for transplantation. Medial ganglionic eminence (MGE) of embryonic forebrain was dissected and suspended in chilled L15 solution (Gibco, 21083027) with 2% (v/v) of DNase I (Roche, 0471672800). All transplantation and subsequent virus injections were performed on the right hemisphere of the animals. For precise targeting, binocular visual cortex (bV1) of adult transplant recipients was mapped using intrinsic optical imaging (described below) at least one week prior to transplantation. The injection sites around bV1 were thinned using a dental drill (Midwest 78044) and FG1/4 carbide burr to allow the injection micropipette to penetrate. The tissue was loaded into a beveled glass micropipette (75 μm; Wiretrol 5 μl, Drummond Scientific Company) and injected using a custom-made hydraulic manipulator (Narishige, MO-10). The cells were injected at ~650-700 μm below the surface of the brain. Each transplant recipient received 20-30 nl per injection for a total of 6-8 injections, all in the same hemisphere. At the end of the procedure, the scalp was sutured using Perma-Hand Silk (Ethicon, J212H) and the animals were returned to the home cage on a heating pad. Refer to Table 1 for the genotype and the age of adult transplant recipients, and the type of donor tissue each received.

Table 2.2: Table of experimental groups.

Figure No.	Donor Tissue	Embryonic region	Host/Recipient	Age of recipient (Day)*	Imaging Method	Cell type imaged	Days after transplantation (DAT)
4.2	No transplant	N/A	PV-cre	26-30	Ca^{2+} imaging	critical period PV cells	N/A
4.4, 4.5, 4.6, 4.7, 4.8	PV-cre;tdTomato	MGE	PV-cre	114-237	Ca^{2+} imaging	Host and transplanted PV cells	35
4.5, 4.6, 4.7 4.8	VGAT-cre;tdTomato	CGE	PV-cre	113-180	Ca^{2+} imaging	Host PV cells	35
4.5, 4.6, 4.7, 4.8	No transplant	N/A	PV-cre	115-204	Ca^{2+} imaging	Age-matched adult PV cells	N/A
4.9A – 4.9E	PV-cre;tdTomato	MGE	C57BL/6 wildtype	140-170	Ca^{2+} imaging	Host excitatory and transplanted PV cells	35
4.9F – 4.9H	No transplant	N/A	C57BL/6	114-164	Ca^{2+} imaging	Age-matched adult excitatory cells	N/A
4.10	No transplant	N/A	C57BL/6 wildtype	26-30	Ca^{2+} imaging	critical period excitatory cells	N/A
4.11	VGAT-cre;tdTomato	MGE	C57BL/6 wildtype	129-178	Intrinsic optical imaging	N/A	35
4.11	VGAT-cre;tdTomato	MGE	PV-cre;ErbB4$^{flx/flx}$	104-132	Intrinsic optical imaging	N/A	35
3.3	PV-cre;TVA	MGE	C57BL/6 wildtype	85-150	N/A	N/A	45-50†

* Age of recipients on the day of transplantation for PV-cre;TVA transplantation experiments. Age on the day of imaging for all the other groups.

† Day of perfusion

2.4 *In vivo* Two-Photon Calcium Imaging

2.4.1 Virus injection for calcium imaging

To label neurons in layer 2/3 of binocular visual cortex, adult transplant recipients or age-matched adult controls received either synapsin-driven AAV1-GCaMP6s virus (Penn Vector Core, CS1118; titer: 7 X 10^{11}- 2 X 10^{12} genome copies (GC)/ml) or cre-dependent

synapsin-driven AAV1-GCaMP6s virus (Penn Vector Core, CS1113; titer: 1 X 10^{12} GC/ml). Refer to Table 1 for details on the experimental groups. All virus injections were done in only the right hemisphere. Animals were anaesthetized with 2% isoflurane (Patterson Veterinary, 07-893-1389) and received an injection of the analgesic Carprofen (0.8mg/ml; Rimadyl) before surgery. For adult transplant recipients, virus injection was performed at bV1 between 10-12 days after transplantation (DAT) in the same hemisphere where the transplanted cells were injected. For age-matched adult mice without transplantation, the injection was made at the center of bV1 based on the intrinsic signal map, which was performed at least a week prior. The virus was injected at ~450-600 μm below the surface of the brain (Volume: 2 sites X 200-240 nl/site, rate:10-12 nl/min) using a beveled glass pipette and a custom-made hydraulic injector.

For labeling cells in critical period mice, the injections were done between postnatal (P) days 2-3. The injections were made at 3-4 mm lateral and 1mm anterior relative to lambda, roughly where bV1 would be (rate: 30-40 nl/min). The exact location of bV1 in critical period mice was identified using intrinsic optical imaging at P16-18. Mice with off-target virus injection were excluded from the subsequent experiments.

2.4.2 Surgical preparation

Three to five days before *in vivo* two-photon calcium (Ca^{2+}) imaging, a custom-printed headplate was installed and fixed to the right skull using Vetbond (3M, Vetbond, 1469SB) and dental acrylic (Lang Ortho-Jet Powder and Ortho-Jet Powder Liquid). A cranial window 4-5 mm in diameter was made over primary visual cortex and covered with a glass coverslip of the same size using Vetbond and dental acrylic. Mice received subcutaneous injections of Carprofen to reduce pain and inflammation for up to three days after the surgery.

2.4.3 Imaging procedures

Two-photon Ca^{2+} imaging procedure was described previously (Salinas et al., 2017). A resonant two-photon microscope (Neurolabware, Los Angeles, CA) with a 16X (Nikon NA = 0.8) objective was used to record Ca^{2+} transients of neurons in layer 2/3 of bV1 (160-350 μm below pia). The laser was set to an excitation wavelength of 910 or 920 nm simultaneously excite GCaMP6s and tdTomato. Emissions were filtered using a 510/84 nm and 607/70 nm BrightLine bandpass filter (Semrock, Rochester, NY). A field of view of approximately 600 X 250 μm was acquired at 12 Hz (660 lines) using Scanbox acquisition software (Scanbox, Los Angeles, CA). For some recordings, an electrically tunable lens (optotune) was used simultaneously record of multiple depths (at least 25 μm apart for up to 3 depths).

For critical period experiments, some animals were anesthetized during the recording with 0.7% isoflurane and chlorprothixene (Sigma, C1671). The first imaging session started at P26-28. Adult transplant MD experiments were performed in head-fixed, awake mice. The first imaging session started at 33-35DAT, when the transplanted cells reached their normal developmental critical period. Each imaging session consisted of measuring each eye's responses to drifting gratings in an alternating pattern for a total of 2-3 sessions for each eye. Because of the sparsity of viral expression, we were able to capture the same PV interneurons in transplant recipients and age-matched adults before and after MD. For excitatory neurons, we located the same fields based on the vasculature.

2.4.4 One-day monocular deprivation

To examine the effect of 1-day monocular deprivation (MD), the eye contralateral to the imaging hemisphere was sutured using Perma-Hand Silk (Ethicon, K809H) immediately

after the first imaging session. To test the effect of neuregulin-1 (NRG1) on the response properties of PV interneurons, some mice received subcutaneous injections of soluble neuregulin-1 (R&D Systems, 396-HB; 0.5 μg per animal every 8 hour) during MD. The suture was carefully removed after 20-30 hours. To allow the eye to fully open, animals were returned to their home cage for 30 minutes after removing the suture. After MD, mice with cataracts, cloudy eyes, and drooping eyelids were excluded from the subsequent experiments and data analysis.

2.4.5 Visual stimulus conditions

Visual stimuli were generated by custom-written Python code using the PsychoPy 1.8 library as described (Salinas et al., 2017). Spherically corrected, full field drifting sinusoidal gratings were presented in eight orientations and five spatial frequencies (0.03-0.48, logarithmically spaced) at 2 Hz temporal frequency. We also showed a blank condition and a full-field flickering condition. The 42 total stimulus conditions were presented in a different random order for each of the 8 repetitions. Each stimulus was presented for 2 seconds and followed by 3 seconds of gray screen for a total of 28 minutes per imaging session. The stimuli were presented to one eye at a time in an alternating pattern for 2-3 sessions per eye. The stimuli were displayed on an Acer V193 monitor (53 X 33 cm, 60 Hz refresh rate, 20 cd/m^2 mean luminance) which was positioned 25 cm from the animal.

2.5 Intrinsic Signal Optical Imaging

2.5.1 Surgical preparation

The procedures for intrinsic signal optical imaging (ISOI) have been previously described (Davis et al., 2015; Sun et al., 2016). ISOI was performed to (a) generate retinotopic

maps of bV1, which were then used to guide transplantation and virus injections, and (b) measure ocular dominance index in transplant recipients. All imaging was performed through intact skull in animals that were anesthetized with chlorprothixene (0.4 mg/ml) and 0.7% isoflurane. An injection of atropine (Med-Pharmex Inc, 54925-063-10; 1 mg/kg) was also given to dilate the pupil and decrease secretion. To prepare for imaging, the skull was covered with agarose (1.5% w/v in 1X PBS) and a 5- or 10-mm glass coverslip. For hour-long experiments, eye ointment was applied around the coverslip to create a seal and prevent the skull from drying out during imaging. Body temperature was maintained by feedback control heating pad during imaging.

2.5.2 Intrinsic signal optical imaging in adult transplant recipients

Intrinsic signal images were collected using a custom-designed macroscope (Nikon 135 X 50 mm lenses) equipped with a Dalsa 1M30 CCD camera. First, a green (530 nm) LED light was used to visualize and capture an image of the surface vasculature. Then the camera was focused ~600 μm beneath the pia surface, and a red (617 nm) LED light was used to acquire the intrinsic signal. For adult MD experiments, all mice underwent both PreMD and PostMD imaging sessions, three to four times each. Each imaging session consisted of measuring the responses through each eye in an alternating pattern for a total imaging duration of 30 to 40 minutes.

2.5.3 Four-day monocular deprivation

For ocular dominance plasticity (ODP) experiments, the eye contralateral to the imaging hemisphere was sutured immediately after the first day of imaging and stayed closed for four days, which has been previously shown to effectively induce cortical plasticity (Davis et al., 2015). To examine the effect of exogenous NRG1 on ocular dominance plasticity

in transplant recipients, some recipients were injected with either saline or NRG1 (0.5 μg per animal every 8 hour) during MD.

2.5.4 Visual stimulus conditions

The MATLAB Psychophysics Toolbox extensions was used to generate visual stimuli (Brainard, 1997; Pelli, 1997). Visual stimuli consisted of contrast modulating sweeping noise. The display of the stimuli was restricted to -5° to +15° visual field azimuth and -18° to +36° visual field elevation. Each recording trial consisted of five-minute presentations of stimuli at 0° and 180°. The stimuli were displayed on an Acer V193 monitor (53 X 33 cm, 60 Hz refresh rate, 20 cd/m^2 mean luminance) which was positioned 25 cm from the animal.

2.6 Retrograde Viral Tracing Using Rabies Virus

Retrograde viral tracing using glycoprotein-deleted rabies virus was previously described (Sun et al., 2014; Sun et al., 2019; Wall et al., 2010). Three weeks after the transplantation of PV-cre;TVA tissue, transplant recipients were anesthetized under 1.5-2% isoflurane and injected with Carprofen before surgery. For labeling the inputs onto normal PV interneurons, we performed retrograde tracing in PV-cre;TVA animals a few days during the juvenile critical period (P29 – P31). A pulled glass pipette (tip diameter, ~30 μm) was loaded with virus and then lowered into the brain (400 μm and 600 μm below the pial surface). A Picospritzer (General Valve, Hollis, NH) was used to deliver the virus. The helper virus (pAAV-Ef1a-DIO-H2B-GFP-2A-oG-WPRE-hGH; Addgene, Plasmid 74289; 1.5 X 10^{13} GC/ml; 2 sites x 200 nl/site) was injected at bV1 at a rate of 8-10 nl/min. To prevent backflow of virus, the pipette remained in the brain for 5 minutes after completion of the injection. After the procedure, mice were allowed to recover in their home cages on a heating pad.

Three weeks after the AAV injection, the rabies glycoprotein (RG)-deleted rabies virus (EnvA-SADΔG-DsRed rabies, 200 nl, ~2 X 10^9 GC/ml) was injected into the same location of the previous helper virus injection in bV1. The rabies virus was allowed to incubate for 9-10 days before the animals were perfused for tissue processing.

2.7 Immunohistochemistry

The mice were perfused with chilled 1XPBS and 4% PFA. The brains were post-fixed overnight and cryoprotected with 30% sucrose. The 50-μm sections containing primary visual cortex were prepared using a microtome (Microm, HM450).

Immunohistolochemistry of free-floating sections was previously described (Sun et al., 2016). Sections were first permeabilized with 0.3% Triton-X in PBS and then blocked with 0.3% Triton-X in PBS containing 5% normal goat serum (Vector Laboratories, S-1000) and 10% bovine serum albumin (Sigma, A7906). After 48-72 hours of incubation in primary antibodies for 48 – 72 hours at 4 °C, sections were rinsed with 1XPBS, and incubated overnight with secondary antibodies. Sections were then mounted with Fluoroshield with DAPI (Millipore-Sigma, F6057), and cover-slipped. To quantify PV+ cells in the transplant brains, selected sections were stained with PV antibody (Sigma, P3088, Mouse, 1:500), followed with Alexa Fluor conjugated secondary (Invitrogen, A21240, Alexa 647 conjugated goat anti-mouse, 1:1000). To identify the starter cells and determine the cell identities of rabies-infected DsRed-positive cells in rabies infected brains, sections containing V1 were co-stained with GFP antibody (Aves, GFP-1010, Chicken, 1:500) and GABA (Sigma, 2052, rabbit, 1:1000) antibodies. Alexa 647-conjugated goat anti-rabbit (Invitrogen, A21245,

1:1000) and Alexa 488-conjugated goat anti-chicken (Invitrogen, A11039, 1:1000) secondary antibodies were used to visualize the staining.

2.8 Whole Brain Clearing and Light-Sheet Imaging

2.8.1 iDISCO+ brain clearing

All samples were cleared as previously described (Renier et al., 2016). For full protocol details and solution reagents, refer to idisco.info.

Pretreatment: Briefly, fixed transplant brains were washed three times in PBS for 1hr to remove PFA. Samples were then subjected to a series of 1hr MeOH dehydration steps of increasing concentration from 20% - 100% at room temperature (RT). After overnight fixation in 2:1 dicholoromethane (DCM, Sigma, 270997): MeOH, samples were washed twice with 100% MeOH. Samples were briefly incubated at 4 °C, then rocked overnight in freshly made, pre-chilled 1:5 30% H_2O_2: 100% MeOH bleaching solution at 4 °C. Upon removal from 4 °C, samples were subjected to a series of 1hr MeOH rehydration steps of decreasing concentration from 80% - 0% at RT.

Immunolabeling: Samples were washed twice in PTx.2 at RT, followed by permeabilization for two days at 37 °C. Samples were again washed twice in PTx.2 at RT, then blocked for three days at 37 °C. To amplify the host AAV1-GCaMP6s and transplanted PV-tdTomato signals, samples were washed twice in PTwH at RT and incubated for 6 days at 37°C with 1:500 chicken anti-GFP (Aves Labs, GFP-1020) and 1:400 rabbit anti-RFP (Rockland, 600-401-379), respectively. Samples were then washed in PTwH for increasing durations of 0 min – 2 hrs for the first day, 2 hrs each for the second. Following a secondary incubation for 6 days at 37°C with 1:500 donkey anti-chicken Alexa 647 (Jackson, 703-605-155) and 1:400 donkey

anti-rabbit Alexa 568 (Abcam, ab175692), samples were washed using the same post-primary protocol.

Clearing: Samples were subjected to a final series of 1 hr MeOH dehydration steps of increasing concentration from 20% - 100% at RT. After another overnight fixation in 2:1 DCM:MeOH, samples were incubated twice for 15 min with 100% DCM. To render the tissue optically clear, samples were lastly incubated with dibenzyl ether (DBE, Sigma, 108014) at RT.

2.8.2 Light-sheet microscopy

Equipped with an s-CMOS camera and multi-view imaging, a light-sheet fluorescence microscope (Zeiss Z.1) was used to image cleared transplant brains as whole brains. Cleared brains were first mounted on custom 3D printed suspension clamps and submerged in a large custom chamber (Translucence) filled with DBE. Using two illumination objectives (EC Plan-Neofluor 5x/0.16), cleared brains were excited by LED lasers (561-50 and 638-75, SBS LP 640) and emissions collected by a collared (n = 1.45) detection objective (LSFM 5x/0.1). Tile scan configurations were calculated using an external multiview-setup program (Zeiss). 16-bit resolution scans were captured at 1X zoom magnification, with laser power (561: 15%, 638: 20%) and exposure time (70 ms) optimized for clarity and high signal-to-noise ratio. Scans retained a constant interval (5.324 μm), overlap (20%), and delay (4 sec) between z-stack tiles.

2.8.3 3D image reconstruction

Overlapping regions between tiles were used for manual realignment and creation of stitched, multi-dimensional image stacks via Arivis. Image stacks were post-processed in

Imaris, applying a gamma correction (0.8) to reduce auto-fluorescence intensity. Orthogonal slice animations were also generated using Imaris.

2.9 Quantification and Data Analysis

2.9.1 Calcium imaging data analysis

The analysis procedures were previously described in more detail (Figueroa-Velez et al., 2017; Salinas et al., 2017). Custom-written Python scripts were used to compute the fluorescence signal of each cell body by subtracting the average neuropil signal from the signal of the soma. Each cell's response to each stimulation period was normalized to the baseline value preceding stimulus presentation ($\Delta F/F_0$). At each spatial frequency, the cell's response to a given orientation θ was defined as the average response across the 8 repeats of that orientation. The peak spatial frequency was defined as the frequency that produces the maximum average response, and this response was chosen as $F(\theta)$. Median peak spatial frequency is plotted in Figure 3.6E, Figure 3.7C, and Figure 3.8C.

The cell's preferred orientation at its peak spatial frequency was then determined as follows:

$$\theta_{pref} = \frac{\sum F(\theta) e^{2i\theta}}{2 \sum F(\theta)}$$

The fitted response $R(\theta)$ was then determined by fitting $F(\theta)$ to a sum of two Gaussians centered on θ_{pref} and $\theta_{pref} + \pi$, with different amplitudes and equal width, and a constant baseline. The amplitude of the fitted response at the preferred orientation was $R(\theta_{pref})$, and this value is reported as a cell's response amplitude in the figures and text. A cell is responsive (1) when its responses to each stimulation across all spatial frequencies reach

significance when compared against the blank screen condition (one-way ANOVA, $p < 0.01$); and (2) when its average peak response $\Delta F/F_0$ is at least 5%.

The cell orientation selectivity index (OSI) was determined using the circular variance method described previously based on the following equation (Figueroa-Velez et al., 2017; Hoy and Niell, 2015; Kerlin et al., 2010; Salinas et al., 2017):

OSI =

$$\sqrt{\left(\sum_i (F(\theta_i) * \sin(2\theta_i))\right)^2 + \left(\sum_i (F(\theta_i) * \cos(2\theta_i))\right)^2} \Big/ \sum_i F(\theta_i)$$

Time-lapse imaging of PV interneurons in transplant recipients and untreated adults allowed us to track the same cells before and after MD. For calculating the percent change in response amplitude (Figure 4.5E), only cells that were responsive during both Pre- and PostMD imaging sessions were included. We first calculated percent change for individual cells, and then calculated the average for each field. The actual data points plotted are therefore the average response amplitude per field (Figure 4.5E). For calculating the percent difference in responsiveness for each field, we included the same cells before and after MD (Figure 4.5D). Each animal contributed 2 – 5 fields.

The ODI for each cell was calculated as (C – I)/(C + I), where C is $R(\theta_{pref})$ for the contralateral eye and I is $R(\theta_{pref})$ for the ipsilateral eye. Contralaterally dominated neurons have an ODI value of 1, and these neurons are labeled as Contra throughout the paper. Ipsilaterally dominated neurons have an ODI value of -1, and they are labeled as Ipsi. Binocular neurons have ODI between -1 and 1. In cases where no significant response was

detected for one eye, response amplitude for that eye was set to 0. Non-responsive cells are those neurons that showed no significant response to either eye.

2.9.2 Intrinsic signal optical imaging data analysis

Custom-written Matlab scripts were used to generate amplitude and phase maps of cortical responses using Fourier analysis as described previously (Davis et al., 2015; Gandhi et al., 2008; Kalatsky et al., 2003; Sun et al., 2016). The Fourier map was then smoothed with a 5 X 5 Gaussian kernel to compute the final amplitude map. The phase map was normalized by subtracting the phase of the cortical responses at 180° from the phase at 0°, to remove hemodynamic delay. Maps of absolute retinotopic phase are shown in terms of visual angle relative to the center of the monitor. Phase maps are then overlaid on top of vasculature image to facilitate the targeting of bV1 in other surgical and imaging procedures.

The ODI for each animal was calculated as (C-I)/(C+I), where C is the average response amplitude for the contralateral eye, and I is the average response amplitude for the ipsilateral eye across 3 or 4 repetitions. OD shift is used as a measure for cortical plasticity and is calculated by subtracting PreMD ODI from PostMD ODI.

2.9.3 Immunohistochemistry image analysis

Immunostained sections were imaged using a confocal microscope (Leica SP8, 20X Objective, Leica Microsystem, Germany). LAS X image processing software (Leica Microsystem) was used to perform image tiling and acquire z-stack. To count the transplanted cells in bV1, sections were sampled at 300 μm intervals. The tdTomato red fluorescence was bright enough to count the transplanted cells without amplification. The percentage of transplanted tdTomato cells that co-expressed PV was calculated by dividing the number of PV^+/$tdTomato^+$ neurons by the total number of $tdTomato^+$ cells.

In rabies infected V1, the starter cells expressed DsRed (rabies), nuclear GFP and GABA. No amplification was needed to identify $DsRed^+$ cells. The cells that only expressed DsRed and GABA were categorized as presynaptic GABAergic neurons. We counted GABA-negative DsRed-positive cells as putative presynaptic excitatory neurons.

2.10 Statistical Analysis

For data plotted as mean ± s.e.m.. either parametric (Brown-Forsythe and Welch one-way ANOVA test followed by Dunnett's T3 multiple comparison test) or non-parametric (two-way ANOVA followed by Bonferroni multiple comparison test, Mann-Whitney U test, Wilcoxon signed-rank test, Kruskal-Wallis one-way ANOVA followed by Dunn's multiple comparison test) statistics was performed. Normality of the data was tested using D'Agostino-Pearson normality test, and non-parametric statistics was performed when the data was not normally distributed. Due to the small sample size, the calcium imaging data of transplanted cells were plotted using box and whisker plots. The central mark indicates the median, the bottom and top edges of the box indicate 25^{th} and 75^{th} percentiles, respectively (Figures 3.6, 3.7 and 3.8). In addition, linear regression and correlation analysis and Fisher's exact test were also performed where appropriate.

CHAPTER 3: TRANSPLANTED PV INTERNEURONS MATURE AND SYNAPTICALLY INTEGRATE INTO ADULT VISUAL CORTEX

3.1 Introduction

Maturation and synaptic integration to the host brain are required for transplanted GABAergic interneurons to produce functional changes in the host brain (Henderson et al., 2014; Priya et al., 2019; Southwell et al., 2010; Upadhya et al., 2019; Zhu et al., 2019). Pair-recordings in slices demonstrate that transplanted interneurons form functional synapses with host neurons (Henderson et al., 2014; Southwell et al., 2010; Zhu et al., 2019). Moreover, silencing the transplanted interneurons *in vivo* using DREADDs reduces the transplant-induced improvement in seizure (Upadhya et al., 2019) and traumatic brain injury (Zhu et al., 2019) models. Collectively, these results imply that transplanted interneurons recover brain functions in various models of neurological disorders by enhancing GABAergic synaptic transmission. The extent of the synaptic integration, however, is not clear since pair-recording limits the sampling to local circuits. In the visual cortex interneurons receive long-range inputs from various brain regions outside of primary visual cortex (Lu et al., 2014).

Previous studies have documented the development of firing properties, synaptic connectivity and *in vivo* tuning properties of the transplanted interneurons (Figueroa-Velez et al., 2017; Larimer et al., 2017). However, it is not clear how the integration of transplanted interneurons alters the responses of the host neurons.

To address these questions, we performed rabies viral tracing and *in vivo* Ca^{2+} imaging in transplant recipients. We found that even though transplanted PV interneurons

are synaptically integrated into the host visual cortex by 35 days after transplantation (DAT), they do not significantly alter the response properties of host PV interneurons or excitatory neurons. We first showed that transplanted interneurons disperse throughout primary visual cortex and express mature markers for parvalbumin (PV) GABAergic interneurons. We then showed that transplanted PV interneurons exhibit mature visual tuning properties by 35DAT. Using retrograde rabies tracing, we also found that transplanted PV interneurons receive extensive local and long-range inputs from the host brain. Local inputs include both excitatory and inhibitory inputs, consistent with previous electrophysiology studies (Larimer et al., 2017; Southwell et al., 2010). Interestingly, the interneuron transplantation does not significantly alter the orientation selectivity index or spatial frequency responses of the host neurons. Overall, these results indicate that the transplanted PV interneurons display mature properties that allow them to regulate cortical plasticity.

3.2 Results

3.2.1 Transplanted interneurons express marker for mature interneurons

Twenty percent of the neurons in the cortex are GABAergic interneurons. During embryonic development, GABAergic progenitors from ganglionic eminence of the embryonic forebrain migrate tangentially to the cortex and other subcortical regions starting around embryonic day 12-14. For parvalbumin interneurons, the progenitors originate specifically from medial ganglionic eminence (MGE). We took advantage of the fact that the progenitors are highly concentrated in the MGE between embryonic day 12-14 and harvested the tissue from MGE for transplantation.

Previous studies have demonstrated that transplanted interneurons disperse widely even in the adult cortex (Davis et al., 2015). Here, we measured the spread of the transplanted PV interneurons in our experimental animals after the *in vivo* Ca^{2+} imaging sessions at around 35-40DAT or 65-70DAT. We harvested MGE from embryos that expressed red fluorescent protein tdTomato specifically in PV interneurons and transplanted into the binocular visual cortex (bV1) of adult mice (~P80 – 120; Fig. 3.1A). The bV1 was located based on the phase map generated using intrinsic signal optical imaging (Fig. 3.1B) at least one week prior to transplantation. The *in vivo* Ca^{2+} imaging of the transplant recipients occurred at 33-35DAT or 60-65DAT. The imaging procedure will be discussed in more detail in the later sections. After repeated imaging sessions, the animals were perfused, and the brains were harvested for post-hoc immunohistochemistry and anatomical analysis (Fig. 3.1A). Fig. 3.1C shows an example of coronal section taken from a transplant recipient that received virus injection calcium indicator GCaMP6s at the center of bV1. The center of the viral infected region was marked as 0 when quantifying the medial-to-lateral spread of the transplanted neurons. I confirmed that the transplanted PV interneurons migrated up to ~1mm from the center of bV1 by 35-40DAT (Fig. 3.1D). They were found in all layers of the visual cortex, however, majority of them resided between layer II/III and layer V (Fig. 3.1E). The distribution of the cells deviated somewhat from what has been reported in the normal cortex (Almási et al., 2019; Tremblay et al., 2016), in which PV interneurons are found in all layers except layer I. The difference might be explained by the fact that we biased our injection to the superficial layer, and therefore there may be some cells that migrated ectopically or stayed in the superficial layer. In the caudal to rostral axis, the transplanted cells were found as far as ~1.4 mm rostral from the posterior visual cortex

(Fig. 3.1F). The spread and survival of the transplanted PV interneuron could be better visualized in 3D in cleared brains (Fig. 3.1G).

In normal development, by P26-28, majority of PV interneurons express parvalbumin. Here, we stained for parvalbumin in our transplant and quantified the percentage of the transplanted tdTomato cells that were co-labeled with PV antibodies. First, we found that genotype of the adult recipients did not determine the final number of transplanted PV interneurons (Fig. 3.2B). Immunostaining results also showed that about 80% of the TdTomato+ cells are also PV+. There was also no difference in the percentage of co-labeled cells between PV-cre or wildtype adult recipients (Fig. 3.2A and Fig. 3.2C). Altogether, these results confirmed previous findings that transplanted MGE progenitors mature and disperse throughout bV1 of adult recipients. By 35DAT, these transplanted cells express mature markers for parvalbumin.

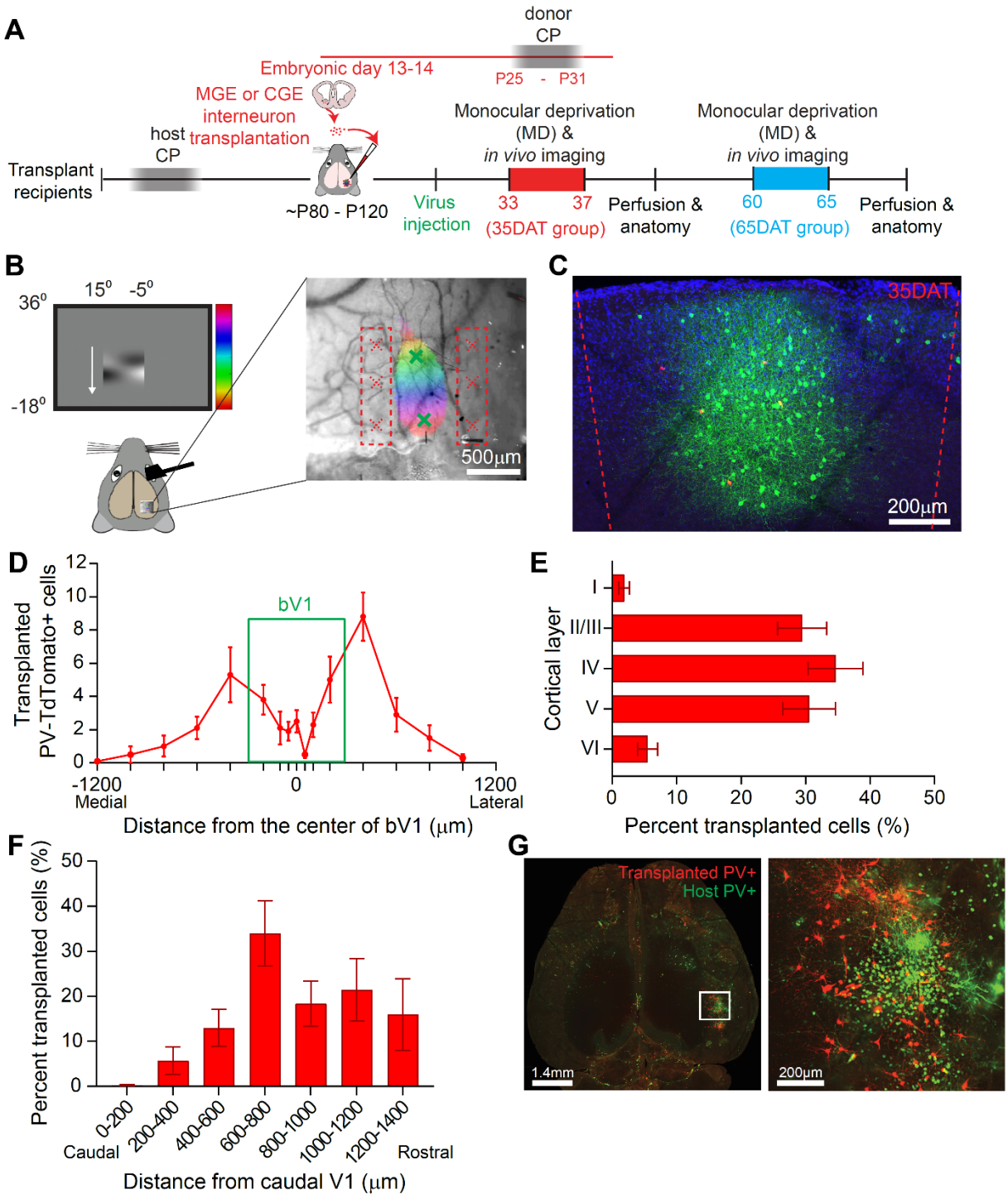

Figure 3.1 Survival and dispersion of transplanted PV interneurons

(A) Schematic of experimental design. (B) Right, intrinsic signal optical imaging was performed to locate binocular visual cortex (bV1). Left, an example phase map of bV1 on the right hemisphere of an adult mouse. The red marks indicate the transplantation sites, and the green marks indicate the virus injection sites. Scale = 500 μm. (C) An example of a coronal section from an MGE-transplant recipient. The MGE-derived parvalbumin (PV) interneurons were labeled with red fluorescent protein tdTomato (red), and the host PV interneurons in bV1 were virally labeled with calcium indicator GCaMP6s. (D) Distribution of transplanted PV-tdTomato+ cells

along the medial-lateral axis. The center of the virus expression was set to be 0 on the x-axis (n = 19 sections from 10 mice). (E) Laminar distribution of transplanted PV-tdTomato cells. (n = 10 mice). (F) Spread of transplanted interneurons in the caudal-rostral axis. The most posterior section collected for analysis is the 0 (n = 13 mice). (G) Left, whole brain image of transplant recipient cleared using iDISCO+ method, scale bar = 1.4 mm. Right, a magnified view of the outlined region above. Transplanted PV interneurons are in red, AAV1-GCaMP6s labeled PV interneurons are in green, and transplanted interneurons that expressed GCaMP6s are in yellow, scale bar = 200 μm. Data are mean ± sem.

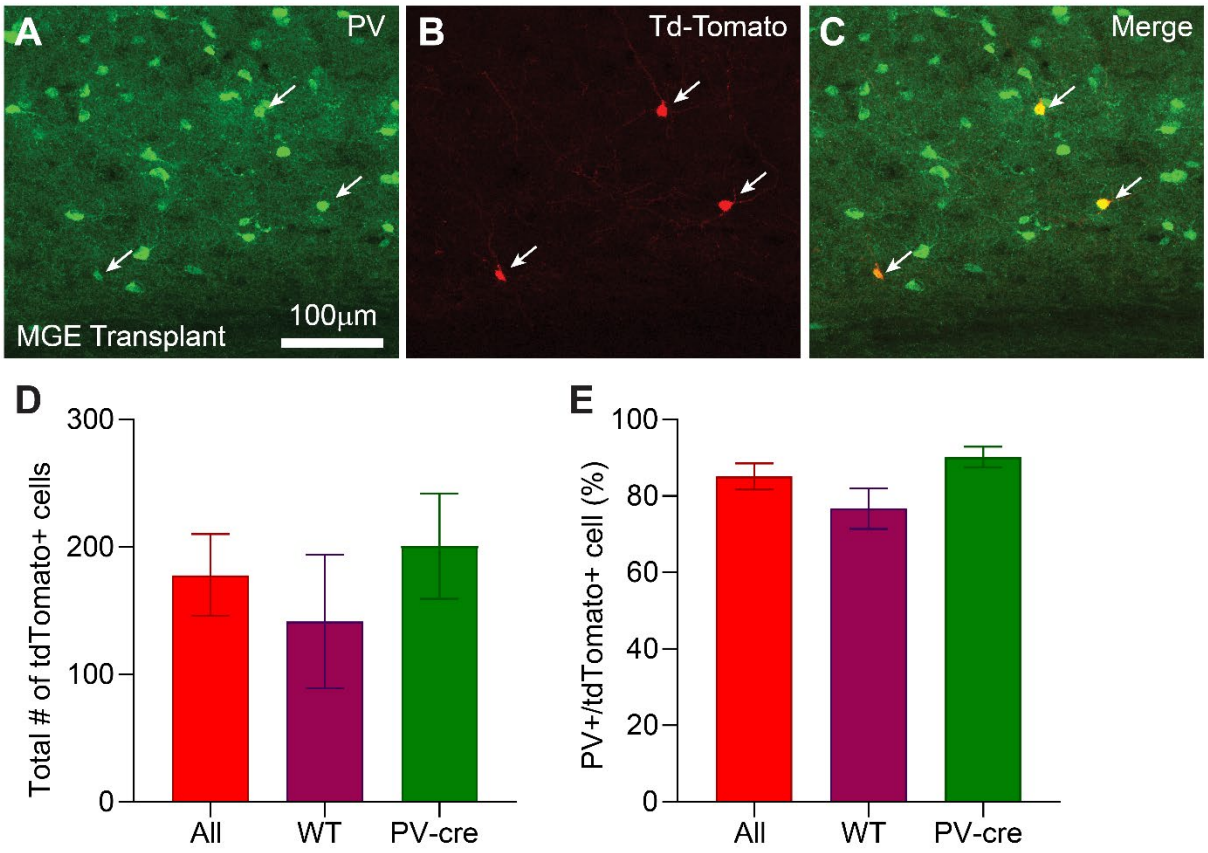

Figure 3.2 Transplanted cells express marker of mature PV interneurons

(A) Example coronal section from a PV-tdTomato MGE recipient at 35DAT stained for parvalbumin (green). Scale bar = 100 μm. (B) In the same section as (A), transplanted PV cells expressed red fluorescent protein tdTomato. (C) Transplanted PV-tdTomato cells stained for parvalbumin (yellow). (D) Estimated number of transplanted cells in adult recipients. (E) Percentage of transplanted tdTomato cells co-labeled with parvalbumin antibody. WT = wildtype adult recipient. PV-cre = PV-cre adult recipient. The genotype of the recipients did not affect total number of transplanted PV+ interneurons. (n = 13 mice).

3.2.2 Transplanted interneurons receive proper local and long-range connections from the host brain

In order to participate in cortical plasticity, transplanted cells must form proper synapses with the host circuit. Previous studies have performed *in vitro* electrophysiology in slice to show that transplanted cells form and receive connections from the host circuit (Southwell et al., 2010; Hunt et al., 2013; Henderson et al., 2014). However, electrophysiological recording can only reveal the synaptic connections within the local circuit. To identify both local and long-range inputs to transplanted PV interneurons, we performed retrograde tracing using rabies virus (Figure 3.3A; Chapter 2 Methods). We harvested tissue from embryos that selectively expressed TVA receptors in PV interneurons and transplanted into the binocular visual cortex of wildtype adult mice. We then injected cre-dependent rabies helper virus with a nuclear GFP tag 3 weeks after transplantation. The rabies virus with DsRed tag was injected at 6-7 weeks after transplantation. The cre-LoxP based approach restricted the helper virus and initial rabies virus infection to transplanted PV interneurons (Chapter 2 Methods; Callaway and Luo, 2014; Sun et al., 2014; Wall et al., 2010). Therefore, the transplanted starter cells should express both nuclear GFP and DsRed. Out of all the rabies-labeled neurons in V1, 12% were transplanted starter cells that expressed both DsRed and nuclear GFP (Figure 3.3F). The transplanted PV starter cells received both local (Figure 3.3B and 3.3C) and long-range inputs (Figure 3.3E) from the host brain like PV interneurons in normal adult mice (Figure 3.4; Lu et al., 2014). The local connections included GABAergic (12%) and putative excitatory inputs (Figures 3.3D, 3.3F and 3.3G). Altogether, these results suggest that the transplanted

cells have differentiated into mature PV interneurons and received proper synaptic inputs from host brain.

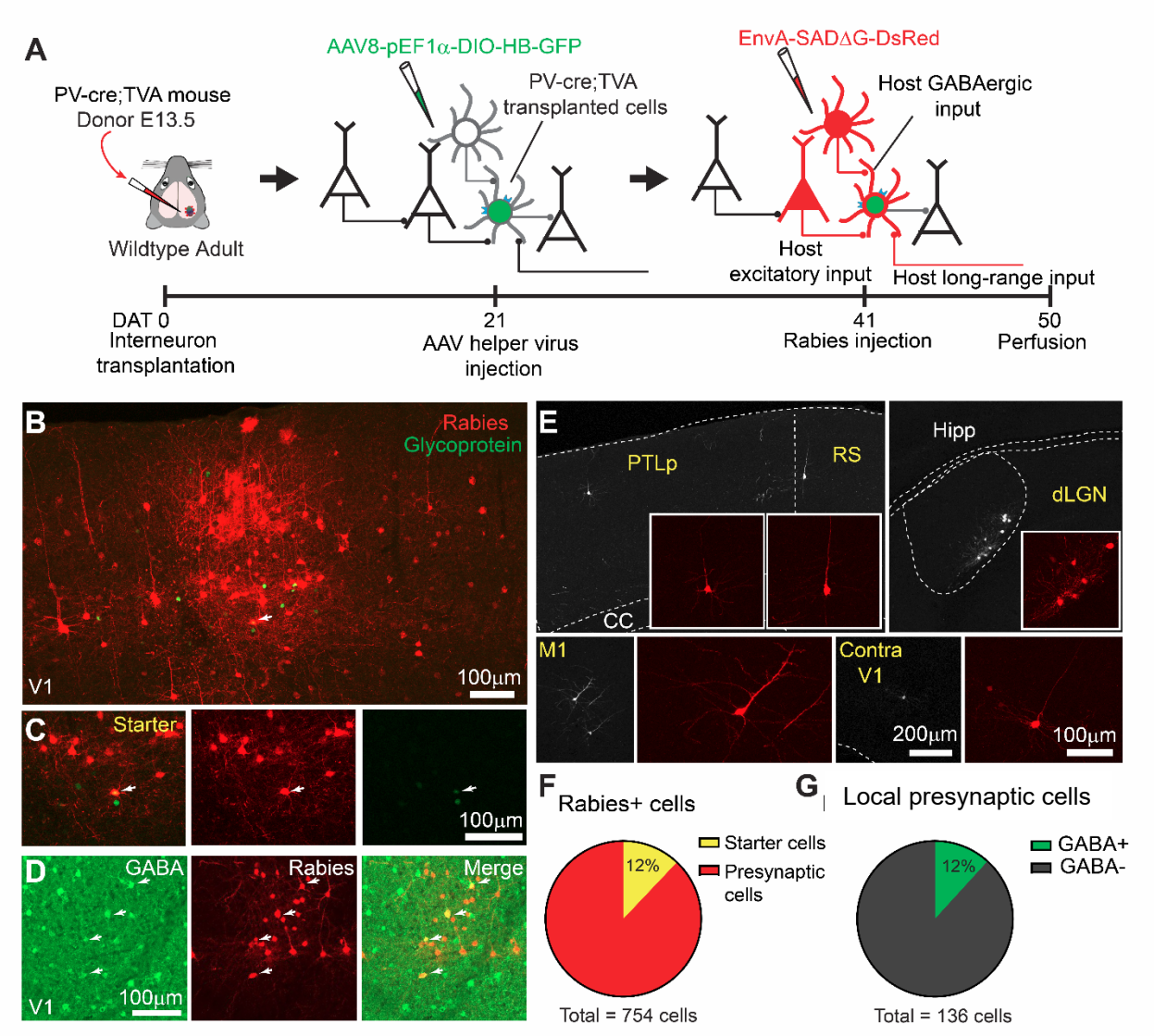

Figure 3.3 Transplanted PV interneurons are integrated into the host circuit

(A) Experimental design. (B) Identification of transplanted starter cells by co-expression of rabies glycoprotein (green) and rabies virus (red). scale bar = 100 μm. 50-μm max projection. (C) Magnified images of the starter cell in B. Scale bar = 100 μm. 3-μm max projection. (D) Transplanted PV cells received both GABAergic (yellow) and putative excitatory inputs (red) from the host cortex. Scale bar = 100 μm. (E) Transplanted PV cells received long-range inputs from various brain regions. Scale bar = 200 μm, 100 μm. (F) Quantification of transplanted starter cells (total number of rabies+ cells counted: 754, number rabies+/GFP+ starter cells: 91, and number of rabies+ only cells: 663, 1 mouse). (G) Quantification of local presynaptic cells that provided inputs to starter transplanted cells (total number of rabies+ presynaptic cells: 136, number of GABA+/rabies+ cells: 16, number of GABA-/rabies+ cells: 120, 1 mouse).

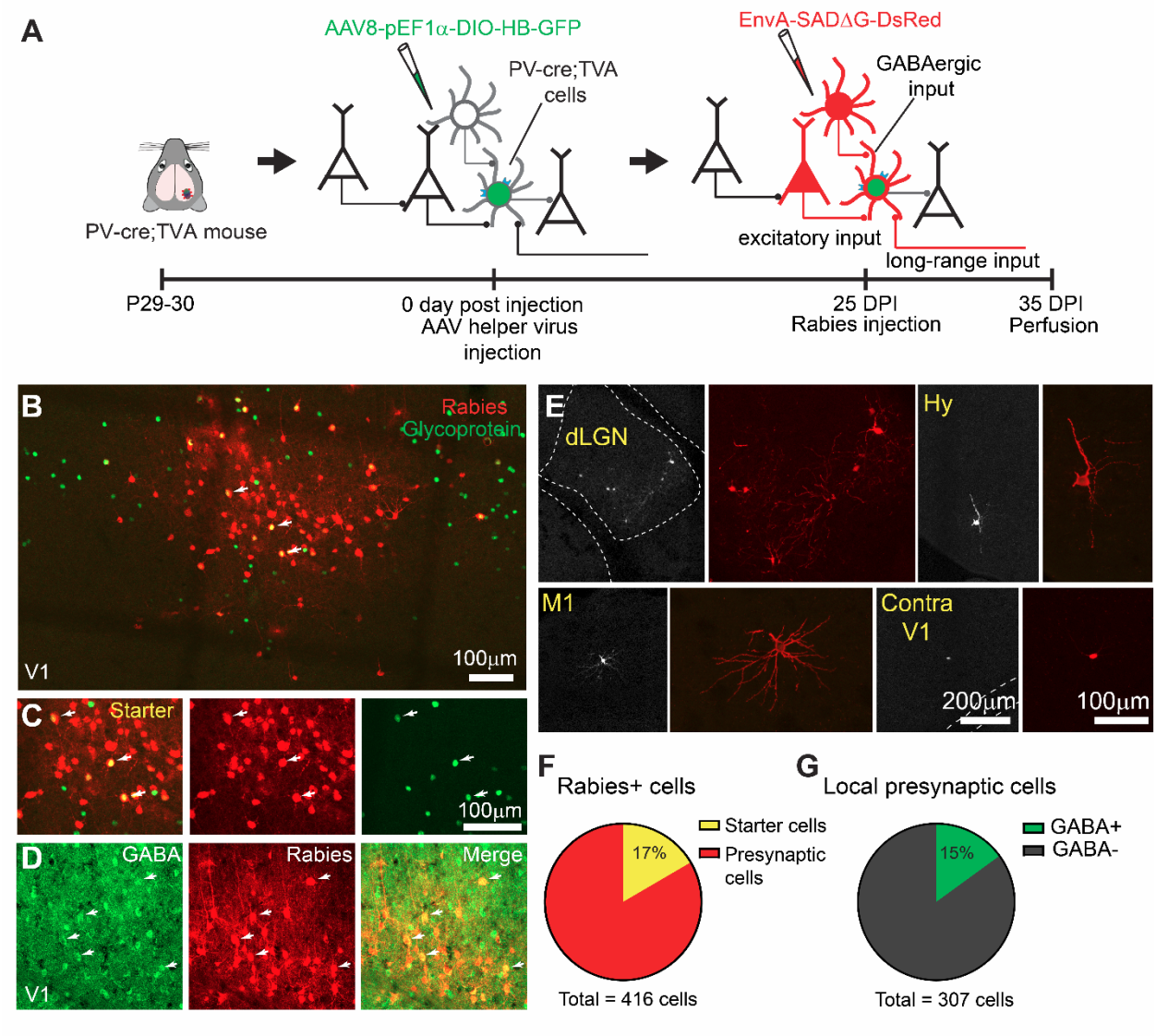

Figure 3.4 Local and long-range inputs to PV interneurons in adult PV-TVA mice

(A) Experimental design. (B) Identification of starter PV cells by co-expression of rabies glycoprotein (green) and rabies virus (red). scale bar = 100 μm. 50-μm max projection. (C) Magnified images of the starter cell in B. Scale bar = 100 μm. (D) PV cells received both GABAergic (yellow) and putative excitatory inputs (red) from the host cortex. Scale bar = 100 μm. (E) PV cells received long-range inputs from various brain regions. Scale bar = 200 μm, 100 μm. (F) Quantification of starter PV cells (total number of rabies+ cells counted: 416, number rabies+/GFP+ starter cells: 69, and number of rabies+ only cells: 347, 2 mice). (G) Quantification of local presynaptic cells that provided inputs to starter transplanted cells (total number of rabies+ presynaptic cells: 307, number of GABA+/rabies+ cells: 46, number of GABA-/rabies+ cells: 261, 2 mice).

Theoretically, the glycoprotein-deleted rabies virus used in our study will only enter the cells that express TVA receptors and infect the direct presynaptic partners if the starter

cells express rabies glycoprotein. To confirm the specificity of rabies virus and to make sure that there was no leakage of the virus, we injected rabies virus into transplant recipients that did not receive helper virus injections. In two of the transplant recipients without helper virus injection, there are no rabies-labeled cells in the local circuit or the more distant brain regions (Figure 3.5). This result confirms that in the local circuit rabies-labeled the cells are indeed the presynaptic cells to the transplanted PV interneurons.

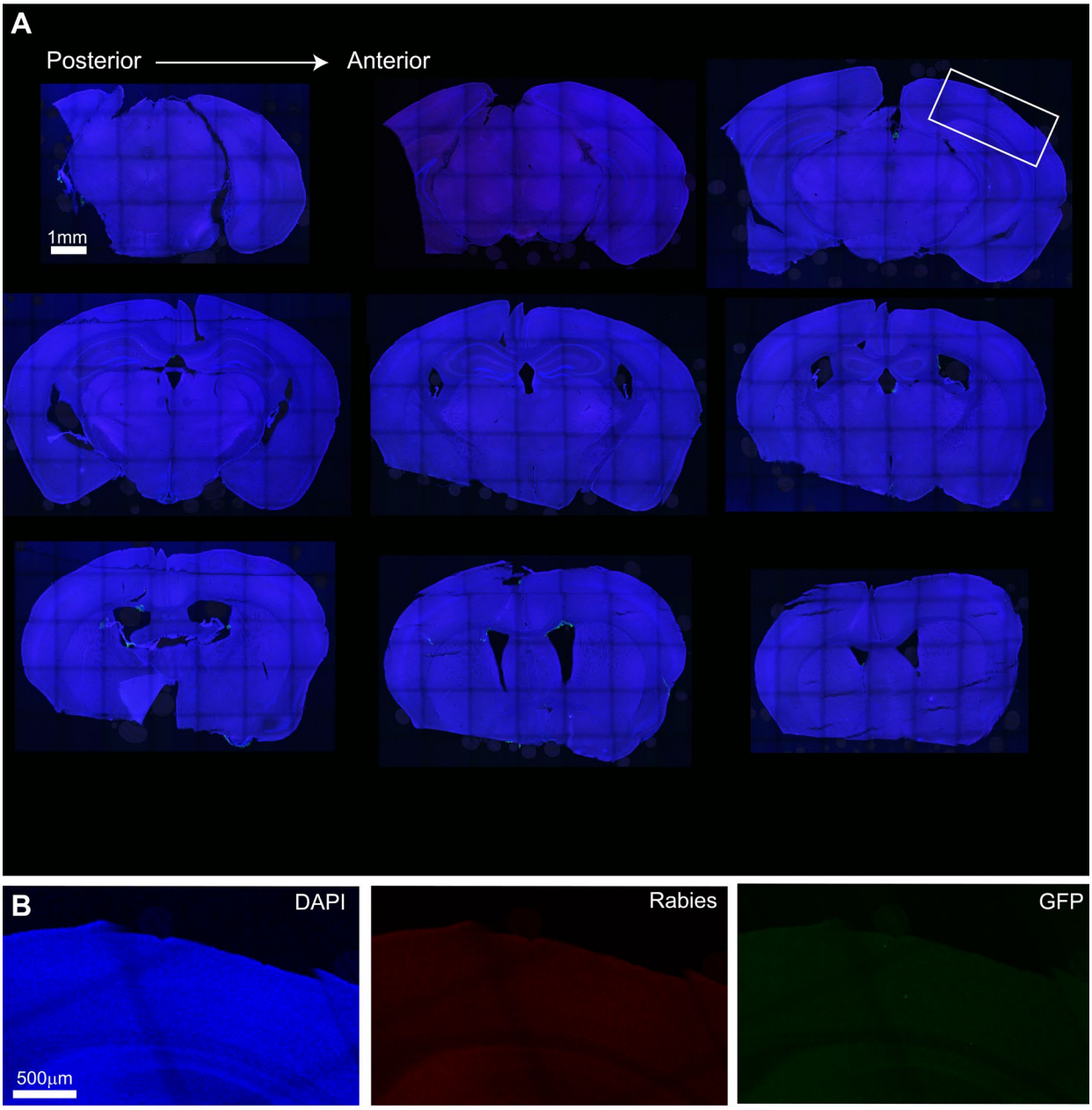

Figure 3.5 No rabies expression was detected in transplant recipients that did not receive helper virus

Two transplant recipients received transplantation of MGE-derived PV interneurons but did not receive helper virus that contained rabies glycoprotein (GFP), which was needed for monosynaptic infection of presynaptic neurons. (A) Example coronal sections from one of these control mice. 50-μm sections were cut and stained with GFP antibody and DAPI. The sections shown here are spaced 600 μm apart and arranged from posterior to anterior. Scale = 1 mm. (B) Magnified view of the boxed region in (A) to show that in binocular V1 where the transplant sites were there was no GFP+ or dsRed+ rabies expression.

3.2.3 Transplanted interneurons exhibit mature interneuron visual responses and tuning properties

The maturation of neurons in the visual cortex is reflected in their visual tuning properties, such as orientation selectivity and spatial frequency preferences. In normal development, by postnatal 26-30, parvalbumin (PV) interneurons exhibit broad orientation tuning which persists throughout adulthood (Kuhlman et al., 2011; Figueroa-Velez et al., 2017). We confirmed the previous findings by performing Ca^{2+} imaging in P26-P28 animals that received viral injection of calcium indicator GCaMP6s. We showed that for both contralateral and ipsilateral eye stimulations, PV interneurons had low orientation selectivity index as reported previously (Figure 3.6C; Contralateral OSI: 0.196 ± 0.001, n = 198 cells; Ipsilateral: 0.186 ± 0.016, n = 88 cells).

Next, we sought to examine whether transplanted PV interneurons also developed broad orientation tuning by the time of reactivated critical period at 33-36 days after transplantation. We harvested interneuron precursors from MGE of 13.5-14-day old embryos and transplanted them into the binocular visual cortex of mature mice. Depending on the genotype of the transplant recipients, we injected either synapsin-driven AAV1-GCaMP6s virus (Penn Vector Core, CS1118; titer: 7 X 10^{11}- 2 X 10^{12} genome copies (GC)/ml) or cre-dependent synapsin-driven AAV1-GCaMP6s virus (Penn Vector Core, CS1113; titer: 1 X 10^{12} GC/ml) to label both the transplanted interneurons and host cells. We performed *in vivo* Ca^{2+} imaging at 33-35DAT and 63-65DAT. We presented the animals with full drifting gratings with 8 orientations and 5 spatial frequencies (0.03-0.48, logarithmically spaced) at 2 Hz temporal frequency. We also showed a blank condition and a full-field flickering condition. The 42 total stimulus conditions were presented in a different random order for

each of the 8 repetitions. Each stimulus was presented for 2 seconds and followed by 3 seconds of gray screen for a total of 28 minutes per imaging session.

There were responsive transplanted PV interneurons at 33-35DAT (Fig. 3.6A top, red) and 63-65DAT (Fig. 3.6A bottom, blue). We next sought to determine the orientation selectivity and peak spatial frequency for these responsive cells. We first calculated the spatial frequency that produced the maximum responses for the cell (peak spatial frequency), and then determined orientation selectivity index of the cell at that spatial frequency.

By 33DAT, the transplanted PV interneurons already exhibited broad orientation tuning (Fig. 3.6B and Fig. 3.6C, red). The property did not change much by 63DAT (Fig. 3.6B and Fig. 3.6C, blue), implying that the transplanted interneurons were fully mature and integrated by the fourth week after transplantation. Interestingly, when compared to P26-28 normal critical period PV interneurons, transplanted PV interneurons in general were more sharply tuned even though the difference did not reach significance. This is not surprising, considering that the adult host brain may lack some developmental factors needed for normal development of these PV interneurons.

3.2.4 Interneuron transplantation does not alter the tuning properties of the adult host neurons

We confirmed that transplanted interneurons developed mature tuning properties by 35DAT, which implies that these cells were integrated into the host circuit. However, it is not clear how interneuron transplantation alters the tuning of host neurons. We examined

visual responses and visual tuning properties of host PV interneurons at 33-35DAT. We did not notice any significant difference in spatial frequency tuning between the transplant recipient and age-matched adult control (Fig. 3.7A – C). For the contralateral eye stimulation, the spatial frequency responses for both groups appeared to extend to the high spatial frequencies at around 2.4 cycle/degree (Fig. 3.7B, top; Fig. 3.7C). In contrast, the responses for the ipsilateral eye stimulation preferred the lower spatial frequencies at 0.6 cycle/degree (Fig. 3.7B, bottom; Fig. 3.7C). More importantly, there was no difference in the peak spatial frequencies between transplant recipients and age-matched adult controls for both contralateral and ipsilateral eye stimulation (Fig. 3.7C).

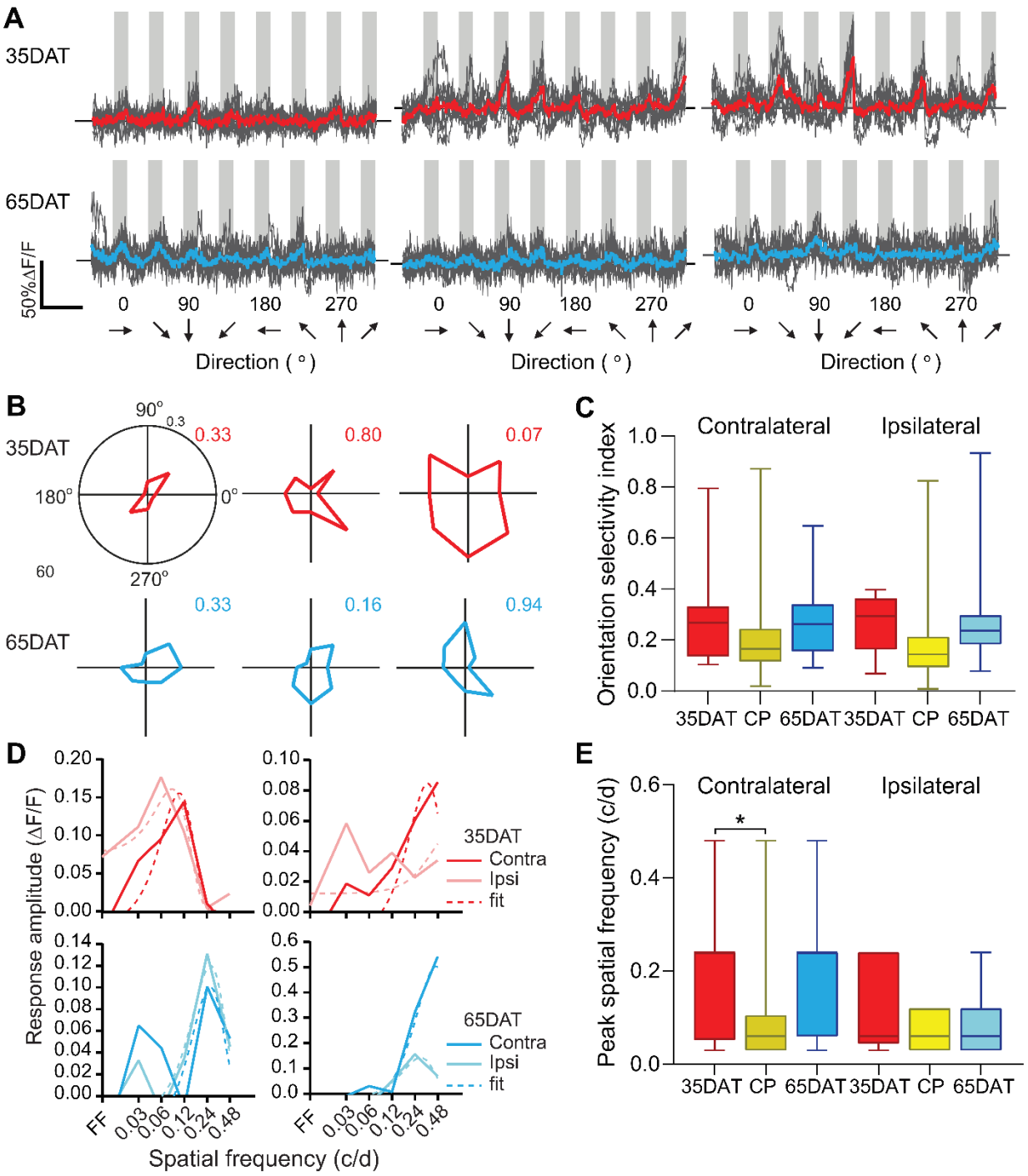

Figure 3.6 Transplanted PV interneurons exhibit mature visual tuning properties

(A) Example responses of visually evoked responses at the peak spatial frequency for transplanted PV interneurons at 35DAT (top; red) and 65DAT (bottom; blue). Light traces present individual trials, and dark traces are the average responses. (B) Peak response at each orientation is represented in polar plots. (C) Box plots of median orientation selectivity index. There was no difference in orientation selectivity between 35DAT and 65DAT transplanted interneurons and critical period (CP) PV interneurons. The central mark indicates the median, the bottom and top edges of the box indicate 25th and 75th percentiles, respectively (Contralateral:

35DAT, n = 7 cells from 5 mice; CP, n = 198 cells from 7mice; 65DAT, n = 17 cells from 3 mice; 35DAT vs. 65DAT p > 0.999, 35DAT vs. CP p = 0.385, Kruskal-Wallis one-way ANOVA test with Dunn's multiple comparison test; Ipsilateral: 35DAT, n = 4 cells from 4 mice; CP, n = 88 cells from 4 mice; 65DAT, n = 11 cells from 4 mice; 35DAT vs. 65DAT p > 0.999, 35DAT vs. CP p = 0.132, Kruskal-Wallis ANOVA test with Dunn's multiple comparison test). (D) Examples of spatial frequency responses of transplanted PV interneurons at 35 and 65DAT. The average responses (solid) at each spatial frequency are overlaid with a difference of Gaussians fit (dotted line). Peak spatial frequency is determined by the maximum of the average response. (E) Box plots of median peak spatial frequency of transplanted PV interneurons at 35 and 65DAT, as well as that of the CP PV interneurons. The central mark indicates the median, the bottom and top edges of the box indicate 25th and 75th percentiles, respectively. There is no difference in peak spatial frequency between 35 and 65DAT transplanted PV interneurons (Contralateral: 35DAT, n = 8 cells from 5 mice; 65DAT, n = 18 cells from 3 mice, CP, n = 56 cells from 2 mice, 35DAT vs. 65DAT p > 0.999, 35DAT vs. CP *p = 0.021, Kruskal-Wallis ANOVA test with Dunn's multiple comparison test; Ipsilateral: 35DAT, n = 5 cells from 4 mice; 65DAT, n = 11 cells from 4 mice, CP, n = 53 cells from 2 mice, , 35DAT vs. 65DAT p > 0.999, 35DAT vs. CP p = 0.624, Kruskal-Wallis ANOVA test with Dunn's multiple comparison test).

Next, we determined if interneuron transplantation altered the orientation tuning of host PV interneurons. We found that at the peak spatial frequency, the host PV interneurons showed characteristic broad orientation tuning (Fig. 3.7D-F). Compared to the tuning of age-matched PV interneuron adult mice, the median OSI of the host PV interneuron in transplant recipients was slightly but not significantly lower (Fig. 3.7F). These results indicate that the interneuron transplantation has little impact on the tuning of the host PV interneurons.

We also examined the tuning properties of the host excitatory neurons in the transplant recipients. As reported previously (Salinas, et al., 2017), there were multiple types

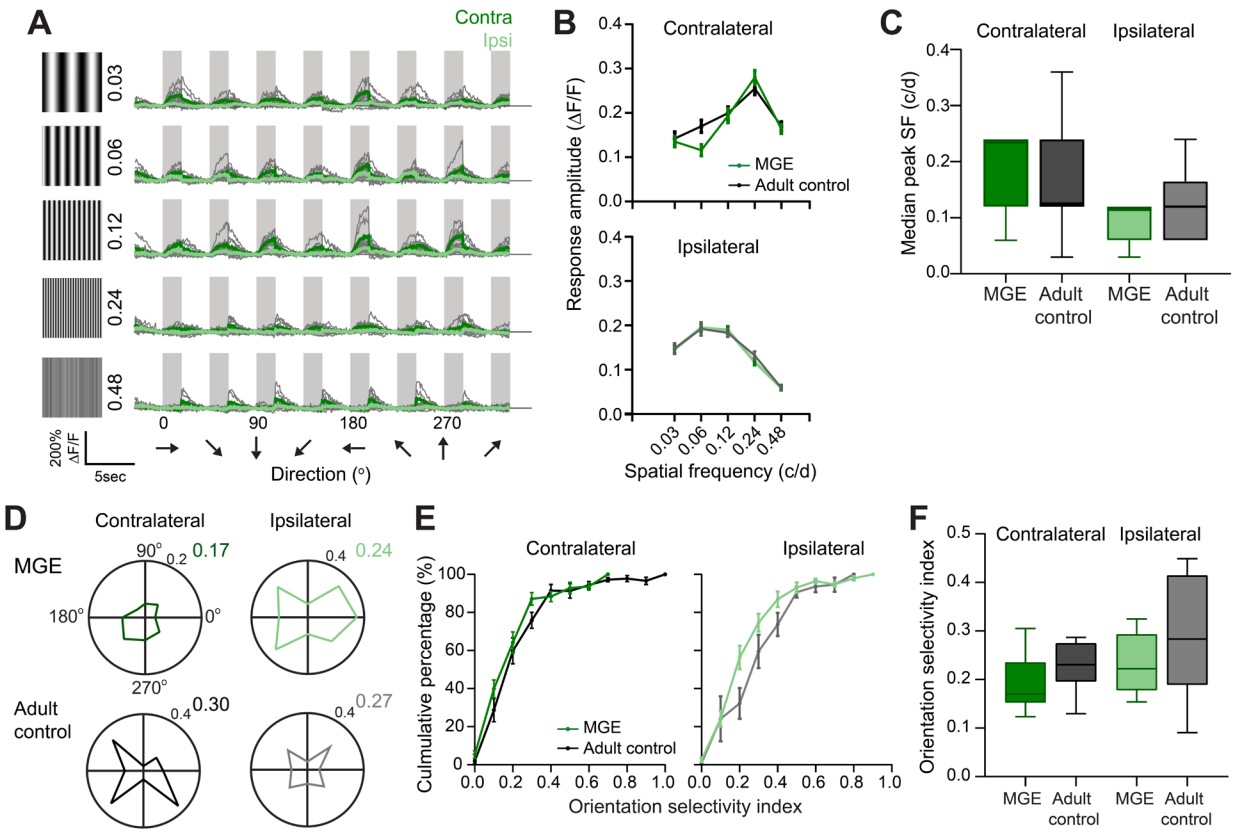

Figure 3.7 Interneuron transplantation does not alter the visual tuning properties of host PV interneurons

(A) Example binocular responses from a host PV interneuron at 35DAT. Gray boxes represent when the visual gratings were shown. Gray traces represent individual trials. Dark green represents averaged responses for contralateral eye stimulation. Light green represents averaged responses for ipsilateral eye stimulation. The peak spatial frequency for the contralateral responses is 0.12 c/d and 0.06 c/d for the ipsilateral responses in the example shown. (B) Composite spatial frequency tuning curves for responses of host and age-matched control PV interneurons. Responses to contralateral eye stimulation of both host and control PV interneurons (top) biased toward higher spatial frequency compared to the responses to the ipsilateral eye stimulation (bottom). The error bars represent s.e.m. (C) There was no difference in median peak spatial frequency between 35DAT host PV interneurons and age-matched control. Box plots of median peak spatial frequency of host PV interneurons in transplant recipients and age-matched adult control. The central mark indicates the median, the bottom and top edges of the box indicate 25th and 75th percentiles, respectively. (Contralateral: 35DAT, n = 11 mice; age matched control, 8 mice, p = 0.814, Mann-Whitney U test; Ipsilateral: p = 0.289, Mann-Whitney U test). (D) Evoked peak response of host PV interneurons at each orientation is represented in polar plots. (E) Left, cumulative distribution of orientation selectivity index (OSI) for contralateral responses of host PV interneurons in MGE transplant recipients (MGE, green, n = 11 mice), age-matched adult control (Adult control, black, n = 8 mice). Right, cumulative distribution of OSI for ipsilateral responses of PV interneurons. (F) Interneuron transplantation did not alter orientation tuning of adult host PV interneurons. Box plots of median orientation tuning of host PV interneurons in transplant recipients and age-matched adult control. The central mark indicates the median, the bottom and top edges of the box indicate 25th and 75th percentiles, respectively. (Contralateral: 35DAT, n = 11 mice; Adult control, n = 8 mice, p = 0.238, Mann-Whitney U test; Ipsilateral: 35DAT, n = 11 mice; adult control, n = 8 mice, p = 0.395, Mann-Whitney U test).

of spatial frequency responses (Fig. 3.8A). Overall, there was no significant difference in spatial frequency tuning responses between 35DAT, age-matched and 65DAT host excitatory neurons. Even though the differences in median peak spatial frequency were not significant, the age-matched excitatory neurons seemed to have higher spatial frequencies, especially for the contralateral eye response (Fig. 3.8C). This suggests that interneuron transplantation may slightly alter the circuit connectivity in bV1. Interestingly, interneuron transplantation significantly lowered the orientation tuning of host excitatory neurons, specifically in the ipsilateral pathway.

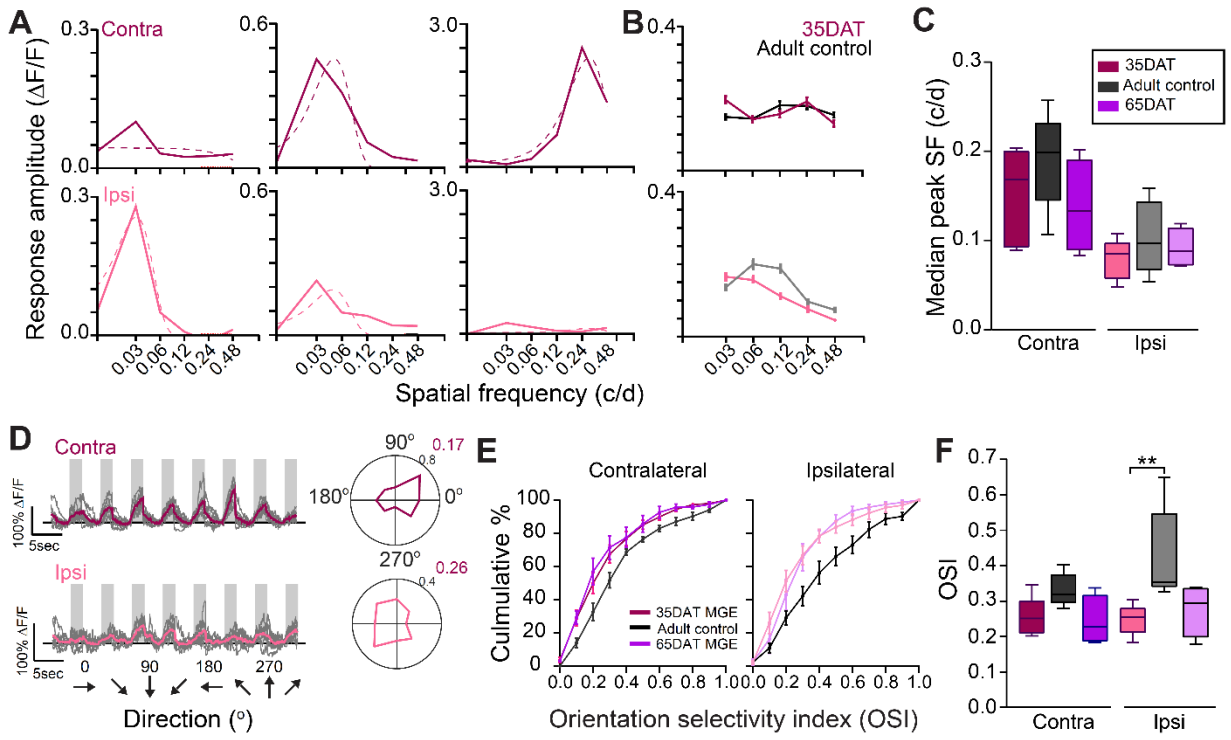

Figure 3.8 Interneuron transplantation does not alter the visual tuning properties of host excitatory neurons

(A) Example spatial frequency tuning curves for contralateral and ipsilateral eye responses. Solid lines represent the average response at each spatial frequency. Dashed lines represent fitted responses. (B) Composite spatial frequency tuning curves for responses of host and age-matched control excitatory neurons. Responses to contralateral eye stimulation of both host and control excitatory neurons (top) biased toward higher spatial frequency compared to the responses to the ipsilateral eye stimulation (bottom). (C) There was no difference in the median peak spatial frequency between 35DAT, age-matched control and 65DAT excitatory

neurons. Box plots of median spatial frequency of 35DAT and 65DAT host excitatory neurons in transplant recipients as well as excitatory neurons in age-matched adult control. The central mark indicates the median, the bottom and top edges of the box indicate 25th and 75th percentiles, respectively. (Contralateral: 35DAT, n = 5 mice; age matched control, 6 mice, 65DAT, n = 4 mice, p = 0.316, Kruskal-Wallis ANOVA test; Ipsilateral: p = 0.552, Kruskal-Wallis ANOVA test). (D) Left, evoked contralateral and ipsilateral responses of a binocular excitatory neurons from transplant recipient at 35DAT. Right, responses are represented in corresponding polar plots. (E) Left, cumulative distribution of orientation selectivity index (OSI) for contralateral responses of host excitatory neurons in 35DAT transplant recipients (35DAT, dark red, n = 5 mice) age-matched adult control (age control, black, n = 6 mice), and 65DAT transplant recipients (65DAT, purple, n = 4 mice). Right, cumulative distribution of OSI for ipsilateral responses of excitatory neurons. (F) Interneuron transplantation did not alter orientation tuning of adult neurons through the contralateral eye stimulation. In contrast, the OSI for the host excitatory neurons through the ipsilateral eye stimulation appeared lower than the age-matched excitatory neurons. Box plots of median orientation selectivity index of 35DAT and 65DAT host excitatory neurons in transplant recipients as well as excitatory neurons in age-matched adult control. The central mark indicates the median, the bottom and top edges of the box indicate 25th and 75th percentiles, respectively. (Contralateral: 35DAT, n = 5 mice; age matched control, 6 mice, 65DAT, n = 4 mice, p = 0.068, Kruskal-Wallis ANOVA test; Ipsilateral: p = 0.003, Kruskal-Wallis ANOVA test, 35DAT vs. Adult control, **p = 0.007, Dunn's multiple comparison test).

We note that the method we used for determining the orientation tuning of the cells deviated from previous studies, in which the stimulus consisted of only one, and usually low, spatial frequency (<0.05cpd; Figueroa-Velez et al., 2017; Kuhlman et al., 2013). To be consistent with the existing literature, therefore, we took a subset of the data presented in Figure 3.6 and 3.7, and plotted orientation tuning at both low (0.03 and 0.06cpd) and peak spatial frequency. The orientation selectivity index for many cells differs depending on the spatial frequency (Fig. 3.9A). However, there was no significant difference in median orientation selectivity index between low spatial frequency and peak spatial frequency.

Recent studies have also demonstrated that orientation tuning of layer 2/3 excitatory cells in the visual cortex is modulated by spatial frequencies (Ayzenshtat et al., 2016; Salinas et al., 2017). Therefore, we decided to probe the relationship between orientation tuning and spatial frequency tuning in PV interneurons further (Figure 3.9). We confirmed that at the single cell level, the responses of PV interneurons to different orientations varied across different spatial frequencies (Figure 3.9B). Here, we showed the direction tuning curves

fitted with a double Gaussian centered at preferred orientation ϑ_{pref} and $\vartheta_{pref} + \pi$ (see Method). Moreover, orientation selectivity index at the peak spatial frequency, the value used to generate orientation selectivity index graphs in Figure 3.6 and Figure 3.7, was not always representative of the overall tuning across all spatial frequencies. These were some preliminary results showing how spatial frequency modulates orientation tuning. Future studies could probe this relationship further and find a better way to represent the data.

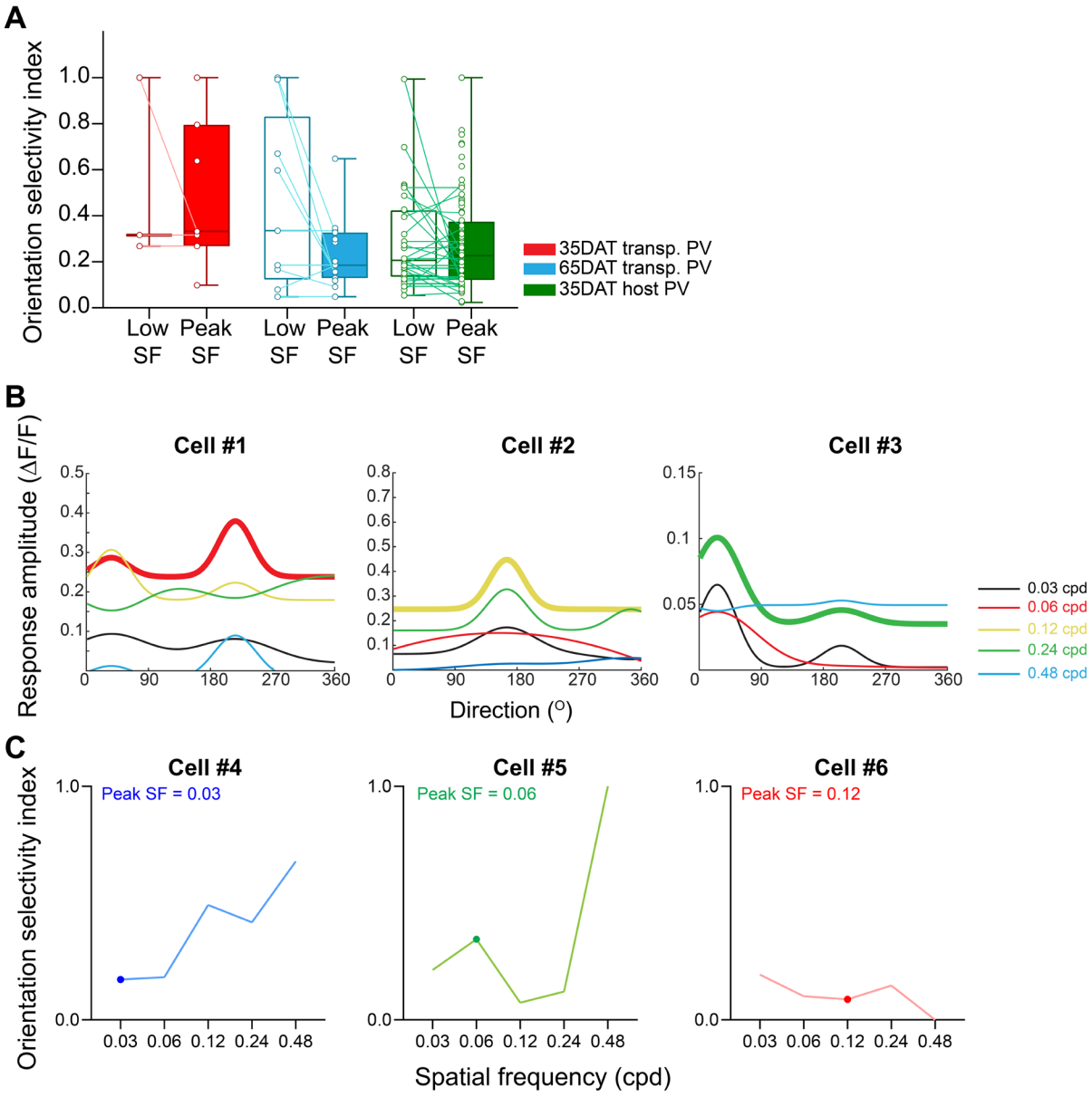

Figure 3.9 Orientation tuning of PV cells is modulated by spatial frequency

(A) Orientation selectivity index of PV cells plotted by low spatial frequency and peak spatial frequency. Overall, there was no significant difference in the median orientation selectivity index between low spatial frequency and peak spatial frequency. (B) Visual responses of example cells across 5 spatial frequencies. At the individual cell level, the orientation tuning was modulated by spatial frequency. (C) Orientation selectivity index at different spatial frequencies. The solid dots represent the orientation index at the peak spatial frequency. Orientation index selectivity varied across spatial frequencies.

3.3 Discussion

Our results show that transplanted interneurons mature, integrate and develop proper tuning properties by the time of reactivated critical period. As shown in previous studies, the transplanted PV interneurons retain the potential to migrate. In our case, the transplanted cells disperse up to 1.4 mm from the injection site. Moreover, for the first time, we show that transplanted PV interneurons receive both local and long-range connections from the host brain, comparable to PV cells in the normal adult cortex. Furthermore, majority of these transplanted PV interneurons express mature markers for parvalbumin. Interestingly, even though transplanted cells are well integrated into the host brain by 33-35DAT, their synaptic integration does not seem to dramatically affect the visual responses and visual tuning properties of the host excitatory and PV interneurons. This observation is consistent with a previous study (Figueroa-Velez et al., 2017), which demonstrates that the maturation of broad orientation tuning of host neurons is not altered by interneuron transplantation.

To our knowledge, our study is the first to show that transplanted PV interneurons receive direct long-range inputs, including those from the other hemisphere and lateral geniculate nucleus (LGN) of the thalamus. The monosynaptic inputs that the transplanted interneurons receive are comparable to the inputs onto endogenous PV interneurons as

reported in previous studies (Lu et al., 2014). Studies in normal development have demonstrated the importance of thalamic (Huh et al., 2020; Jaepel et al., 2017; Sommeijer et al., 2017) and callosal inputs (Pietrasanta et al., 2012; Restani et al., 2009) in ocular dominance plasticity, but it is not clear how these long-range inputs to transplanted PV cells contribute to the plasticity of the visual cortex. In future studies, the combination of rabies tracing and *in vivo* calcium imaging could be used to dissect the role of different long-range inputs in transplant-reactivated cortical plasticity.

Furthermore, it would be interesting to use rabies tracing to investigate how the host circuitry is altered by transplanted interneurons. Previous *in vitro* paired whole cell recordings provide inconsistent results. While Southwell et al. (2010) reports that the transplanted cells are more likely to form connections with the host excitatory neurons, Larimer et al. (2017) demonstrates that the transplanted interneurons are ~50% less likely to form synaptic connections onto host excitatory neurons. This discrepancy can be partly explained by the interneuron cell diversity. Neither of these two studies identify the cell types that are recorded in the study. In future studies, we can perform both rabies and *in vitro* electrophysiology to specifically examine the synaptic connections between transplanted PV interneurons and the host excitatory neurons. We can also examine how interneuron transplantation alters the synaptic connectivity between host PV interneurons and host excitatory neurons.

Overall, our results in agreement with previous studies. We demonstrate that the transplanted interneurons are mature and able to disperse and integrate into the host circuit by the reactivated window for plasticity. In next chapter, we will explore how the visual

experience affects the response of the transplanted interneurons and how the changes contribute to the expression of ocular dominance plasticity in the adult recipients.

CHAPTER 4: Embryonic interneuron transplantation re-sensitizes the adult host cortex to sensory experience

4.1 Introduction

The modification of inhibitory signaling in the adult brain using the transplantation of embryonic inhibitory neurons has emerged as a promising strategy to recondition dysfunctional or diseased neural circuits (Chohan and Moore, 2016; Spatazza et al., 2017; Southwell et al., 2014; Tyson and Anderson, 2014). Previously, we have demonstrated that embryonic interneuron transplantation reverses visual deficits in adult mice by reactivating a second critical period for cortical plasticity (Davis et al., 2015). Since the reactivated window for plasticity coincides with the developmental critical period of transplanted interneurons, it has been hypothesized that transplanted cells add a young inhibitory circuit to the mature brain that executes a cell-intrinsically timed developmental program that induces cortical plasticity (Davis et al., 2015; Southwell et al., 2010; Tang et al., 2014; Priya et al., 2019). While anatomical and electrophysiological properties of transplanted interneurons have been well characterized (Spatazza et al., 2017; Larimer et al., 2017), there is little understanding of how sensory experience affects the activity of transplanted interneurons and host neurons in intact animals.

During the development of the visual cortex, a sudden reduction in the activity of parvalbumin (PV) GABAergic interneurons is essential for the experience-dependent plasticity of excitatory circuits. The changes in PV interneuron responses depend on neuregulin1 (NRG1), which regulates the excitability of PV interneurons by binding to ErbB4 receptors on these neurons (Mei and Xiong, 2008; Vullhorst et al., 2009; Wen et al., 2010).

After brief monocular deprivation by eyelid suture (MD), NRG1/ErbB4 mediates the loss of excitatory drive onto PV interneurons (Sun et al., 2016). The resulting loss of PV cell activity is necessary for the subsequent reorganization of the excitatory circuit (Kuhlman et al., 2013; Sun et al., 2016). When the activity of PV interneurons is maintained, the ocular dominance plasticity is blocked (Figure 4.1; Gu et al., 2016; Sun et al., 2016). The level of NRG1 within PV interneurons peaks during the critical period but gradually decreases as the cortex matures (Grieco et al., 2020; Sun et al., 2016). These results suggest that NRG1/ErbB4 signaling may only be involved in juvenile cortical plasticity.

We sought to determine whether the same developmental processes underlying developmental OD plasticity are involved in transplant-induced plasticity, namely: (a) whether MD reduces transplanted PV interneuron activity; (b) whether the reduction in transplanted PV interneuron activity is mediated by NRG1/ErbB4 signaling; and (c) whether the reduction in transplanted PV interneuron activity is necessary for transplant-induced plasticity. To answer these questions, we performed in vivo Ca^{2+} imaging in transplant recipients and track the same cells before and after MD. Surprisingly, we found that brief MD greatly reduces the visual activity of adult host PV interneurons but has little effect on transplanted interneurons. Moreover, our study demonstrates that not only is NRG1 signaling essential for transplant-reactivated cortical plasticity, but also that the signaling depends on the ErbB4 receptors in the host PV interneurons. These results suggest that interneuron transplantation reactivates NRG1/ErbB4, a signaling pathway normally involves in developmental cortical plasticity, within the adult host PV interneurons and allow them to participate in the second critical period.

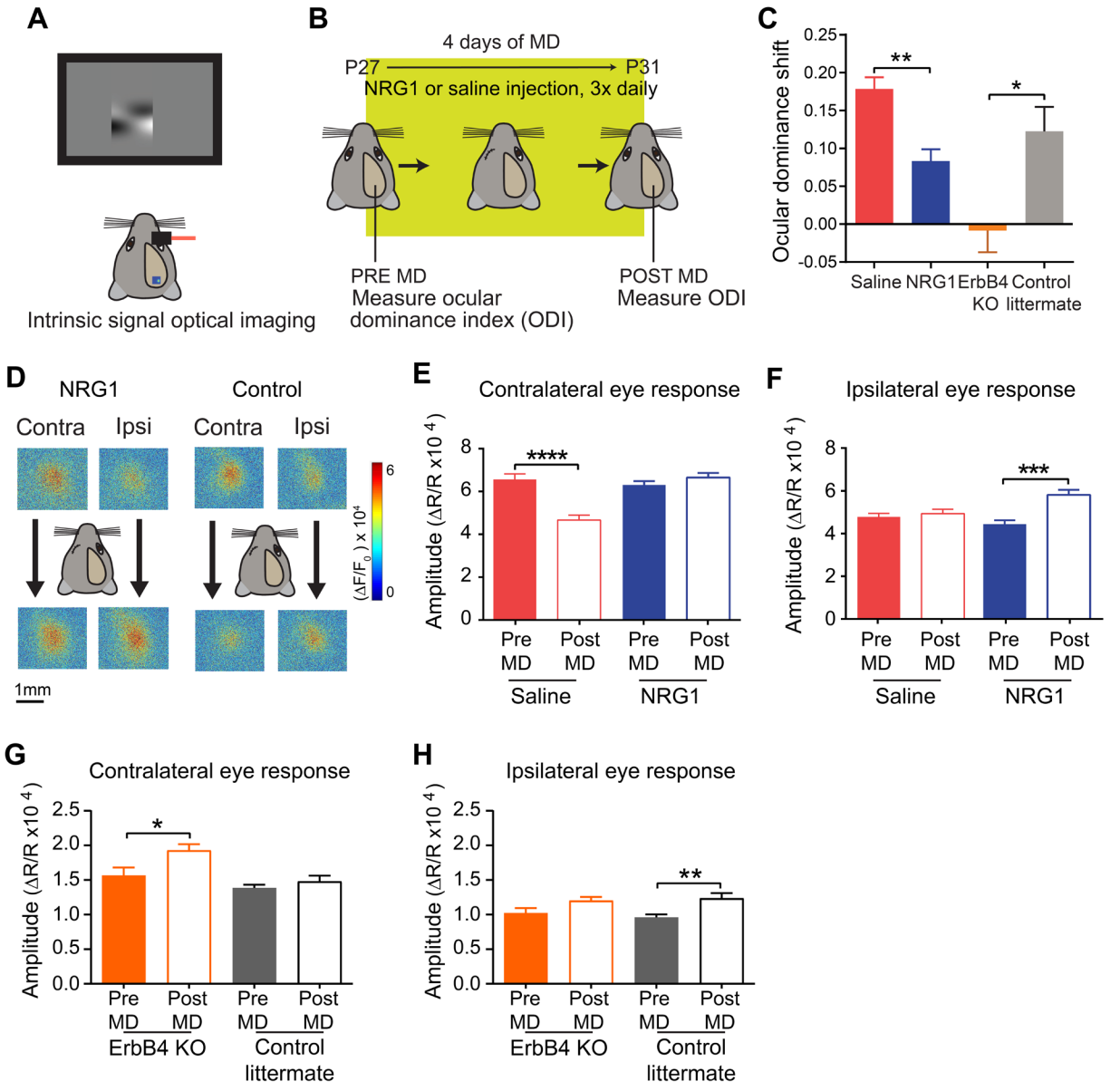

Figure 4.1. Manipulation of NRG1/ErbB4 signaling in PV Neurons prevents critical period ocular dominance plasticity

(A) Schematic of intrinsic signal optical imaging. (B) Schematic of experimental design. (C) Ocular dominance shift is reduced in NRG1-treated critical period animals (n = 6, blue) compared with control critical period animals (n = 7, red). **p = 0.004 (Mann-Whitney U test). OD shift is also reduced in PV-specific ErbB4 knockout (KO) animals (PV-Cre; ErbB4flx/flx, n = 6 mice, orange) compared with their ErbB4flx/flx littermates (n = 8 mice, gray). *p = 0.014 (Mann-Whitney U test). (D) Examples maps of contralateral and ipsilateral visual response from an NRG1-treated animal (left) and a control animal (right) before (top panels) and after (bottom panels) 4 days of MD. (E) Contralateral (deprived) input changes for control: Pre-MD (n = 7 mice, 24 responses) versus Post-MD (n = 7 mice, 23 responses). ****p = 0.0001 (Mann-Whitney U test). No contralateral input change observed in NRG1 treated animals: pre-MD (n = 7 mice, 22 responses) versus post-MD (n = 5 mice, 16 responses), p = 0.3 (Mann-Whitney test). (F) In contrast, ipsilateral input increases in NRG1-treated animals: PreMD (n = 6 animals, 18 responses) versus Post-MD (n = 6 mice, 15 responses). ***p = 0.0002 (Mann-Whitney U test). No ipsilateral input change observed in control animals: Pre-MD (n = 6 animals, 23 responses) versus

Post-MD (n = 6 animals, 23 responses). p = 0.6 (Mann-Whitney test). In PV-ErbB4 KO animals, there is a significant increase in the contralateral input: PreMD (n = 6 mice, 21 responses) versus Post-MD (n = 6 mice, 22 responses), *p = 0.022. No ipsilateral input change is observed: Pre-MD (n = 6 mice, 21 responses) versus Post-MD (n = 6 mice, 22 responses), p = 0.0812. In contrast, in ErbB4flx/flx littermates, there is a significant increase in the ipsilateral input: Pre-MD (n = 8 mice, 36 responses) versus Post-MD (n = 8 mice, 35 responses), **p = 0.005 (Mann-Whitney U test). No contralateral input change observed: Pre-MD (n = 8 mice, 35 responses) versus Post-MD (n = 8 mice, 36 responses), p = 0.97 (Mann-Whitney U test). In (E)–(H), the error bar represents the SEM. The figure was generated by XiaoTing Zheng and published in Sun et al. (2016, Neuron).

4.2 Results

4.2.1 Sensory deprivation reduces the responses of juvenile PV interneurons

Previous studies have shown that visual deprivation rapidly decreases the responses of PV interneurons, and a series of *in vitro* experiments shows that the reduction can be prevented by treating PV interneurons with exogenous NRG1 (Sun et al., 2016). Here, we confirmed previous results in juvenile critical period (P26-28) mice using *in vivo* two-photon calcium (Ca^{2+}) imaging of GCaMP6s. We recorded visually evoked activity of layer 2/3 PV cells in binocular visual cortex using cre-dependent AAV1-Syn-GCaMP6s injections into PV-cre mice (Figure 4.2A to 4.2C). We presented the animals with full field drifting sinusoidal gratings were presented in eight orientations and five spatial frequencies (0.03-0.48, logarithmically spaced) at 2 Hz temporal frequency. We also showed a blank condition and a full-field flickering condition. The stimulus conditions were presented in a different random order for each of the 8 repetitions. A cell is responsive (1) when the cell's responses to each stimulation across all spatial frequencies reached significance when compared against the blank screen condition (one-way ANOVA, $p < 0.01$); and (2) when the cell's average peak responses $\Delta F/F_0$ across 8 trials is at least 5%. One to two days of monocular deprivation (MD) rapidly reduced the overall responsiveness of PV interneurons. We determined the overall responsiveness by calculating: (a) the percentage of responsive cells (Figure 4.2D) and (b) response strength of responsive cells (Figure 4.2E). We found that one day MD reduced both

the percentage of responsive PV interneurons (Figure 4.2D) and response amplitude (Figures 4.2B and 4.2E) of PV interneurons, consistent with previous studies (Kuhlman et al., 2013; Sun et al., 2016). A second group of mice received subcutaneous injections of soluble NRG1 (3x daily) immediately after eye suturing. We showed that treatment with exogenous NRG1 during MD prevented the reduction in PV cell activity (Figures 4.2D and 4.2E).

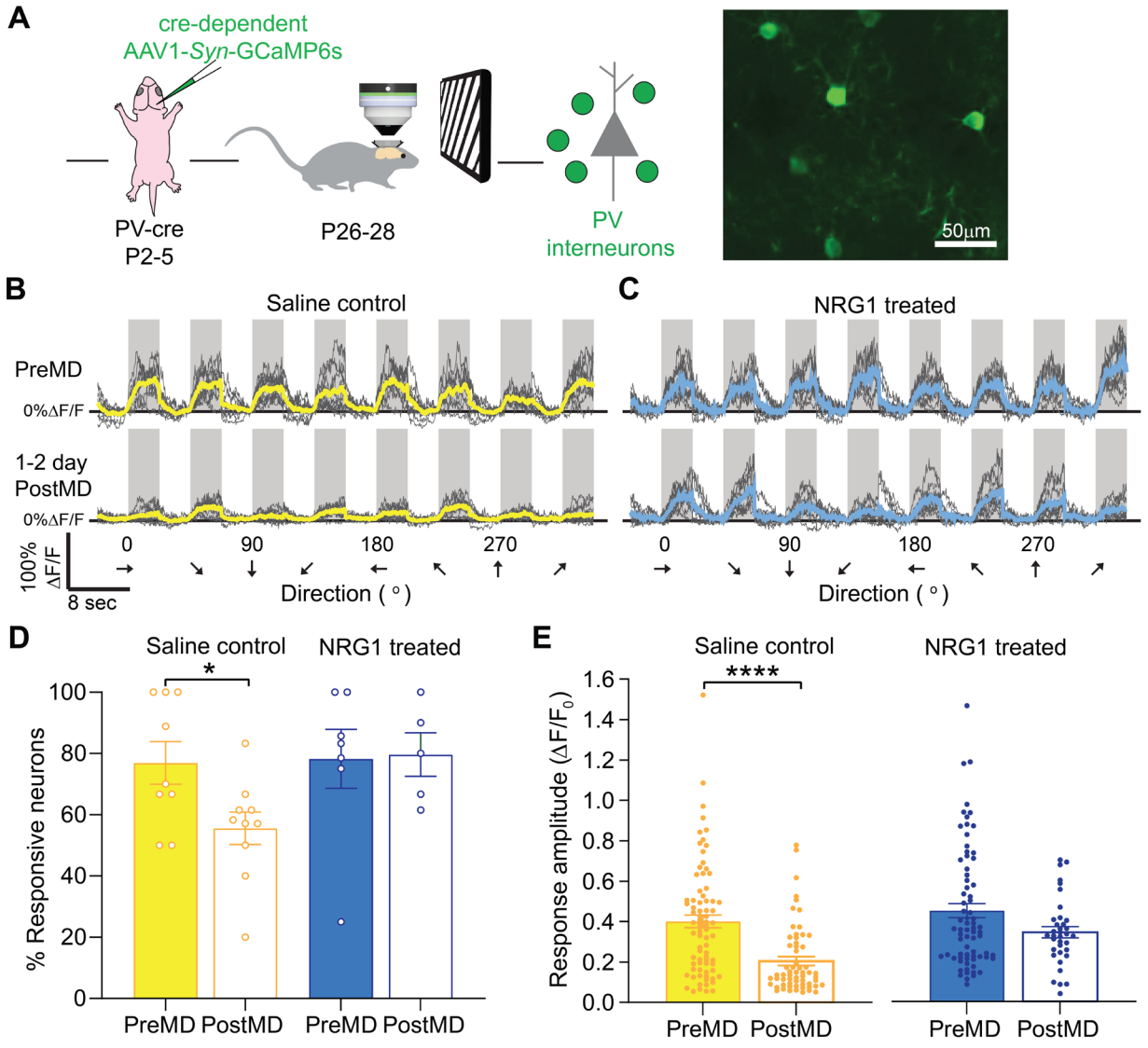

Figure 4.2. Sensitivity of juvenile PV interneurons to brief MD depends on NRG1 signaling
(A) Left, Schematic of experimental design for viral labeling PV interneurons in neonates and Ca^{2+} imaging in critical period animals. Right, *In vivo* image of visually responsive PV interneurons (green). Scale bar = 50 µm.

(B) Visually evoked responses of PV interneurons through the deprived eye before and after MD in saline controls. (C) Visually evoked responses of PV interneurons through the deprived eye before and after MD in neuregulin1 (NRG1) treated mice. (D) 1D MD significantly decreased the percent of responsive PV interneurons (PreMD: n = 9 fields from 3 mice; PostMD: n = 10 fields from 3 mice; *p = 0.036, Mann-Whitney U test). Exogenous NRG1 prevented the reduction in PV cell responsiveness (PreMD: n = 7 fields from 2 mice; PostMD: n = 5 fields from 2 mice; p = 0.909, Mann-Whitney U test). (E) 1D MD also reduced the response amplitude of PV interneurons through the contralateral, deprived eye stimulation (ΔF/F0: PreMD, 0.401 ± 0.031, n = 78 cells from 5 mice; PostMD, 0.205 ± 0.022, n = 61 cells from 3 mice; ****p < 0.0001, Mann-Whitney U test). Exogenous NRG1 blocked the reduction in response amplitude of PV interneurons. (ΔF/F0: PreMD, 0.449 ± 0.035, n = 73 cells from 3 mice; PostMD, 0.342 ± 0.028, n = 36 cells from 2 mice; p = 0.266, Mann-Whitney U test). Data are mean ± SEM.

4.2.2 Sensory deprivation does not alter the responses of transplanted PV interneurons

To test whether transplanted cells were responsive to sensory manipulation, we performed *in vivo* time-lapse two-photon Ca^{2+} imaging to examine the effects of brief monocular deprivation on layer 2/3 transplanted PV cell activity (Figure 4.3). First, we transplanted PV-tdTomato interneurons into the binocular visual cortex of adult mice and confirmed that the transplanted PV interneurons dispersed and expressed mature interneuron markers. We found transplanted PV-tdTomato+ cells in all layers of the visual cortex (Figure 3.1). Immunostaining revealed that more than 80% of these transplanted cells were PV+ (Figures 4.3).

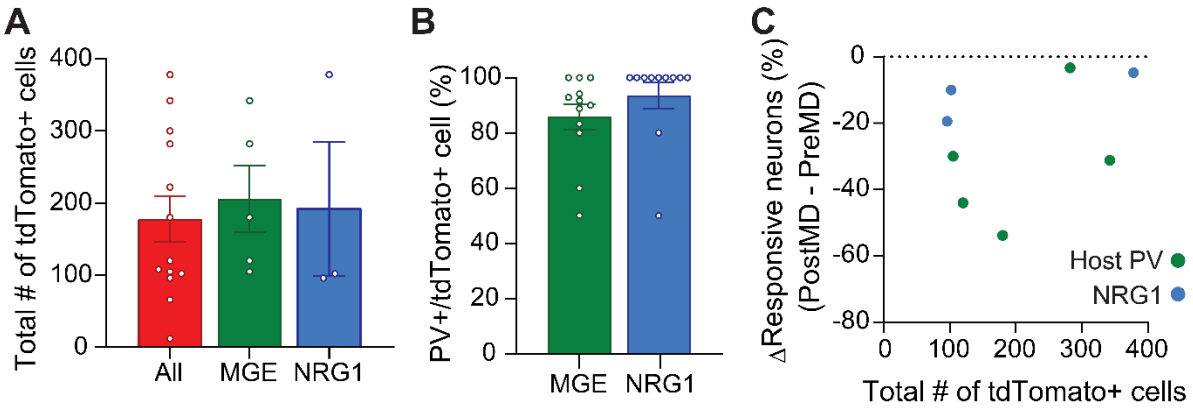

Figure 4.3. Number of transplanted cells is not correlated with the magnitude of reduction in host PV interneuron responsiveness

(A) Estimated number of transplanted PV-tdTomato cells in all MGE transplant recipients (n = 13 mice, red, including "MGE" and "NRG1" groups). MGE includes transplant recipients for which host PV cells were imaged in Ca^{2+} imaging experiments at 35DAT (n = 5 mice). NRG1 includes transplant recipients for which host PV cells were imaged but also treated with exogenous soluble NRG1 (n = 3 mice; see also Figure 3). There was no difference between the estimated total number of transplanted PV-tdTomato cells between MGE and NRG1 treated groups. (B) Quantification of transplanted PV-tdTomato cells coexpress PV. More than 80% of transplanted cells co-expressed PV in both MGE (n = 12 sections from 3 mice) and NRG1 groups (n = 11 sections from 2 mice). (C) No correlation between the total number of transplanted PV-tdTomato cells and the change in responsiveness was observed in MGE or NRG1 treated recipients (R^2 = 0.112)

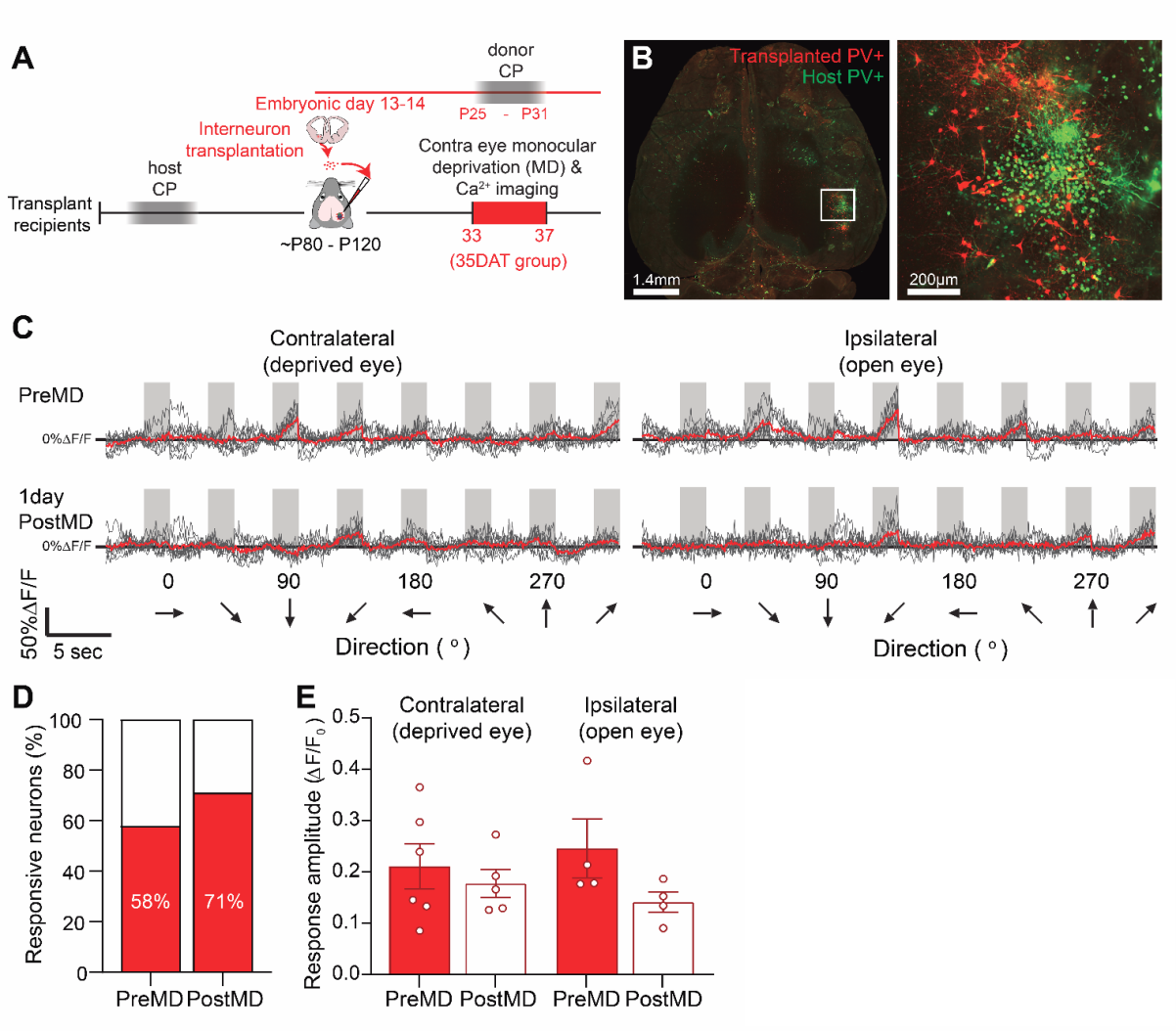

Figure 4.4. Transplanted PV interneurons are not sensitive to MD

(A) Experimental timeline. The calcium imaging of transplanted PV interneurons was performed at either 33-35 days after transplant (35DAT) or 65-70 DAT. (B) Left, whole brain image of transplant recipient cleared using iDISCO+ method, scale bar = 1.4 mm. Right, a magnified view of the outlined region above. Transplanted PV interneurons are in red, AAV1-GCaMP6s labeled PV interneurons are in green, and transplanted interneurons that expressed GCaMP6s are in yellow, scale bar = 200 µm. (C) Visually evoked responses at the peak spatial frequency before and after MD of an example transplanted PV interneuron. (D) Responsiveness of transplanted PV interneurons remained unchanged after 1D MD. Fraction of responsive and non-responsive

neurons before and after MD was not significantly different (PreMD: n = 12 cells from 5 mice; PostMD: n = 7 cells from 3 mice, p = 0.656, Fisher's exact test). (E) Response amplitude of transplanted PV interneurons at 35DAT before and after 1D MD through the contralateral, deprived eye (PreMD: n = 6 cells from 5 mice; PostMD: n = 5 cells from 4 mice) and ipsilateral eye stimulation (PreMD and PostMD: n = 4 cells from 4 mice). The response amplitude of transplanted PV interneurons did not change after 1D MD for either the contralateral or ipsilateral eye.

We labeled the transplanted PV cells with either cre-dependent or synapsin-driven AAV-1 GCaMP6s (Figure 4.4A). The Ca2+ imaging was performed at 33-35 days after transplantation (DAT) when the age of transplanted PV interneurons was equivalent to P26-P28 critical period PV cells. After the first day of imaging, the eye contralateral to the imaged cortex was closed by eyelid suture for 20-24 hours. Whereas MD reduced the responsiveness and response amplitude of PV cell activity in juvenile critical period mice (Figure 4.2), we were surprised to find no change in the overall responsiveness (Figure 4.4D) or the response amplitude of transplanted PV interneurons (Figure 4.4E).

4.2.3 Sensory deprivation reduces the responsiveness of host PV interneurons

Since transplanted cells failed to respond significantly to sensory deprivation, our results are inconsistent with the notion that transplanted cells recapitulate the developmental program for cortical reorganization. Next, we examined whether interneuron transplantation restores sensitivity to visual deprivation in host PV interneuron. To record the visually evoked responses of layer 2/3 host PV interneurons, we transplanted PV-tdTomato positive interneurons into PV-cre adult mice. Then, we labeled the host PV cells with cre-dependent synapsin-driven AAV-1 GCaMP6s (Figure 4.5A). We observed no difference in the baseline responsiveness of PV interneurons between experimental groups before MD (Figure 4.7B). As shown in Chapter 3, the tuning properties of host PV interneurons were also not altered by transplantation (Figure 3.7). We found no significant

difference in median peak spatial frequency (Figure 3.7C) or orientation selectivity index (Figure 3.7F) in PV interneurons between MGE transplant recipients and adult controls before MD.

In contrast to the negligible effect we found in the transplant PV interneurons, the overall responsiveness of host PV interneurons was greatly reduced after one day of MD. We noticed that the decrease in the percentage (35-40%) of responsive PV interneurons (Figure 4.5D; green) and the reduction of response amplitude (30%; Figure 4.5E; green) were significantly greater in 35DAT MGE transplant recipients compared to untreated adult controls (Figures 4.5D and 4.5E; Figures 4.6B and 4.6E, black). Previously, studies have shown that interneurons derived from caudal ganglionic eminence (CGE) do not induce cortical plasticity (Davis et al., 2015; Larimer et al., 2016). Here, we found that MD-induced reduction in host PV interneuron responsiveness in CGE transplant recipients was equivalent to that in untreated adult control (Figures 4.5D and 4.5E; Figure 4.6B, turquoise). These results suggest that the deprivation-induced reduction in host PV cell responsiveness is specific to MGE transplant recipients.

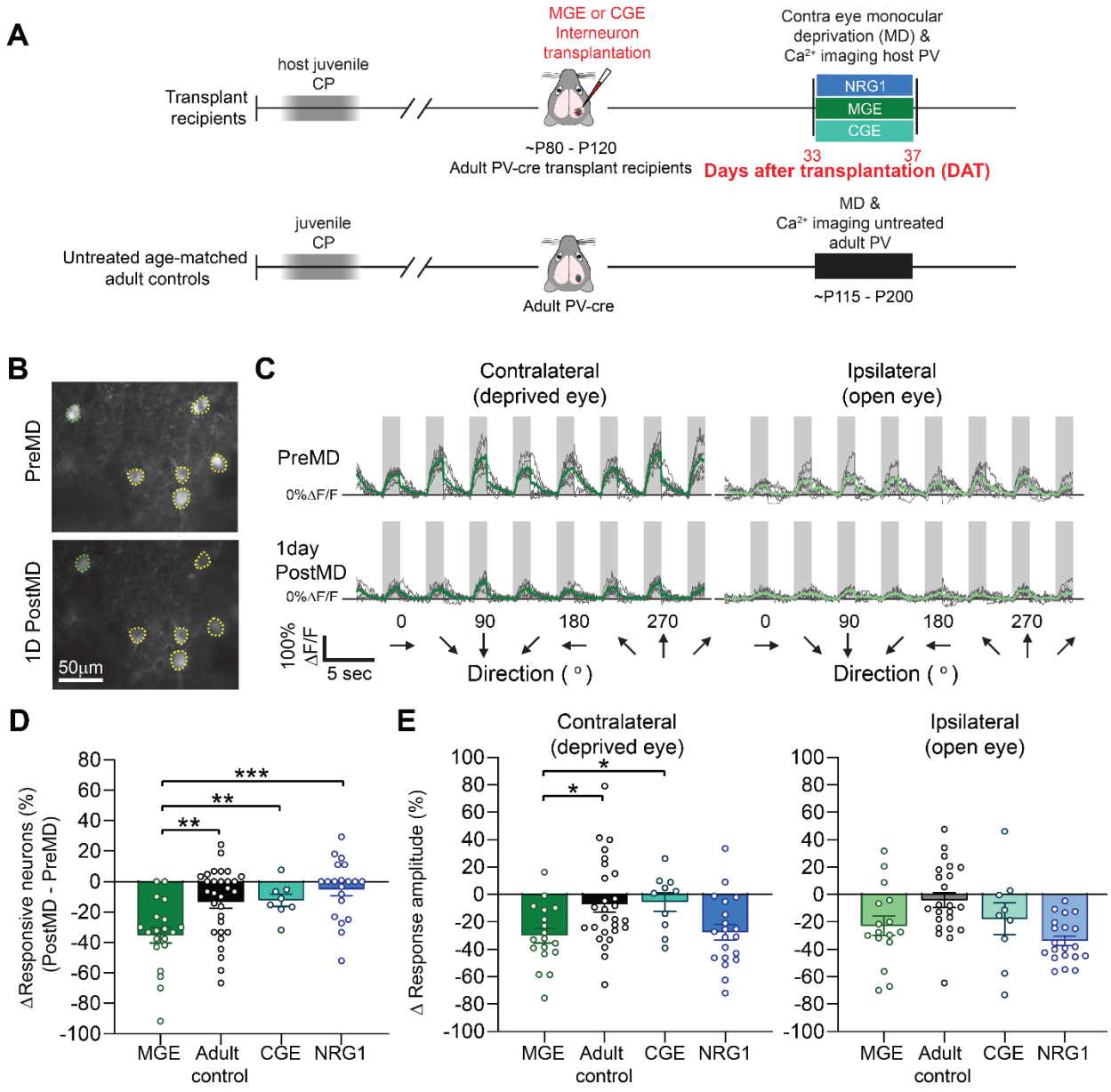

Figure 4.5. Transplant-induced sensitivity of host PV interneurons to brief MD depends upon NRG1 signaling

(A) Experimental timeline. (top) Calcium imaging of host PV interneurons in MGE transplant recipients (green), MGE recipients treated with NRG1 (blue) or CGE transplant recipients (turquoise) were performed at 33-35 days after transplantation. (bottom) Imaging of PV interneurons in untreated adult control mice was performed around postnatal day (P) 115 (black). (B) *In vivo* image of GCaMP6s-labeled host PV interneurons in a MGE transplant recipient before and after 1D MD. Responsive cells are outlined in yellow and green. Scale bar = 50µm. (C) Visually evoked responses at the peak spatial frequency for the cell outlined in green in panel (B). (D) MGE: host PV interneurons from MGE transplant recipients at 35DAT. Adult control: PV interneurons from age-matched adults that receive no transplantation. CGE: host PV interneurons from CGE transplant recipients at 35DAT. NRG1: host PV interneurons from MGE transplant recipients that have been treated with exogenous NRG1 at 35DAT. 1D MD reduced the overall responsiveness of host PV interneurons in 35DAT transplant recipients (MGE: n = 20 fields from 6 mice, green; adult control: n = 30 fields from 8 mice, black; 35DAT CGE: n = 8 fields from 5 mice, turquoise; NRG1: n = 20 fields from 5 mice, blue; 35DAT MGE vs. adult control: **p = 0.0054; 35DAT MGE vs. 35DAT CGE: **p = 0.0051; 35DAT MGE vs. NRG1: ***p = 0.0002, Brown-Forsythe and Welch ANOVA followed by Dunnett's T3 multiple comparisons test). (E) 1D MD resulted in a large reduction in the response amplitude of 35DAT host PV interneurons through both the deprived eye, which is not observed in the adult control or adults received CGE transplant. However, exogenous NRG1 did not prevent the reduction

in the response amplitude of host PV interneurons (Contra: 35DAT MGE vs. adult control, *p = 0.019; 35DAT MGE vs. 35DAT CGE: *p = 0.026; 35DAT MGE vs. NRG1: p = 0.983; Ipsi: 35DAT MGE vs. adult control, p = 0.1697; 35DAT MGE vs. 35DAT CGE: p = 0.9739; 35DAT MGE vs. NRG1: p = 0.4357, Brown-Forsythe and Welch ANOVA followed by Dunnett's T3 multiple comparisons test). Data are mean ± SEM.

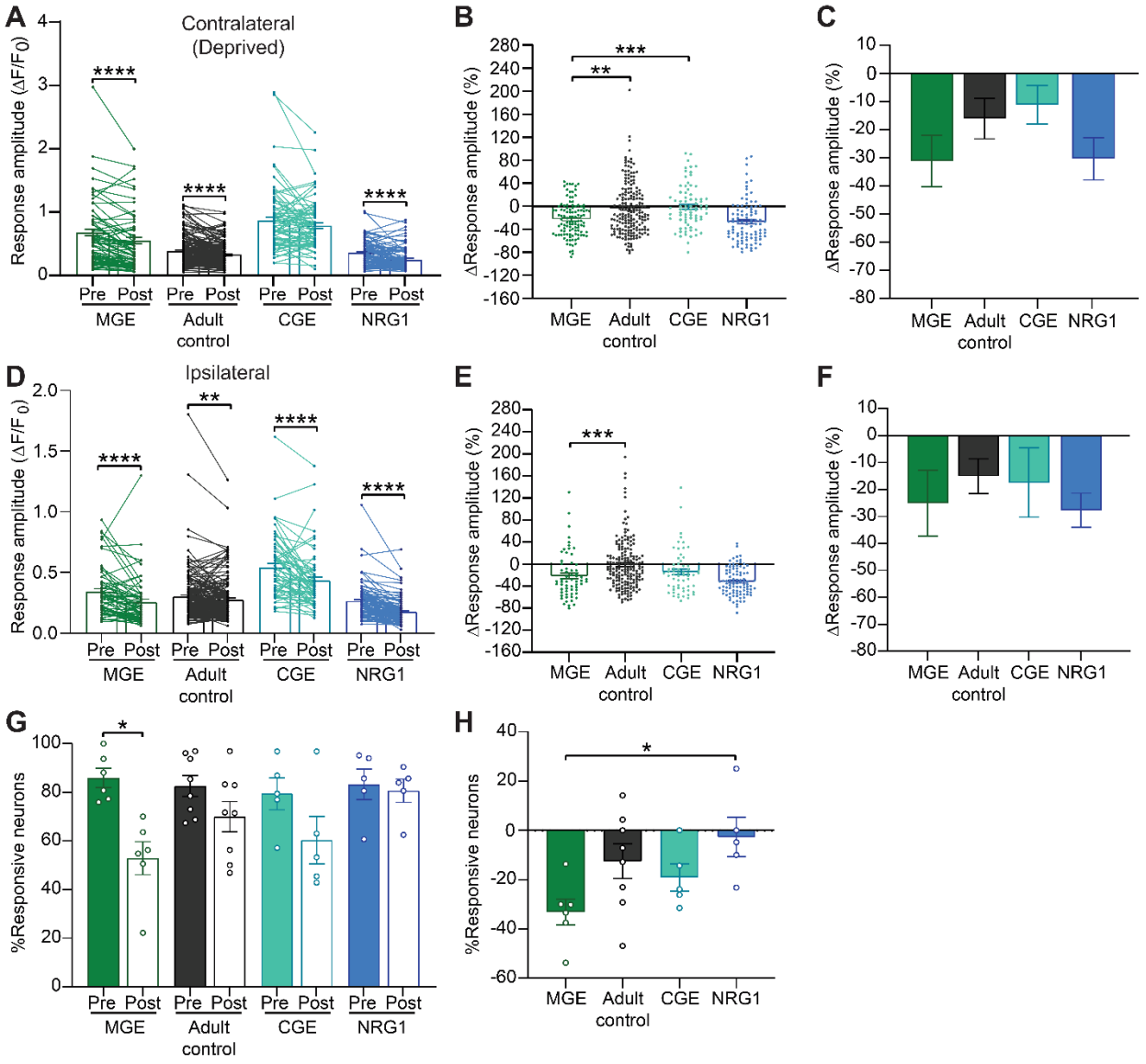

Figure 4.6. Change of responsiveness of host PV interneurons at the single-cell level and at the individual animal level

(A) Visual responses of the same host PV interneurons before and after 1D MD. MD reduced response amplitude of host PV interneurons through the deprived eye in 35DAT MGE transplant recipients, adult control and 35DAT MGE transplant recipients with NRG1 treatment (MGE: n = 111 cells; adult control: n = 189 cells; 35DAT CGE: n = 77 cells; NRG1: n = 94 cells; ****p<0.0001, Wilcoxon matched-pairs test). (B) The reduction in response amplitude was significantly greater in 35DAT MGE transplant recipients compared to adult control and CGE transplant recipients (**p = 0.0068, ***p=0.0006, Kruskal-Wallis one-way ANOVA test with Dunn's multiple comparison test). (C) The trend remained when plotted by animal, although the difference was not statistically significant. (D) Visual responses of host PV interneurons through the ipsilateral, open eye after 1D MD (MGE: n = 62 cells; adult control: n = 180 cells; 35DAT CGE: n = 61 cells; NRG1: n = 96 cells; **p = 0.005, ****p < 0.0001,

Wilcoxon matched-pairs test). (E) The reduction in response amplitude was again significantly greater in 35DAT MGE transplant recipients when compared to that in the adult control. There was no difference the reduction of PV cells between 35DAT MGE transplant recipients, CGE recipients or NRG1 treated recipients (***p = 0.0004, Kruskal-Wallis one-way ANOVA test with Dunn's multiple comparison test). (F) The trend persisted when plotted by animal. (G) Percent responsive PV cells before and after MD in each animal. The percent of responsive PV cells was significantly lower in the 35DAT MGE transplant recipients after MD (MGE: n = 6 mice; adult control: n = 8 mice; CGE: n = 5 mice; NRG1: n = 5 mice; *p = 0.031, Wilcoxon matched-pairs test). (H) NRG1 treatment prevented the MD-induced reduction in the percent of responsive neurons in 35DAT transplant recipients (*p = 0.016, Kruskal-Wallis one-way ANOVA test with Dunn's multiple comparison test).

4.2.4 Exogenous NRG1 blocks the reduction in binocular PV interneuron responses

The expression of NRG1 in PV interneurons is developmentally regulated (Grieco et al., 2020; Sun et al., 2016). Its expression in the visual cortex peaks during the critical period in development but decreases significantly in the adult cortex. The high expression of NRG1 within PV interneurons during the critical period allows these cells to regulate experience-dependent plasticity. We demonstrated previously that exogenous NRG1 prevents the reduction in PV interneuron responses which subsequently blocks cortical plasticity (Figures 4.2D and 4.2E; Sun et al., 2016). To determine if the reduction in host PV interneuron responses also depends on NRG1, we treated a second group of MGE transplant recipients with soluble NRG1 during one day of MD (0.5 μg per animal every 8 hour, s.c.). While exogenous NRG1 did not prevent the reduction in the response amplitude of host PV interneurons after MD (Figures 4.5E and 4.5F; Figures 4.6B and 4.6E, blue), we found that it blocked the drop in the percentage of responsive PV interneurons (Figure 4.5D; Figures 4.6G and 4.6H, blue). Post-hoc immunostaining shows that there was no difference in the overall number of transplanted TdTomato+ cells between the two experimental groups (Figure 4.3A), and more than 80% of TdTomato+ cells that were positive for PV in both transplant recipients with NRG1 and without NRG1 (Figure 4.3B). Furthermore, the overall number of transplanted interneurons was not correlated with the percent change in responsiveness

(Figure 4.3C). Taken together, our results suggest that interneuron transplantation reactivates a developmental program within adult host PV interneurons that re-sensitizes them to visual deprivation.

To further examine how NRG1 affects the host PV interneuron responses, we again performed Ca^{2+} imaging to measure visually evoked responses of PV interneurons after one day of MD in transplant recipients treated with NRG1. Time-lapse recording enabled us to track the same host PV interneurons before and after MD and measure deprivation-induced ocular dominance plasticity at the single-cell level. Before deprivation, a large fraction of host PV interneurons were visually responsive (80-83%; Figure 4.7B), and a little more than 40% of all cells recorded had binocular responses (Figure 4.7D). We did not observe any difference in the percentage of responsive cells (Figure 4.7B) or binocular responses between all experimental groups (Figure 4.7D). Like the excitatory neurons in normal adult mice (Salinas et al., 2017), there were also PV interneurons that responded only to the contralateral or ipsilateral inputs (Figures 4.7A, 4.7C and 4.7D).

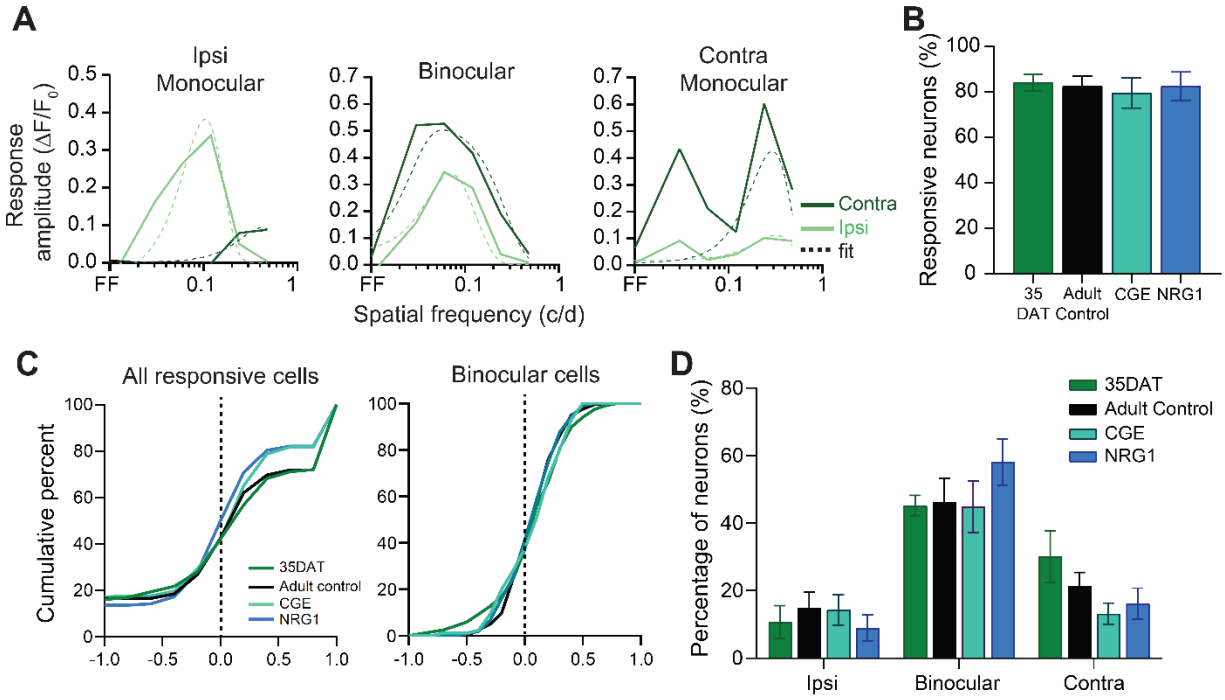

Figure 4.7. Interneuron transplantation does not alter the responsiveness of host interneurons.

(A) Different types of spatial frequency responses for host PV interneurons. (B) There was no difference in the % responsive host PV interneurons between MGE transplant recipients (35DAT and NRG1), age-matched adult controls (Adult Control) and CGE transplant recipients before MD. (C) Left, The ocular dominance index distributions for all responsive cells were similar between all four experimental groups; Right, the distributions for only binocular cells were also very similar across all four groups. (D) Percentage of responsive host PV interneurons grouped by response types. There was no difference between any of the experimental groups across different response types.

We determined whether MD differentially affected these groups of host PV interneurons and how exogenous NRG1 counteracted the effect of MD. We found that MD-induced reduction of responsiveness was most pronounced in binocular PV interneurons (Figures 4.8A and 4.8E), which was prevented in transplant recipients treated with soluble NRG1 (Figures 4.8D and 4.8H). With NRG1 treatment, not only did a higher percentage of binocular cells remain binocular, but many previously monocular and unresponsive cells also became binocular (Figure 4.8K). Consequently, the overall percent of responsive binocular PV interneurons remained stable after MD in transplant recipients treated with NRG1. Although many PV interneurons in the untreated adults (Figure 4.8B) and CGE transplant recipients (Figure 4.8C) also exhibited ocular dominance plasticity at the single-cell level, there was no selective reduction in the responsiveness of binocular cells (Figures 4.8F and 4.8G). In fact, there is no change in ODI after 1 day MD across all four experimental groups when analyzed by animals (Figure 4.8I).

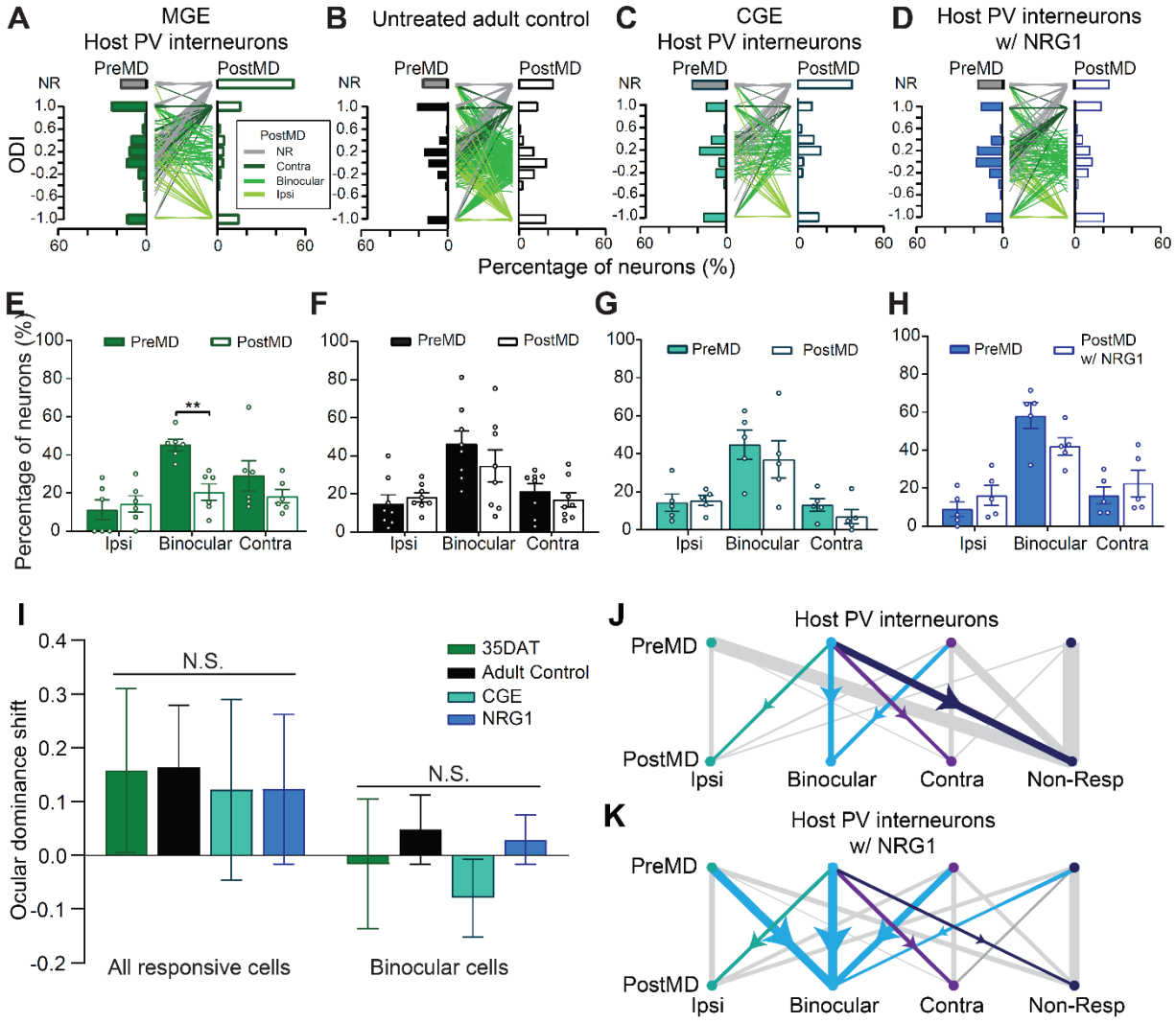

Figure 4.8. NRG1 prevents the selective reduction of binocular responses in host PV interneurons

(A-D) Single-cell ODI distribution of PV interneurons before and after MD in (A) 35DAT MGE transplant recipients (n = 260 cells from 6 mice), (B) adult age-matched adult controls (n = 435 cells from 8 mice), (C) CGE transplant recipients (n = 150 cells from 5 mice), and (D) MGE transplant recipients with NRG1 treatment (n = 202 cells from 5 mice) The colors of the lines are determined by the cell's PostMD ODI. Non-responsive cells (NR): gray; contralateral only cells: dark green; binocular cells: medium green; ipsilateral cells: light green. (E-H) Same data as (A-D) but plotted by animal. (E) 1D MD selectively reduced the percentage of responsive binocular PV interneurons in MGE transplant recipients (n = 6 mice, green, **p = 0.0018, Two-way ANOVA followed by Bonferroni's multiple comparison test). No significant reduction in the percentage of responsive binocular PV interneurons in (F) age-matched adult control (n = 8 mice, Two-way ANOVA followed Bonferroni's multiple comparison test) or (G) CGE transplant recipients (n = 5 mice; Two-way ANOVA followed by Bonferroni's multiple comparison test). (H) NRG1 treatment prevented the reduction in responsiveness of binocular PV interneurons after MD (n = 5 mice. Two-way ANOVA followed by Bonferroni's multiple comparison test). (I) There was no significant difference in OD shift of all responsive cells or binocular cells between all four experimental groups. (All cells: MGE, n = 6 mice; Adult Control, n = 8 mice; CGE, n = 5 mice; NRG1, n = 5 mice; p = 0.98; Binocular cells, p = 0.742, Kruskal-Wallis ANOVA test). (J) Distribution of host PV interneurons across different cell responses before and after MD in 35DAT MGE transplant recipients. The

thickness of the lines indicates the proportion of neurons within that specific response group. For example, the thickness of the lines connecting PreMD Ipsi to PostMD Non-Resp indicates that majority of the ipsilateral cells became non-responsive after MD. Binocular cells are color-coded by their Post-MD responses. (K) Changes in the distribution of host PV interneurons across different cell responses in 35DAT MGE transplant recipients that received NRG1 treatment during MD. Not only more binocular cells remained binocular after MD, but previously ipsilateral and contralateral cells also became binocular. Data in (E), (F), (G), (H) and (I) are mean ± SEM.

4.2.5 Interneuron transplantation accelerates reorganization of binocular excitatory neuron responses

During development, MD-induced reduction in the visual responses of PV interneurons results in an enhancement of visual activity in excitatory cells (Figure 4.10B and 4.10C; Kuhlman et al., 2013; Sun et al., 2016). To test whether reduction in host PV inhibition resulted in a similar increase in excitatory neuron response amplitude, we transplanted PV-tdTomato interneuron progenitors from MGE into wildtype C57BL adult mice, and then labeled the host cells using non-cre dependent synapsin-driven AAV-1 GCaMP6s (Figure 4.9A). When plotted by cell, MD seemed to produce a significant reduction in the response amplitude of host excitatory neurons at 35DAT (Figure 4.9C). However, the extent of the reduction was small, and it disappeared when plotted by animal (Figure 4.9D). When we analyzed all cells and determined whether MD altered the overall responsiveness of excitatory neurons, we were surprised to find that one day of MD produced a selective reduction in the percentage of binocular excitatory neurons (Figure 4.9E), which was not apparent in the juvenile critical period animals (Figure 4.10D) or adult control mice (Figure 4.9H). During the critical period, the reorganization of binocular responses usually occurs after a longer period of MD. The fact that the transplant recipients exhibited cortical

reorganization after one day of MD suggests that interneuron transplantation accelerates cortical plasticity.

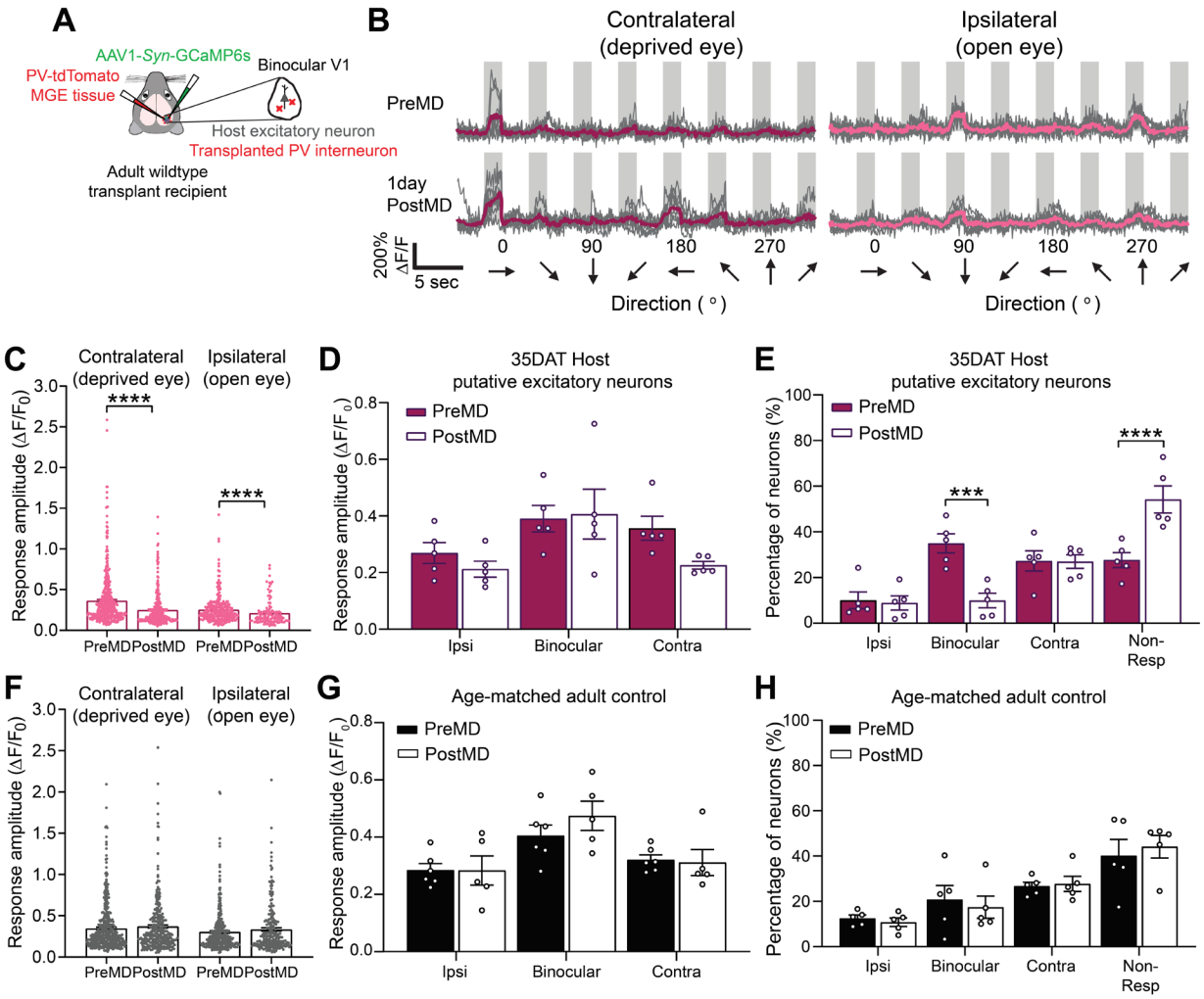

Figure 4.9. Interneuron transplantation selectively reorganizes binocular responses in host cortex
(A) Schematic of experimental design for transplantation and viral labeling host excitatory neurons. (B) Visually evoked responses before and after MD of example host excitatory neurons at 35DAT. (C) At the single-cell level, MD significantly reduced the response amplitude of host excitatory neurons through both the deprived and open eye. (D) When plotted by animal, there was no significant change in the response amplitude after MD across all three cell types (n = 5 mice; two-way ANOVA with Bonferroni's multiple comparison test). Ipsi includes neurons that only have significant ipsilateral eye responses, contra includes neurons that only have significant contralateral eye responses. Binocular includes neurons that have both ipsilateral and contralateral responses, but only the dominant eye response amplitude is plotted here. (E) However, percentage of binocular host excitatory neurons was reduced after 1D MD (n = 5 mice. ***p = 0.0002; ****p < 0.0001, two-way ANOVA with Bonferroni's multiple comparison test). (F) In contrast, MD did not change the response amplitude of adult control excitatory neurons. (G) No change in the response amplitude of excitatory neurons was observed at the animal level either (PreMD: n = 6 mice; PostMD: n = 5 mice; two-way ANOVA with Bonferroni's multiple comparison test). (H) The percentage of responsive cells also remained unchanged after 1D MD in age-matched control mice (Two-way ANOVA with Bonferroni's multiple comparison test).

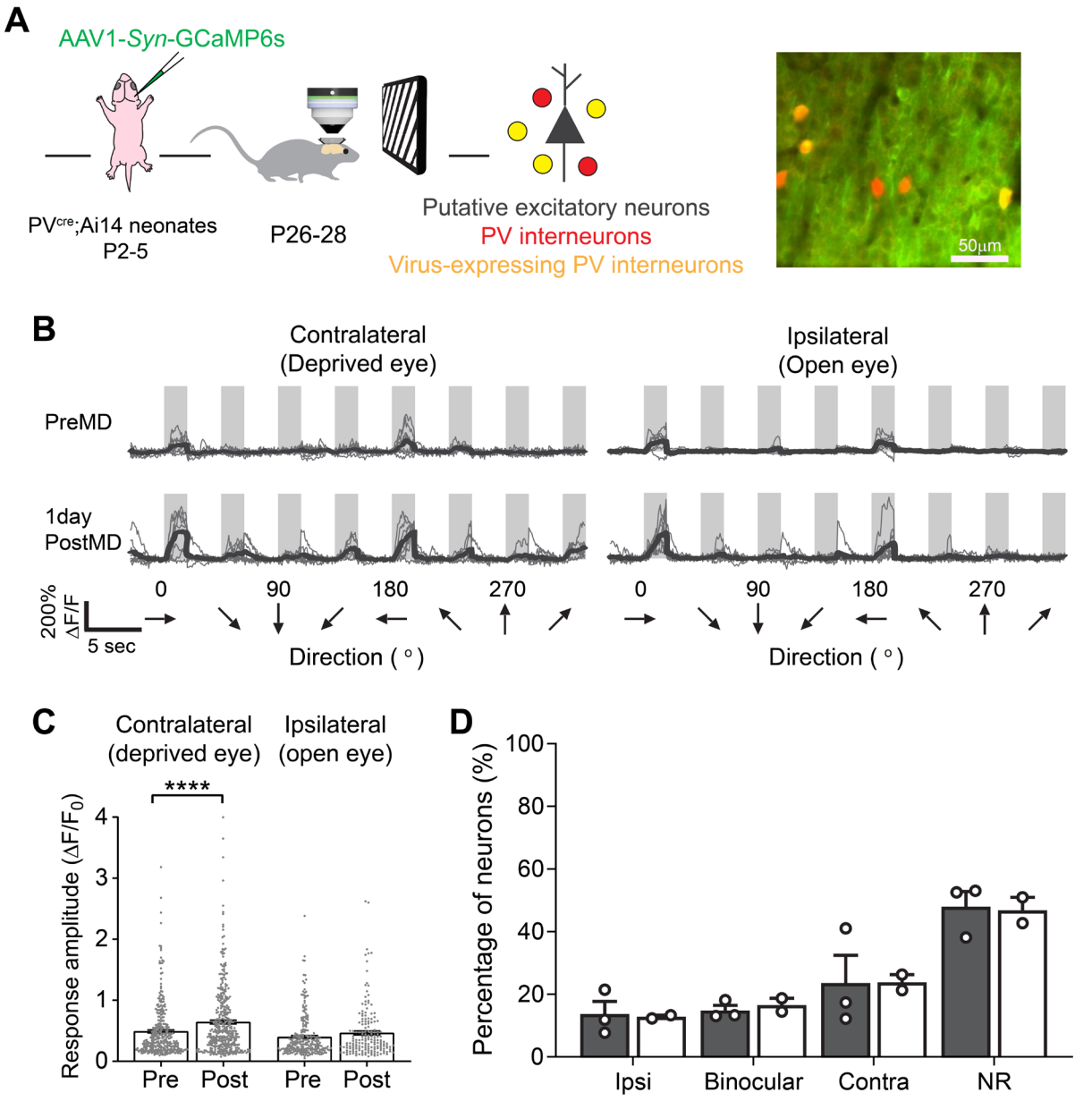

Figure 4.10. Excitatory neurons increase in responses after MD during developmental critical period
(A) Schematic of experimental design for viral labeling excitatory neurons in neonates and Ca^{2+} imaging in critical period animals. (B) Example traces of evoked visual responses before (top) and after (bottom) 1D MD for contralateral (left) and ipsilateral (right) eye stimulation. (C) During juvenile critical period, the response amplitude of excitatory neurons was significantly increased through the contralateral, deprived eye stimulation. (Contralateral: PreMD, n = 333 cells from 4 mice; PostMD, n = 373 cells from 3 mice; Ipsilateral: PreMD, n = 247 cells from 3 mice; PostMD, n = 173 cells from 2 mice. Contra: ****$p < 0.0001$; Ipsi: $p = 0.109$, Mann-Whitney U test). (D) However, unlike in the transplant recipients, there was no change in the percentage of responsive binocular neurons after 1D MD in critical period mice (Two-way ANOVA with Bonferroni's multiple comparisons test). Data are mean ± SEM.

4.2.6 NRG1/ErbB4 signaling within host PV interneurons is necessary for transplant-induced ODP

Finally, we asked if NRG1-mediated reduction in host PV interneuron responsiveness is necessary for transplantation-induced cortical reorganization. Like in the juvenile critical period, we found that transplant-induced ocular dominance shift measured using intrinsic signal optical imaging was prevented in transplant recipients treated with exogenous NRG1 (Figure 4.11). In transplant recipients receiving saline injections, four days of MD produced a significant reduction in the cortical responses through the deprived eye, and thus resulted in a significant shift in ocular dominance index (Figure 4.11C). In contrast, in transplant recipients treated with soluble NRG1, the reorganization of cortical responses was blocked (Figure 4.11C). Considering that exogenous NRG1 also blocked the reduction in the overall responsiveness of host PV interneurons (Figure 4.5), this result suggests that NRG1-mediated reduction of host PV cell responsiveness was necessary for cortical reorganization in transplant recipients.

To directly test the possibility that NRG1-dependent plasticity operated through the ErbB4 receptors on the host PV interneurons, we transplanted embryonic MGE tissue into adult recipients in which the ErbB4 receptors were genetically ablated in the host PV interneurons selectively (PV-cre;ErbB4$^{flx/flx}$). We found that interneuron transplantation failed to reactivate cortical plasticity in these mutant mice (Figures 4.11D and 4.11E), which further supports that the NRG1/ErbB4 signaling in the host PV interneurons is necessary for transplant-mediated cortical plasticity. Consistent with previous studies, the number of transplanted cells in each group could not account for the differences observed in ocular dominance plasticity across these three groups (Figure 4.12D). We also did not observe a

correlation between the extent of plasticity and the number of transplanted cells (Figure 4.12E).

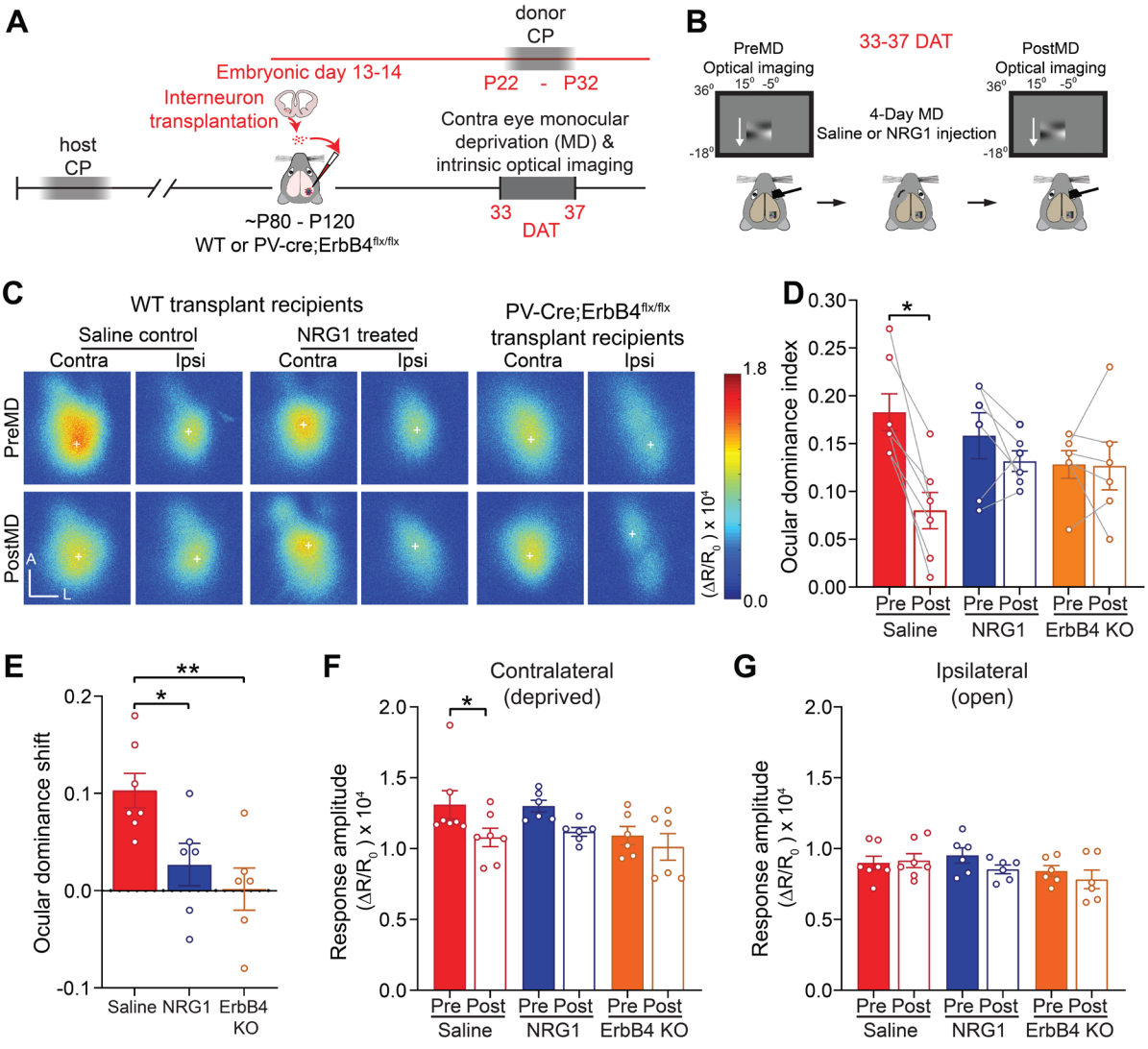

Figure 4.11. Transplant-induced ODP depends on NRG1/ErbB4 signaling
(A) Experimental timeline. (B) Intrinsic optical imaging was performed to measure ocular dominance plasticity (ODP) in adult transplant recipients around 33-35 days after transplantation (DAT). The wildtype adult recipients received either saline or soluble neuregulin1 (NRG1) during four days of monocular deprivation (MD). (C) Examples of response amplitude before and after 4D MD. Scale bar = 500 µm. (D) Four-day MD resulted in a shift of ocular dominance index (ODI) in transplant recipients that received saline injections. Injections of soluble NRG1 diminished transplant-induced ODI shift. Interneuron transplantation also failed to reactivate ODP in PV-cre;ErbB4$^{flx/flx}$ adult recipients. ODI is calculated as (Contra response amplitude – Ipsi response amplitude) / (Contra response amplitude + Ipsi response amplitude) (Saline n = 7 mice, red; NRG1 n = 6 mice, blue. PV-cre;ErbB4$^{flx/flx}$ n = 6 mice, orange. Saline: *p = 0.0156, NRG1: p = 0.344, PV-cre;ErbB4$^{flx/flx}$: p = 0.844, Wilcoxon matched-pairs signed rank test). (E) Ocular dominance shift is calculated as (PreMD ODI – PostMD ODI). Ocular dominance shift was significantly reduced in the transplant recipients treated with NRG1 and in PV-cre;ErbB4$^{flx/flx}$ adult recipients (Saline vs. NRG1: *p = 0.033, Saline vs. PV-cre;ErbB4$^{flx/flx}$: **p = 0.005, one-way ANOVA followed by Bonferroni's multiple comparison test). Data are mean ± SEM. (F) Contralateral

(deprived) input was significantly reduced after MD in Saline control (n = 7 mice, *p = 0.016, Wilcoxon matched-pairs signed rank test). No contralateral input change observed in NRG1 treated transplant recipients (n = 6 mice, p = 0.063, Wilcoxon matched-pairs signed rank test) or PV-cre;ErbB4$^{flx/flx}$ recipients (n = 6 mice, p = 0.344, Wilcoxon matched-pairs signed rank test). (G) No ipsilateral input change observed in Saline control (p = 0.469, Wilcoxon matched-pairs signed rank test), NRG1 treated transplant recipients (p = 0.125, Wilcoxon matched-pairs signed rank test), or PV-cre;ErbB4$^{flx/flx}$ recipients (p = 0.313, Wilcoxon matched-pairs signed rank test). In (D)–(G), the error bar represents the SEM.

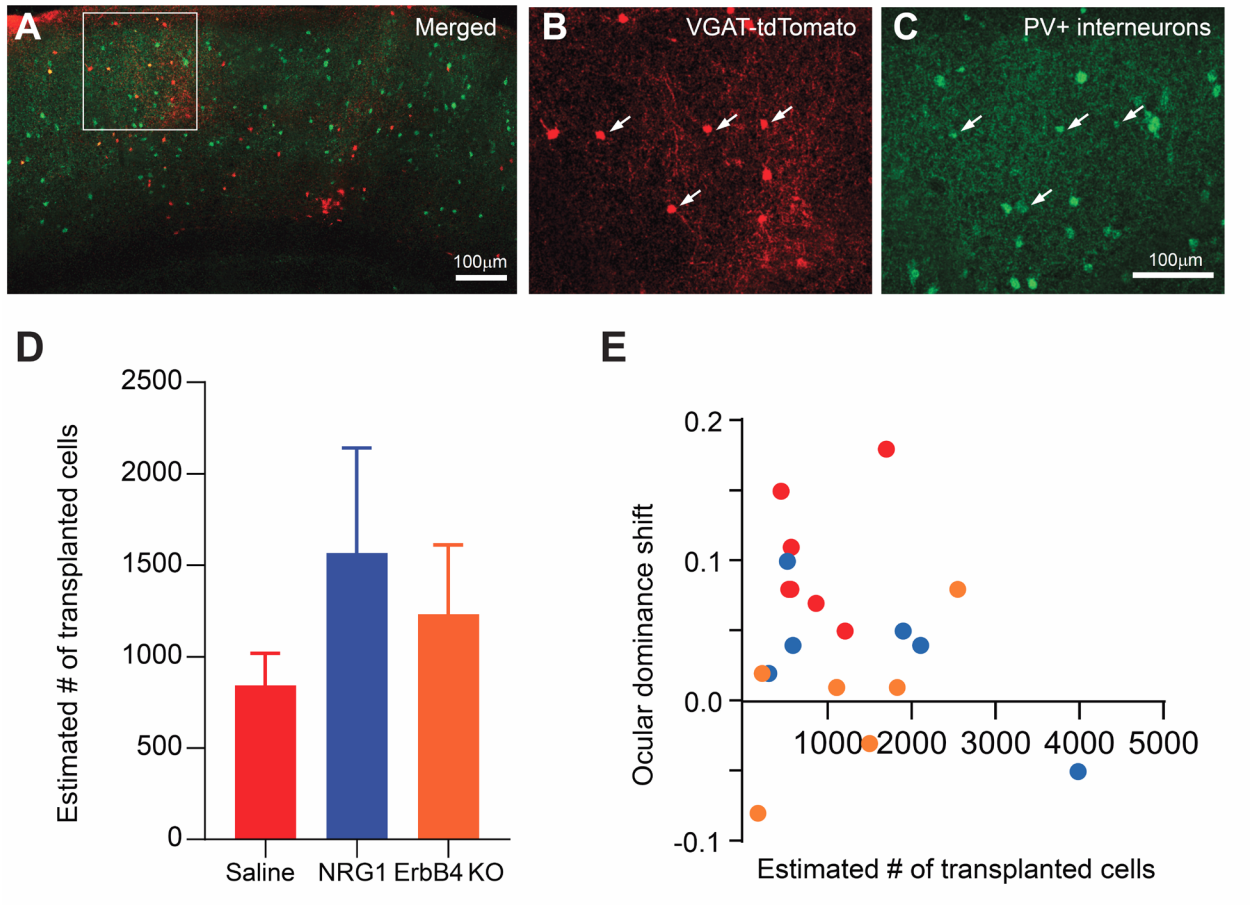

Figure 4.12. The extent of ODP is not correlated with the number of transplanted cells
(A) An example coronal section from an adult mouse that received VGAT-tdTomato MGE transplantation. Transplanted VGAT+ cells (red) dispersed throughout all layers, and a subset of the transplanted cells expressed marker for mature PV interneurons (green). (B-C) Magnified images of the region outlined in (A). (D) Quantification of VGAT-tdTomato-positive transplanted cells (Saline: n = 7 mice; NRG1: n = 6 mice; PV-cre;ErbB4$^{flx/flx}$: n = 6 mice. p = 0.690, Kruskal-Wallis one-way ANOVA). The error bar represents the SEM. (E) Estimated number of transplanted cells plotted against ocular dominance shifts for recipients injected with saline (red) or NRG1 (blue), and PV-cre;ErbB4$^{flx/flx}$ recipients (orange). There was no correlation between the number of transplanted cells and ocular dominance shift (R^2 = 0.234).

4.3 Discussion

Using *in vivo* time-lapse Ca^{2+} imaging, our study obtained the first functional data on the effect of interneuron transplantation on the cortical responses of host neurons at single-cell resolution. We demonstrate that MGE interneuron transplantation reinstates a NRG1/ErbB4-dependent reduction of host PV interneurons upon sensory deprivation. First, we show that brief MD results in a rapid reduction in the visual activity of host PV interneurons, to a similar degree as observed in during the developmental critical period (Figures 4.2 and 4.5). Second, the reduction in host PV interneuron responsiveness is blocked by exogenous NRG1 (Figures 4.5, 4.6 and 4.8). Third, exogenous NRG1 also blocks cortical reorganization that depends on the function of ErbB4 receptors on host PV interneurons (Figure 4.11). Taken together, these results suggest that transplanted cells modify host interneurons to create a new critical period for synaptic plasticity.

Our results are surprising because they counter the prevailing idea that transplanted interneurons play a direct role in gating the plasticity of the host circuitry. Even though the transplanted PV interneurons show normal receptive field properties and proper synaptic integration in our study, visual deprivation has little effect on the activity of transplanted PV interneurons. A recent study, in which MGE cells from VGAT-mutant embryos fails to induce plasticity in the host visual cortex, appears to support our initial hypothesis that transplanted PV cell activity regulates the induction of plasticity (Priya et al., 2019). Since the transplanted $VGAT^{-/-}$ interneurons in that study did not fully mature, reflected in their abnormally developed axonal and dendritic processes, release of the necessary factors for the rejuvenation of NRG1/ErbB4 signaling in the host PV interneurons may have been prevented. In support of our conclusion, another recent transplantation study shows that

suppressing the activity of transplanted interneurons after MD does not prevent the expression of transplant-induced OD plasticity (Hoseini et al., 2019). Together these two pieces of information strongly support our idea that host and not transplanted PV cells mediate the reactivated plasticity.

Our study provides the first mechanistic insight into transplant-induced cortical reorganization. We highlight the role of NRG1/ErbB4 signaling within a specific cell type – host PV interneurons – in mediating the cortical reorganization.

The mechanisms for NRG1, however, may be different between the normal critical period and transplant-induced critical period. During the developmental critical period, exogenous NRG1 prevents the reduction in both the percentage of responsive PV interneurons and PV cell activity after one day of MD and subsequently blocks cortical plasticity (Gu et al., 2016; Sun et al., 2016). In transplant recipients, NRG1 prevents the reduction in the percentage of responsive host PV interneurons but not their response amplitude. The downstream signaling of NRG1 remains unclear. Our evidence indicates that NRG1 activates the ErbB4 receptors on the host PV interneurons, but this needs to be further examined since other cell types, including transplanted cells, may also express ErbB4 receptors (Batista-Brito et al., 2017). Future studies can also probe what upstream signals are responsible for reinstating NRG1/ErbB4 signaling in host PV interneurons. It is not how interneuron transplantation alters the expression of NRG1 and ErbB4 receptors in the adult host neurons.

In summary, our findings suggest that interneuron transplantation reactivates cortical plasticity by rejuvenating the plasticity program within the host PV interneuron circuit. The mechanism that we describe here resembles parabiosis, in which factors

released by young blood cells are thought to restore function to older host blood, muscle and neural stem cells (Conboy et al., 2005; Conese et al., 2017; Ruckh et al. 2012). In this young-to-old neural transplant paradigm, perhaps the transplanted young inhibitory cells create a second critical period by introducing rejuvenating factors into the adult host brain. Host PV interneurons may then receive these factors and become re-sensitized to sensory experience. The identification and isolation of these factors would enable development of non-invasive therapeutics for treating neurological diseases.

CHAPTER 5: CONCLUSION AND GENERAL DISCUSSION

5.1 Overview of Findings

To the best of our knowledge, our study is the first attempt to identify cell type-specific molecular mechanisms underlying interneuron transplant-induced cortical plasticity. Our findings indicate that interneuron transplant-induced cortical plasticity is mediated by the *host* PV interneurons. We first confirm that transplanted interneurons disperse, mature, and integrate into the host circuit. By 33 – 35 days after transplantation, the tuning properties of transplanted PV interneurons are comparable to those during normal critical period. However, integration of these cells does not alter the visual tuning properties of the host PV interneurons. More importantly, brief visual deprivation has very little effect on the responsiveness of the transplanted PV interneurons. What we find, instead, is that in transplant recipients, one day monocular deprivation (MD) reduces the responsiveness of the host cells. The deprivation mainly affects the binocular responses of the host PV interneurons, whereas the ipsilateral and contralateral-only responses remain intact.

A recent transplantation study done in young mouse pups, however, partially supports our results. The study reports that silencing the transplanted interneurons does not prevent the MD-induced ocular dominance plasticity in transplant recipients (Hoseini et al., 2019). Optogenetic inactivation of transplanted interneurons is performed after four days of MD, while our study looks at the initial effect of MD on the transplanted PV cells. It would be interesting for future studies to examine the effect of silencing the transplanted interneurons before MD.

Another important finding of our study is that the heightened sensitivity to visual manipulation in the host PV interneurons depends on a developmental molecular pathway – NRG1/ErbB4 signaling. We definitively demonstrate with a genetic (ErbB4KO) and a pharmacological approach (NRG1 treatment) that blocking the NRG1/ErbB4 pathway in host PV interneurons prevents transplant-induced plasticity. Our findings significantly advance our understanding of the cellular and molecular mechanisms of interneuron transplantation and shift focus to the host PV interneurons.

In the following sections, we will address the limitations of our study and the remaining questions for future studies. First, the experiments in our study heavily depend on Ca^{2+} imaging. While this approach has its advantages, it does not provide a complete picture of the transplant circuitry. Second, by narrowing our focus to PV interneurons, we are able to investigate cell-type specific mechanism on cortical plasticity. The limitation is that this simplification may not capture the complexity of the interneuron circuitry. Lastly, we use OD plasticity as a proxy for cortical rejuvenation. However, interneuron transplantation may reprogram the host brain at the gene level in ways that extend beyond OD plasticity.

5.2 Circuit Mechanisms for Transplant-induced Cortical Plasticity

The differentiation and maturation of transplanted interneurons have been extensively studied in the interneuron transplantation field (Chohan and Moore, 2016; Spatazza et al., 2017; Southwell et al., 2014). While physiological and immunohistochemical characterization of the transplanted interneurons are important and valuable, they shed

very little light on the mechanisms of cortical plasticity. Our study is the first to provide a cellular-resolution, time-lapse view of the reorganization of cortical circuits after transplantation. Using time-lapse Ca^{2+} imaging, we show that the host interneurons, and not transplanted cells, become re-sensitized to changes in sensory experience after transplantation.

One major limitation of our study is the low yield of transplanted interneurons using Ca^{2+} imaging. It is possible that the reason we do not observe any change in transplant interneuron responses after MD is because of the low sample size. For our current study, we used viral approach to deliver GCaMP6 into transplanted PV interneurons, which constitutes about 20-40% of MGE cells. In the future, we can harvest cells from transgenic embryos where all PV cells are labeled with GCaMP6. This transgenic line became available at the Allen Institute after my project was well under its way. Another approach we can take is to harvest PV interneurons from PV-cre;DREADDs mouse embryos (JAX, stock # 026219; Zhu et al., 2019; Upadhya et al., 2019), in which all the PV interneurons will express DREADDs. We can directly manipulate PV interneuron activity and examines its role in OD plasticity in the transplant recipients.

Furthermore, while *in vivo* Ca^{2+} imaging technique has many advantages, it cannot easily tell us how the synaptic connectivity between cells are affected by visual deprivation and how these changes contribute to the resulting plasticity. One important remaining question is what causes the reduction in the host PV interneuron responsiveness after MD (Figure 5.2). During the normal critical period, MD-induced reduction in layer 2/3 PV interneuron responses is due to a reduction of excitatory inputs from layer 4 and layer 5

pyramidal cells (Figure 5.1; Kuhlman et al., 2013). In future studies, we can perform *in vitro* circuit mapping experiments in addition to Ca^{2+} imaging to test whether there is a reduction in the excitatory inputs to the host PV interneurons. However, to answer this question, we must understand how the host circuit is altered by the interneuron transplantation.

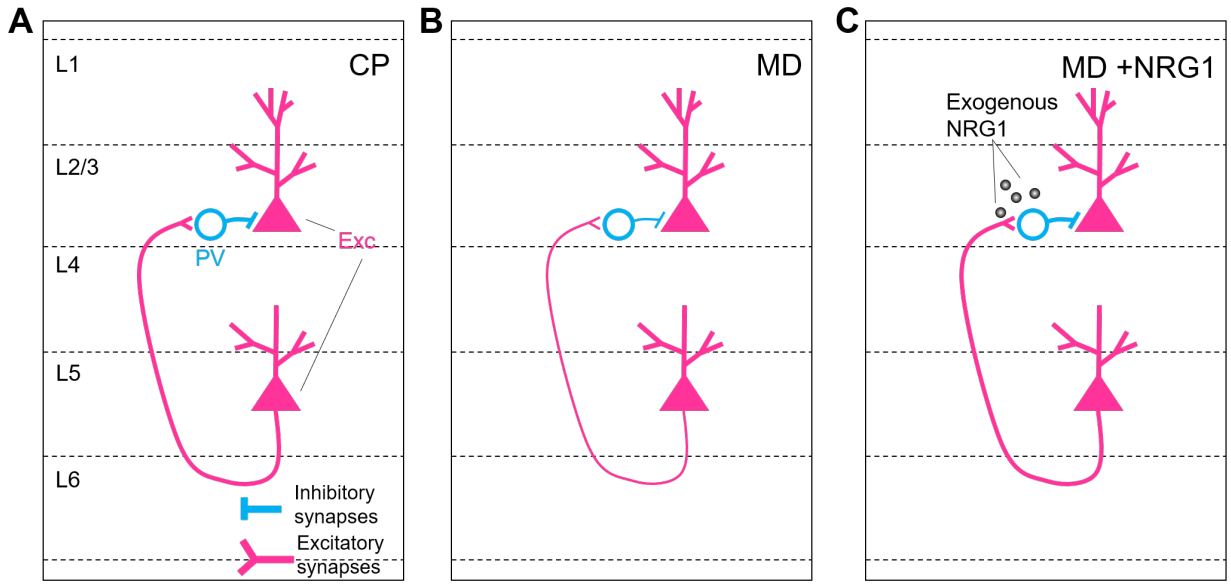

Figure 5.1 Exogenous NRG1 prevents MD-induced reduction in excitatory drive onto layer 2/3 PV interneurons during development.

(A) In the binocular visual cortex, Layer 2/3 PV interneurons receive excitatory inputs from layer 2/3, 4 and 5 excitatory neurons. PV interneurons, in turn, preferentially target the soma of the excitatory neurons. (B) Brief MD reduces the layer 4 and 5 excitatory inputs onto PV interneurons, which results in a reduction of somatic inhibition on the layer 2/3 excitatory neurons. (C) Exogenous NRG1 during MD prevents the reduction in excitatory inputs and subsequently prevents the reduction of the somatic inhibition.

With additional new inhibitory neurons, the overall circuit in the transplanted hemisphere may be more complex (Figure 5.2). The rabies tracing experiments show that transplanted PV interneurons integrate properly into the host circuit. They receive both inhibitory and excitatory inputs (Figure 5.2A). We do not know, however, how the integration of the new inhibitory interneurons alters the inputs to the host PV interneurons. Do they compete for inputs from the same neurons? How does the host circuit keep the

balance of inhibition and excitation in the visual cortex? More importantly, are there synaptic changes to the host PV interneurons that result in the renewed sensitivity to the visual manipulation? It is possible that the transplanted PV interneurons are competing for excitatory inputs, and now there is less excitatory control of the host PV interneurons so that they respond more readily to the visual manipulation. Previous studies show that the excitatory synapses received by the host PV interneurons are fewer but stronger compared to those received by the transplanted interneurons (Southwell et al., 2010). Unfortunately, Southwell et al. (2010) does not record from age-matched control to show that sparse inputs received by the host inhibitory neurons are specifically due to transplantation and not due to developmental changes in the excitatory inputs.

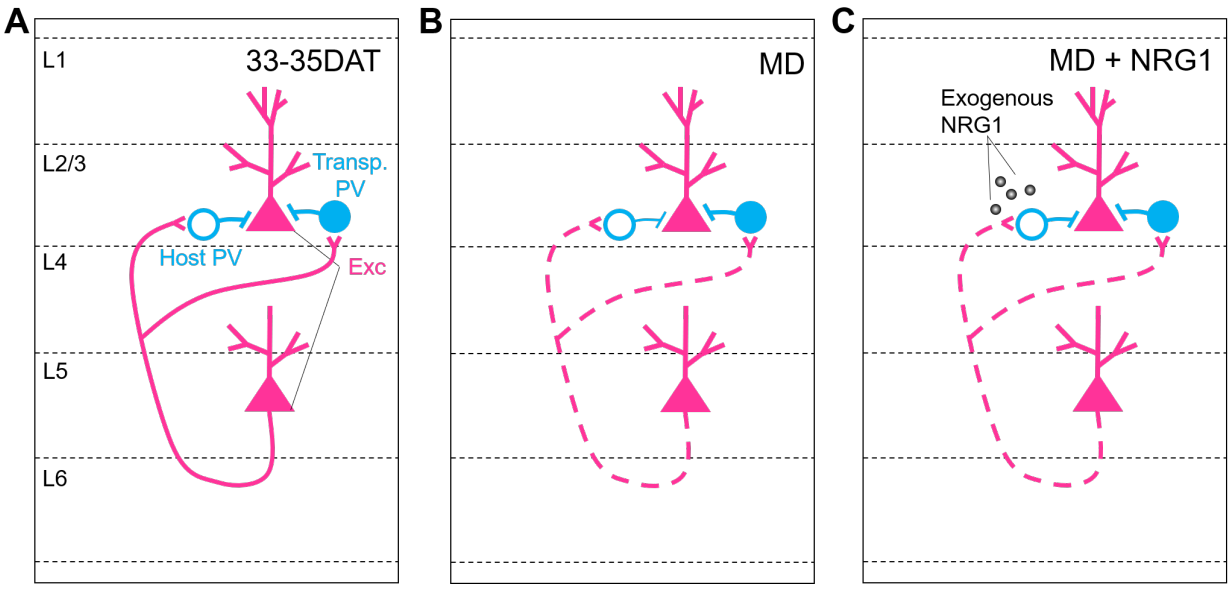

Figure 5.2 Exogenous NRG1 prevents MD-induced reduction in host PV interneuron responsiveness, but the cause is not known.

(A) Rabies tracing experiments show that transplanted PV interneurons (solid blue) integrate properly into the host circuit. They receive both excitatory and inhibitory inputs (not shown) from the host cells. (B) Ca^{2+} imaging results indicate that MD leads to a reduction in host PV interneuron responsiveness (empty blue) but has little effect on the transplanted interneurons (solid blue). Dashed lines indicate that we do not know yet whether MD results in reduction of presynaptic excitatory inputs onto host PV interneurons like during the normal developmental critical period. (C) Exogenous NRG1 during MD prevents reduction in host PV interneuron responsiveness. However, we do not know where NRG1 is acting.

Another interesting observation is that adding more inhibitory neurons to cortex does not seem to induce dysfunction; instead, it has been shown repeatedly that interneuron transplantation can correct deficits in the dysfunctional cortex. It was first illustrated by Southwell et al. (2012) that the cortex can incorporate a large number of inhibitory neurons without affecting the number of the host interneurons. Subsequent interneuron transplantation studies have provided both physiological evidence as well as behavioral evidence that interneuron transplantation does not overtly change the properties of the cortex. For example, on our hand, we have shown that interneuron transplantation does not change the tuning properties of the host neurons. Other properties such as ocular dominance index remains comparable between transplant recipients and age-matched adult controls. In other studies (Martinez-losa et al., 2018; Southwell et al., 2020), interneuron transplantation into wildtype, healthy animals also does not significantly alter the behavioral performance of those animals on various learning and memory tasks. It seems that the transplantation only exerts its effect when the cortex is perturbed. These studies imply that to incorporate additional inhibition, the host cortex responds through a homeostatic mechanism so that the overall excitation and inhibition balance is maintained. To test this hypothesis and understand the effect of interneuron transplantation on the connectivity of host circuit, we would have to perform circuit mapping experiments.

5.3 Structural Brakes on Transplant-induced Cortical Plasticity

Many cellular and molecular signaling pathways are involved in cortical plasticity in normal development. One class of these molecules are involved in structural consolidation of inhibitory synapses late in development or in adulthood, such as perineuronal nets (PNN). These extracellular structures consisting of chondroitin sulfate proteoglycans surround the cell bodies of PV interneurons in the adult cortex and limit the synaptic plasticity by providing a structural barrier. It has been shown that removing these extracellular structures can reactivate plasticity in adult mice (Pizzorusso et al., 2002).

At first it seems counterintuitive that interneuron transplantation can serve as a brake on inhibition since adding more inhibitory cells is likely to increase the level of inhibition in the host circuit. The story is a little more complicated though. A transplantation study in the amygdala shows that interneuron transplantation reduces the level of the perineuronal nets on the host PV interneuron and therefore reinstates synaptic plasticity within the host amygdala circuit (Yang et al., 2016). In contrast, the study from our lab does not find reduction of PNN in the host visual cortex after transplantation; instead, we find that transplanted PV interneurons show precocious expression of PNN compared to the PV interneurons in normal development (Bradshaw et al., 2018).

These results suggest that the host circuit may have influence over the structural development of the transplanted interneurons. Whereas interneuron transplantation reduces PNN expression in the host amygdala cells, it has little effect on the host PV interneuron in the visual cortex. Nevertheless, it does not mean that interneuron transplantation in V1 does not affect other aspects of structural plasticity in the circuit such

as myelination and axonal arborization of host cells, both of which have been implicated in cortical plasticity.

One may wonder if adding any new cells could make the host brain more plastic structurally – new cells could somehow break the structural integrity of the host circuit. However, this is not supported by our current study or previous studies (Davis et al., 2015; Larimer et al., 2016). The cells from other regions of the embryonic brain (caudal and lateral ganglionic eminence) do not induce OD plasticity in host animals.

Decline in axon growth is another brake on cortical plasticity. Myelin associated inhibitor Nogo and Nogo-66-receptor 1 inhibits axon growth both in the brain and the spinal cord. Additionally, Nogo signaling restrains adult cortical plasticity by also limiting PV interneuron-mediated circuit disinhibition. By knocking out Nogo receptors specifically in PV cells in adult mice, the visual cortex exhibits critical period-like plasticity after brief MD (McGee et al. 2005; Stephany et al., 2016). Even though the overall expression of GAD65 remains intact in Nogo receptor mutant mice (McGee et al., 2005), one day MD significantly reduces the excitatory inputs onto PV interneurons in adult mutant mice (Stephany et al., 2016). These results suggest that Nogo signaling pathway puts a brake on cortical plasticity by preventing PV-mediated circuit disinhibition after the closure of the juvenile critical period. How interneuron transplantation alters Nogo signaling has not been studied. It is possible that the transplant disrupts Nogo signaling in the host PV cells and stimulates axon growth to promote cortical plasticity.

5.4 One Ring Does Not Rule Them All: The Role of Somatostatin Interneurons

Interneurons are a diverse population of cells that exhibit distinct electrophysiological properties, anatomical features, laminar distributions, postsynaptic targets and synaptic connectivity with excitatory as well as inhibitory neurons. Depending on the regions of the brain, the same cell type can behave differently (Hattori et al., 2017). For cortical plasticity in the visual cortex, PV interneurons may be the main player in circuit disinhibition (Kuhlman et al., 2013). For the disinhibitory circuit underlying associative learning in the motor cortex, SOM and VIP together may be the ringmasters (Chen et al., 2015). In our study, we narrow our focus on the role of PV interneurons in transplant-induced cortical plasticity in the visual cortex. However, we cannot ignore the complexity of the interneuron circuit.

Medial ganglionic eminence is a region in the embryonic forebrain that gives rise to majority of the parvalbumin and somatostatin inhibitory interneurons in the cortex. In our study, we use PV-tdTomato line to focus on PV interneurons, but the tissue transplanted contains both PV and SOM interneurons. A previous studying using cell-type specific ablation indicates that either PV or SOM interneurons alone can induce plasticity (Tang et al., 2014). In our study, we show that manipulating PV cell activity with exogenous NRG1 treatment or ablation of ErbB4 receptors are enough to prevent ocular dominance plasticity. However, this does not necessarily mean that SOM interneurons are not involved in other aspects of transplant-induced plasticity.

Based on the results from developmental studies, SOM interneurons and PV interneurons are very likely to employ different mechanisms for inducing plasticity (Figure

5.3A). While somatic inhibition provided by PV interneurons is important in the initial disinhibition of the excitatory circuit and allows the excitatory synapses to participate in a Hebbian plasticity, the role of PV inhibition is more permissive. SOM interneurons, on the other hand, are in a better position to directly orchestrate the competition of eye-specific excitatory inputs that ultimately leads to the expression of OD plasticity as SOM interneuron axons mainly target the distal dendrite of the excitatory neurons (Scheyltjens and Arckens, 2016; Trachtenberg, 2015). Although only 4% of somatostatin synapses are formed on the soma of the excitatory neurons, its connectivity to PV interneurons also allow them to modulate somatic disinhibition (Yaeger et al., 2019). This recent study reveals that SOM interneurons transiently but powerfully control both localized dendritic inhibition and somatic disinhibition during the developmental critical period.

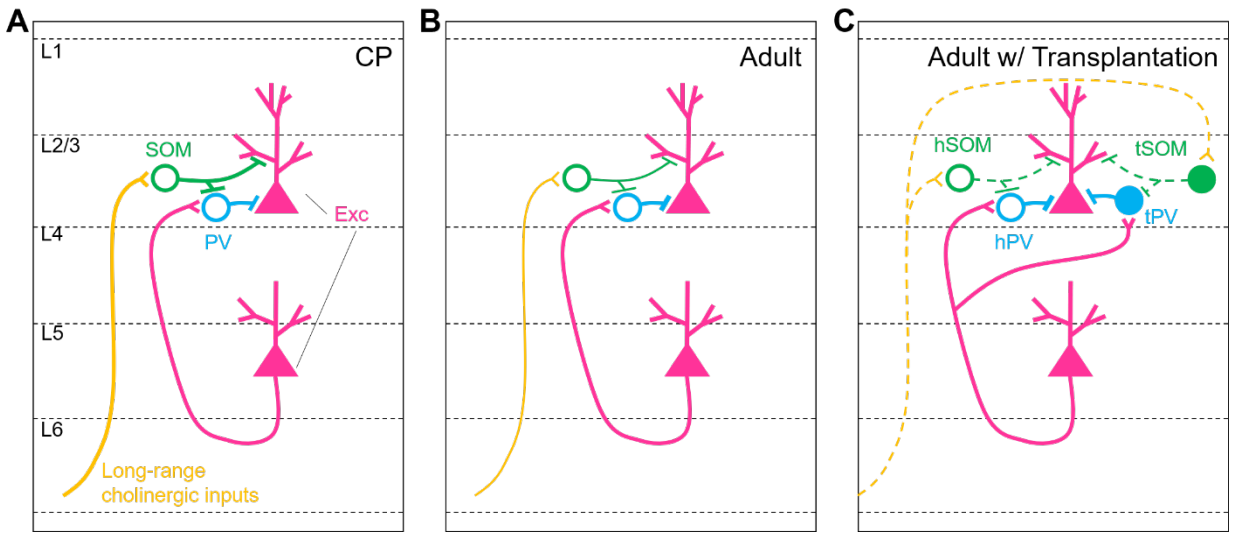

Figure 5.3 A more complete diagram of the interneuron circuitry in the visual cortex.

(A) While PV interneurons preferentially target the soma of the layer 2/3 excitatory neurons, SOM interneurons mainly target the distal dendrites of the excitatory neurons. Additionally, SOM interneurons also inhibit other layer 2/3 PV interneurons. When the presynaptic cholinergic inputs are activated, SOM interneurons indirectly disinhibit the soma of the excitatory neurons by inhibiting PV interneurons, and at the same time inhibit the dendritic shaft of the excitatory neurons. Localized SOM inhibition is thought to regulate the specificity of excitatory inputs. (B) In the adult cortex, the cholinergic inputs to SOM interneurons is reduced, which results in a reduction of dendritic inhibition but an increase in somatic inhibition on the layer

2/3 excitatory neurons. The contribution of SOM inhibition in cortical plasticity is not well understood. (C) For our experiments, we transplant both PV and SOM interneurons into the bV1 of adult animals. While we have learned much about the transplanted PV interneurons, we do not yet know how SOM interneurons integrate into the circuit and how their responses are affected by visual deprivation. Dashed lines indicate the synaptic inputs that could be altered by interneuron transplantation.

To have a more complete picture of the circuitry in the transplanted the cortex, therefore, it is important to map the wiring of not just PV interneurons but also the SOM interneurons. Optogenetic activation of SOM interneurons disinhibits PV interneurons in the visual cortex during the developmental critical period (Yaeger et al., 2019). However, it is not known what effect MD has on SOM interneuron activity and at what time scale. If MD also reduces SOM interneuron activity, then it makes sense that in our study MD shows no overall change in PV interneuron activity since SOM and MD can have opposing effects on PV interneurons.

Transplanted SOM interneurons may also have direct influence on the structural plasticity of excitatory dendritic spines in the host visual cortex. Spine motility is one of the hallmarks of MD-induced cortical plasticity during development (Oray et al., 2004). Dendritic inhibition is important for learning and memory in other cortical regions (Chen et al., 2015; Cummings and Clem, 2020). How the plasticity of the SOM axonal terminals is involved in structural and functional plasticity of excitatory synapses and the expression of cortical plasticity is less clear. Given the diversity of the interneuron population, it is crucial to probe the cell type specific effects on transplant-induced cortical plasticity.

It is also important to note that PV interneurons are also a diverse group of cells. They are subdivided into basket cells and chandelier cells based on the morphology of their axonal arbors. The seminal study by Fagiolini et al. (2004) demonstrates that fast-spiking basket

cells but not chandelier cells are important for regulating the onset of the critical period. One limitation of our study was that we did not confirm which PV cell type was included in the data analysis. It might not pose a serious problem for the transplanted cells since the age of the transplant tissue was restricted to E13.5-E14, during which chandelier cells comprise less than 5% of all PV cells in the MGE (Inan et al., 2012). The percentage of chandelier cells triples by E15, and the birth continues along the ventral germinal zone late into the embryonic development, even after the MGE disappears (Taniguchi et al., 2013). Because of the timing for tissue harvest, we believe that most of the transplanted cells in our study are fast-spiking basket PV cells. In the future, we could perform immunostaining and cellular reconstruction to characterize the morphology of the transplanted cells and to confirm their cellular identity.

Since we are not aware of any transgenic lines that specifically label basket PV cells, it would be much more difficult to tease apart the two PV cell types in the adult host brain. We identified host PV cells by injecting cre-dependent calcium indicator into PV-cre adult cortex. This means that we likely included both cell types in our current study. There is evidence that late-born chandelier cells are more superficial and pressing against the border of layer 1 and layer 2 in the cortex (Taniguchi et al., 2013). In future imaging experiments, we could focus on deeper layer 2/3 to target the basket cells. We could further confirm the cellular identity post-hoc by immunostaining and reconstruction.

5.5 Molecular Mechanisms for Transplant-Induced Cortical Rejuvenation: NRG1/ErbB4, ODP and Beyond

5.5.1 NRG1/ErbB4 Signaling

In normal development, NRG1/ErbB4 signaling influences PV interneuron activity by regulating the excitatory inputs on those cells (Figure 5.1; Gu et al., 2016; Sun et al., 2016). The expression of NRG1 in PV interneurons is developmentally regulated (Figure 5.4; Grieco et al., 2020; Sun et al., 2016). The peak expression of NRG1 in PV interneurons coincides with the peak of cortical plasticity in development. The downregulation of NRG1 in adulthood implies that it does not play an important role in adult cortical plasticity. With interneuron transplantation, we find that manipulating NRG1/ErbB4 signaling within host adult PV interneurons can prevent transplant-induced cortical plasticity. These results suggest that interneuron transplantation may reinstate this developmentally restricted signaling pathway in the adult PV interneurons. But we do not know how.

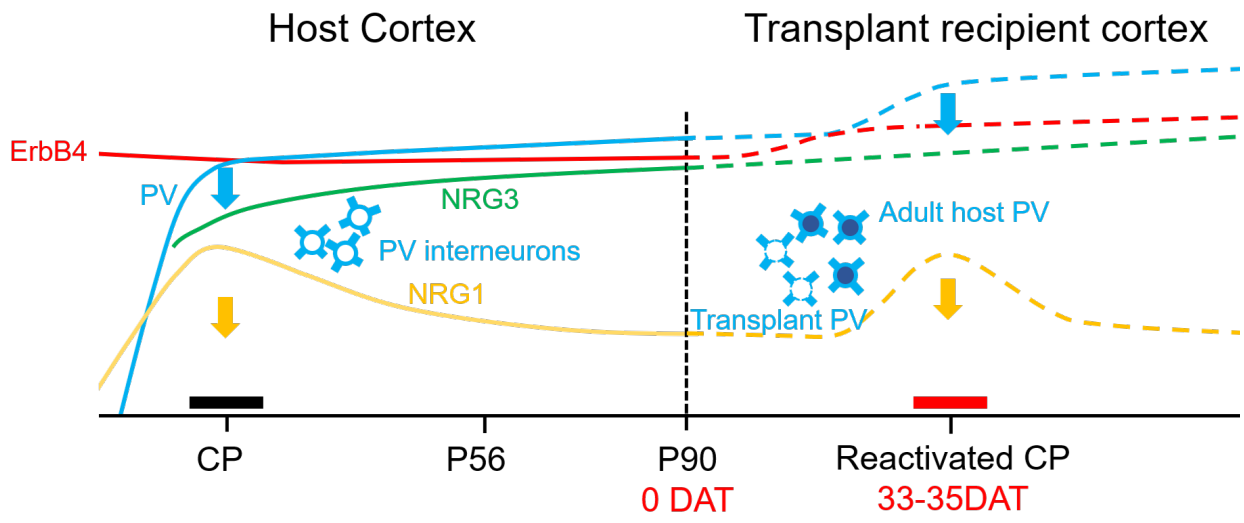

Figure 5.4 A summary diagram for ErbB4, NRG1 and NRG3 expression in PV interneurons in the normal cortex as well as transplant recipient cortex. The level of NRG1 in PV interneurons peaks during the developmental critical period (CP). After brief MD, the level of NRG1 in PV intenreurons trasiently drops (yellow arrow) which results in a reduciton of PV interneuron responsiveness (blue arrow). NRG3 may also be affected (not shown), but the change of NRG3 is not specific to PV intenreurons (Grieco et al., 2020). As the

animal matures, the level of NRG1 in PV interneurons decreases. Interneuron transplantation may reinstate the juvenile level of NRG1 (dashed yellow) in the cortex since the age of transplanted PV interneurons (dashed blue outline) at 33-35DAT is equivalent to that of critical period PV interneurons (solide blue outline). A brief MD during the reactivated CP results in a rapid reduction of host PV interneuron responsiveness (blue arrow).

Since there are many other NRG isoforms in the adult brain (Figure 5.4; Grieco et al.., 2020; Mei and Nave, 2014), it is not clear whether other NRGs are also involved in transplant-induced cortical plasticity. In adult cortex, the expression of NRG3 remains high. Like NRG1, the expression level of NRG3 in PV interneurons is activity dependent. Both brief MD and long-term dark rearing downregulate the mRNA expression of NRG3 in PV interneurons (Grieco et al., 2020). NRG1 and NRG3 both activate ErbB4 receptors, but NRG1 has a higher affinity for ErbB4 receptors (Hobbs et al., 2002). The exogenous NRG1 used in our study activates ErbB4 receptors, and the effect it has in ocular dominance plasticity may reflect more of the downstream pathway of ErbB4 receptors rather than the direct role of NRG1. It is possible that exogenous NRG1 competes with the various forms of endogenous NRG for binding to ErbB4 receptors on either the transplanted neurons or the host PV interneurons. Since our Ca^{2+} imaging results show that exogenous NRG1 diminishes the MD-induced reduction of host PV interneuron responsiveness, it is likely that exogenous NRG1 binds to ErbB4 receptors on host PV interneurons. To directly test this, we can perform immunohistochemistry staining for ErbB4 activation on transplanted and host PV interneurons in the transplant recipients that receive exogenous NRG1 after MD. ErbB4 receptors are phosphorylated when they are activated (Mei and Nave, 2014; Mei and Xiong, 2008; Sun et al., 2016), so we can stain for pErbB4 and compare the level of phosphorylation in transplanted vs. host PV interneurons.

It is important to note that the NRG1/ErbB4 manipulations performed in our current study were not region-specific. ErbB4 receptors are expressed mainly in PV interneurons, but the expression is not restricted to the primary visual cortex. Therefore, both PV-cre;ErbB4 knockout and subcutaneous injections of NRG1 are likely to have widespread effects on the sensorimotor systems in the transplant recipients. To achieve region-specific effect of NRG1, we could implant a minipump and connect it to an intracranial catheter that delivers NRG1 directly into the visual cortex. Considering that the mice in the current study already have to go through a series of invasive surgeries, for future studies the experimental design may need to be revised to accommodate the additional surgeries for minipump implantation.

To directly test whether the NRG1 within the transplanted interneurons is important in transplant-induced cortical plasticity, we can harvest MGE cells from NRG1-knockout (KO) embryos. If NRG1 from transplanted interneurons is necessary, then MGE cells from the KO embryos will not induce OD plasticity when transplanted into wild-type adult visual cortex. However, if NRG1 from the transplanted interneurons is not needed, then it suggests that pathways other than or upstream to NRG1/ErbB4 signaling may be involved in inducing OD plasticity.

5.5.2 Parabiosis

Our findings suggest that interneuron transplantation reactivates cortical plasticity by rejuvenating the plasticity program within the host PV interneuron circuit. An interesting question is whether interneuron transplantation simply reinstates the critical period level

of NRG1 or the host PV interneurons are rejuvenated by other factors released by the transplanted interneurons and sensitivity to NRG1 is one of the outcomes.

It is conceivable that transplanted PV interneurons express high levels of NRG1, since the transplanted cells at 33-35DAT are of a similar age to critical period PV interneurons (Figure 5.4). We can perform immunohistochemistry to examine the NRG1 protein expression in transplanted and host PV interneurons. Additionally, we can perform cell-type specific translating ribosome affinity purification to examine the NRG1 mRNA expression. The strategy has been previously used to determine different NRG mRNA levels in normal mouse cortex (Grieco et al., 2020). Then the next question would be how the level of NRG1 within transplanted cells induces plasticity of the host PV interneurons. To answer this question, we can perform high-resolution *in vivo* imaging to examine NRG1 trafficking from transplanted interneurons and examine whether NRG1 is released by the transplanted PV interneurons and bind to the ErbB4 receptors on host PV interneurons.

Sensitivity to NRG1 in host PV interneurons may be a downstream effect of the rejuvenated state of host PV interneurons. But how are the host PV interneurons rejuvenated in the first place? One rejuvenating mechanism can act similarly to parabiosis, in which factors released by young blood cells are thought to restore function to older host blood, muscle and neural stem cells (Conboy et al., 2005; Conese et al., 2017; Ruckh et al. 2012). In our neural transplant paradigm, perhaps the transplanted young inhibitory cells create a second critical period by releasing soluble rejuvenating factors, including but not limited to NRG1, into the adult host brain and thus restoring juvenile-like sensitivity to the adult PV interneurons (Figure 5.5).

5.5.3 Direct Nuclear Reprogramming

Ocular dominance plasticity is one of the most extensively studied mechanisms in the brain. It is useful for indicating the state and function of the cortex because it has a well-defined critical period in development and the process is age dependent. It is also useful because OD plasticity during developmental critical period and in adults are qualitatively different (Frenkel and Bear, 2004; Lehmann and Löwel, 2008; Sato and Stryker, 2008). OD plasticity has also been used in our lab to measure the rejuvenated state of the brain. As we have pointed out, measuring OD plasticity alone does not inform us about circuit, structure and molecular changes in the transplant brain. Perhaps OD plasticity is the downstream of more direct and fundamental molecular changes to the neurons in transplant cortex. Rejuvenation of the cortex can occur through direct gene reprogramming of the neurons. Identifying the specific target genes will not only help understand the transplant-induced cortical plasticity, but it will also answer the broader question of how interneuron transplantation rejuvenates the brain.

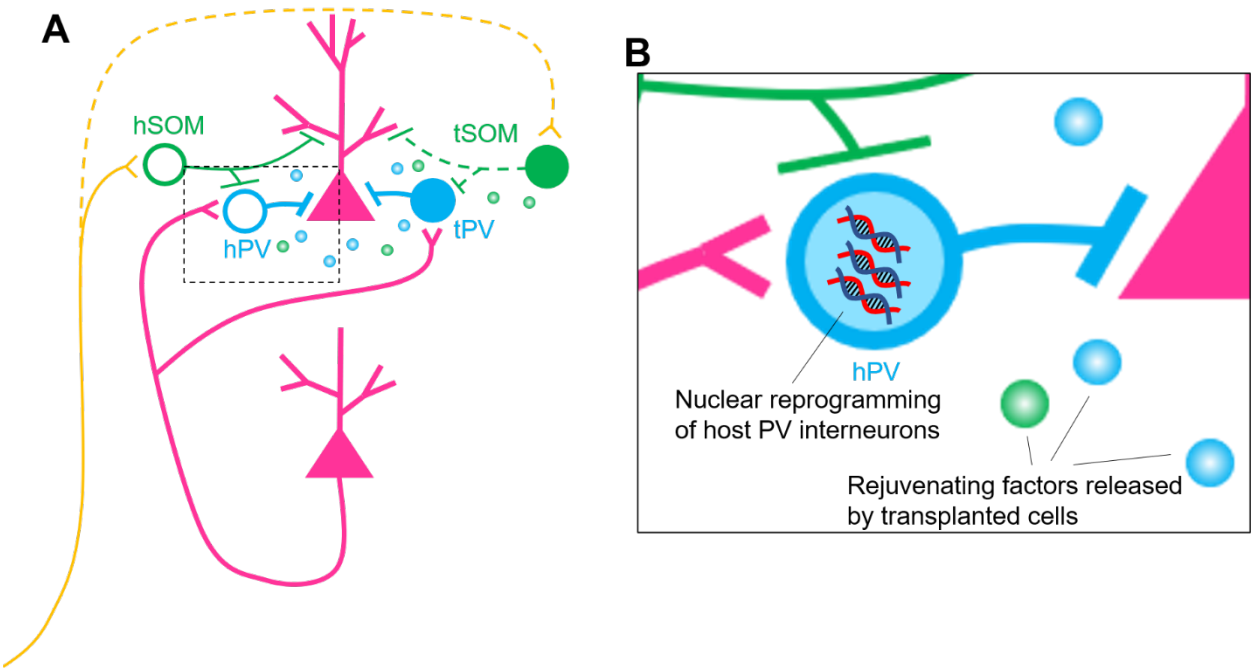

Figure 5.5 Direct reprogramming and rejuvenating of host PV interneurons.

(A) Interneuron transplantation could rejuvenate the host interneurons by releasing some rejuvenating factors. (B) Rejuvenation of the host interneurons may occur at the genetic level. The rejuvenating factors released by the transplanted interneuron may stimulate expression of genes in adult host interneurons that are normally expressed only in young PV interneurons.

5.5.4 Mechanisms Beyond NRG1/ErbB4 Signaling

In our study, we focus our attention on a single signaling pathway, but it is unlikely that NRG1/ErbB4 is the only mechanism involved in reactivating cortical plasticity. In future studies, we can perform single-cell transcriptomics of transplant recipient brains and identify a broader range of signaling pathways that may be altered or rejuvenated by interneuron transplantation.

A central idea in the field of cortical plasticity is the inhibitory threshold for critical period plasticity, which posits that a first threshold level of inhibition must be reached for visual experience to trigger cortical plasticity during early development. As the intracortical

inhibition continues to increase and crosses a second threshold, the brain shows diminished cortical plasticity with a parallel increase in the plasticity brakes (Fagiolini et al., 2000; Sale et al., 2010). This idea is supported by studies on the role of BDNF in PV cell maturation and critical period plasticity. Studies performed in mice with overexpression of brain-derived neurotrophic factor showed accelerated maturation of inhibitory neurons and a precocious onset and closure of critical period (Hanover et al., 1999; Huang et al., 1999). It is interesting to note that in both studies, the expression of ocular dominance plasticity is normal.

The idea of inhibitory thresholds also guides the studies in the reactivation of adult cortical plasticity. Studies using pharmacological treatment or chemogenetics have successfully demonstrated that directly lowering the intracortical inhibition can promote ocular dominance plasticity in the adult cortex (Harauzov et al., 2010; Kuhlman et al., 2013). For example, the antidepressant fluoxetine has been shown to promote ocular dominance plasticity in the adult mouse visual cortex by reducing the level of intracortical inhibition (Maya Vetencourt et al., 2008). Other studies have shown that removing the plasticity brakes in the adult cortex can also promote plasticity. We have presented studies on two of these brakes, namely PNN and myelin-associated inhibitors. One other brake is p75 neurotrophin receptor. Its normal function is to promote PV cell maturation and connectivity when associated with proBDNF during early postnatal development. The p75 receptor level persists in the adult cortex, and when the animals are treated with exogenous proBDNF, ocular dominance plasticity can be reactivated (Baho et al., 2019). The mechanism includes destabilization of PV interneuron connectivity. Altogether, these studies demonstrate the importance of PV maturation and inhibition for the onset of critical period plasticity and for promoting adult cortical plasticity. However, whether the same factors are involved in the

expression of experience-dependent plasticity is not well understood. Some evidence to date shows that some neurotrophin factors are needed to set up the machinery for PV cell maturation for cortical plasticity, but the factors may not necessarily be needed for the expression of experience-dependent cortical plasticity. For example, monocular deprivation induces normal ocular dominance shift in BDNF-overexpressing mice even though the onset for the plasticity occurs earlier than the normal critical period (Hanover et al., 1999; Huang et al., 1999). BDNF only has mild effect on ocular dominance shift when infused directly into the rat cortex during monocular deprivation (Lodovichi et al., 2000). Similarly, removal of PNN in the adult cortex promotes cortical plasticity, but how the nets modulate the expression of ocular dominance plasticity is not well understood.

How interneuron transplantation alters these processes is not completely understood. Previous work from our lab has demonstrated that interneuron transplantation does not disrupt PNN expression in the adult host PV cells (Bradshaw et al., 2018). Adding interneurons also adds more inhibition to the cortex; therefore, it contrasts with the prevailing idea of reducing intracortical inhibition to reactivate cortical plasticity. The single-cell transcriptomics of transplant cortex will reveal how these wide-range of signaling pathways are affected by interneuron transplantation. We can then perform *in vivo* and *in vitro* physiology to fully understand the circuit and cellular mechanisms involving the factors whose expression has been altered by transplantation.

5.6 Conclusion

In summary, this thesis shows for the first time that transplant-induced plasticity is mediated by NRG1/ErbB4 signaling within the host PV interneurons. For a long time, the field has focused on development and integration of transplanted interneurons and believed that the plasticity is reactivated by the addition of the new inhibitory circuit. We show that monocular deprivation has little effect on the transplanted interneurons. Instead, the interneuron transplantation heightens the sensitivity of host PV interneurons to visual deprivation. Furthermore, we demonstrate that NRG1/ErbB4 signaling – a pathway involved in normal critical period plasticity – within host PV interneurons is necessary for transplant-reactivated plasticity. Here we provide a cell type-specific mechanism for transplant-induced plasticity in the visual cortex. This is significant because it provides a means to directly manipulate the circuit to reactivate plasticity. It also directs future studies to focus the search of molecular mechanisms within the host circuit.

In the normal MGE, the young interneuron progenitors are destined to journey long and far, and along the way, they are given instructions and guidance. This is how they normally grow and develop into their unique selves. In our transplantation paradigm, these young progenitors are transported to a different time and space. They are taken from the embryonic brain where they are bathed in all kinds of growth factors and guidance cues to a land that may not be so nourishing. In our hands, these transplanted cells seem to fare well enough in the strange land. Even without the normal cues, they differentiate into mature PV interneurons and exhibit proper tuning properties. The puzzle is that their responses are not affected by the visual manipulation, and from another study, their responses also do not

affect the expression of OD plasticity when they are at the age to participate in cortical plasticity. So what are they doing in the host brain to induce plasticity? How do they re-sensitize the host interneurons and make them become more vulnerable to visual manipulation? What if these transplanted neurons do not behave like normal interneurons at all due to the lack of proper growth molecules and guidance cues? In fact, transplanted interneurons could employ any of the mechanisms mentioned above (i.e., synaptic rewiring, paracrine or direct nuclear reprogramming) to induce plasticity, but whether they act like the normally developing interneurons still remains to be explored.

REFERENCES

Almási, Z., Dávid, C., Witte, M. and Staiger, J.F. (2019). Distribution patterns of three molecularly defined classes of GABAergic neurons across columnar compartments in mouse barrel cortex. *Front Neuroanat* 13, 45.

Baho, E., Chattopadhyaya, B., Lavertu-Jolin, M., Mazziotti, R., Awad, P.N., Chehrazi, P., Groleau, M., Jahannault-Talignani, C., Vaucher, E., Ango, F., Pizzorusso, T., Baroncelli L. and Di Cristo, G. (2019). p75 Neurotrophin receptor activation regulates the timing of the maturation of cortical parvalbumin interneuron connectivity and promotes juvenile-like plasticity in adult visual cortex. *J. Neurosci* 39, 4489-4510.

Batista-Brito, R., Vinck, M., Ferguson, K.A., Chang, J.T., Laubender, D., Lur, G., Mossner, J.M., Hernandez, V.G., Ramakrishnan, C., Deisseroth, K., Higley, M.J. and Cardin, J.A. (2017). Developmental dysfunction of VIP interneurons impairs cortical circuits. *Neuron* 95, 884-895.

Bavelier, D., Levi, D.M., Li, R.W., Dan, Y. and Hensch, T.K. (2010). Removing brakes on adult brain plasticity: from molecular to behavioral interventions. *J Neurosci.* 30, 14964–14971.

Bradshaw, K.P., Figueroa-Velez, D.X., Habeeb, M. and Gandhi, S.P. (2018). Precocious deposition of perineuronal nets on parvalbumin inhibitory neurons transplanted into adult visual cortex. *Sci Rep* 8, 7480.

Brainard, D. H. (1997). The psychophysics toolbox. *Spat Vis* 10, 433–436.

Buonanno, A. and Fischbach, G.D. (2001). Neuregulin and ErbB4 receptor signaling pathways in the nervous system. *Curr Opin Neurobiol* 11, 287-96.

Callaway, E. M., and Luo, L. (2015). Monosynaptic circuit tracing with glycoprotein-deleted rabies viruses. *J Neurosci* 35, 8979-85.

Chen, S.X., Kim, A.N., Peters, A.J. and Komiyama, T. (2015). Subtype-specific plasticity of inhibitory circuits in motor cortex during motor learning. *Nat Neurosci* 18, 1109-15.

Chen, T. W., Wardill, T.J., Sun, Y., Pulver, S.R., Renninger, S.L., Baohan, A., Schreiter, E.R., Kerr, R.A., Orger, M.B., Jayaraman, V., Looger, L.L., Svoboda, K., and Kim, D.S. (2013). Ultrasensitive fluorescent proteins for imaging neuronal activity. *Nature* 499, 295-300.

Chohan, M. O., and Moore, H. (2016). Interneuron progenitor transplantation to treat CNS dysfunction. *Front Neural Circuits* 10, 64.

Conboy, I.M., Conboy, M.J., Wagers, A.J., Girma, E.R., Weissman, I.L., and Rando T.A. (2015). Rejuvenation of aged progenitor cells by exposure to a young systemic environment. *Nature* 433, 760–764.

Conese, M., Carbone, A., Beccia, E. and Angiolillo, A. (2017). The fountain of youth: a tale of parabiosis, stem cells, and rejuvenation. *Open Med (Wars)* 12, 376-383.

Cummings, K.A. and Clem, R.L. (2020). Prefrontal somatostatin interneurons encode fear memory. *Nat Neurosci* 23, 61-74.

Davis, M.F., Figueroa Velez, D.X., Guevarra, R.P., Yang, M.C., Habeeb, M., Carathedathu, M.C., and Gandhi, S.P. (2015). Inhibitory neuron transplantation into adult visual cortex creates a new critical period that rescues impaired vision. *Neuron* 86, 1055-1066.

Fagiolini, M. and Hensch, T.K. (2000). Inhibitory threshold for critical-period activation in primary visual cortex. *Nature* 404, 183-6.

Fagiolini, M., Fritschy, J.M., Löw, K., Möhler, H., Rudolph, U and Hensch, T.K. (2004). Specific GABAA circuits for visual cortical plasticity. *Science* 303, 1681-3.

Falls, D.L. (2003). Neuregulins: functions, forms, and signaling strategies. *Exp Cell Res* 284, 14-30.

Fazzari, P., Paternain, A.V., Valiente, M., Pla, R., Luján, R., Lloyd, K., Lerma, J., Marín, O. and Rico, B. (2010). Control of cortical GABA circuitry development by Nrg1 and ErbB4 signalling. *Nature* 464, 1376-80.

Figueroa Velez, D. X., Ellefsen, K. L., Hathaway, E. R., Carathedathu, M. C. & Gandhi, S. P. (2017). Contribution of innate cortical mechanisms to the maturation of orientation selectivity in parvalbumin interneurons. *J Neurosci* 37, 820-829.

Flames, N., Long, J.E., Garratt, A.N., Fischer, T.M., Gassmann, M., Birchmeier, C., Lai, C., Rubenstein, J.L. and Marín, O. (2004). Short- and long-range attraction of cortical GABAergic interneurons by neuregulin-1. *Neuron* 44, 251-61.

Frenkel, M.Y. and Bear, M.F. (2004). How monocular deprivation shifts ocular dominance in visual cortex of young mice. *Neuron* 44, 917-23.

Gandhi, S. P., Yanagawa, Y. & Stryker, M. P. (2008). Delayed plasticity of inhibitory neurons in developing visual cortex. *PNAS* 105, 16797-16802.

Garcia, R.A., Vasudevan, K. and Buonanno, A. (2000). The neuregulin receptor ErbB-4 interacts with PDZ-containing proteins at neuronal synapses. *Proc Natl Acad Sci U S A* 97, 3596-601.

Gordon, J.A. and Stryker, M.P. (1996). Experience-dependent plasticity of binocular responses in the primary visual cortex of the mouse. *J Neurosci* 16, 3274-86.

Grieco, S. F., Wang, G., Mahapatra, A., Lai, C., Holmes, T. C. & Xu, X. (2020). Neuregulin and ErbB4 expression is regulated by development and sensory experience in mouse visual cortex. *J Comp Neurol.* 528, 419-432.

Gu, Y., Tran, T., Murase, S., Borrell, A., Kirkwood, A., and Elizabeth M. Quinlan (2016). Neuregulin-dependent regulation of fast-spiking interneuron excitability controls the timing of the critical period. *J Neurosci.* 36, 10285-10295.

Harauzov, A., Spolidoro, M., DiCristo, G., De Pasquale, R., Cancedda, L., Pizzorusso, T., Viegi, A., Berardi, N. and Maffei, L. (2010). Reducing intracortical inhibition in the adult visual cortex promotes ocular dominance plasticity. *J Neurosci* 30, 361-71.

Hattori, R., Kuchibhotla, K.V., Froemke, R.C. and Komiyama, T. (2017). Functions and dysfunctions of neocortical inhibitory neuron subtypes. *Nat Neurosci* 20, 1199-1208.

Heimel, J.A., van Versendaal, D. and Levelt, C.N. (2011). The role of GABAergic inhibition in ocular dominance plasticity. *Neural Plast.* 2011, 391763.

Henderson K. W., Gupta, J., Tagliatela, S., Litvina, E., Zheng, X. T., Van Zandt, M. A., Woods, N., Grund, E., Lin, D., Royston, S., Yanagawa, Y., Aaron, G. B., and Naegele, J. R. (2014). Long-term seizure suppression and optogenetic analyses of synaptic connectivity in epileptic mice with hippocampal grafts of GABAergic interneurons. J Neurosci. 34, 13492–13504.

Hensch, T.K. (1998). Local GABA circuit control of experience-dependent plasticity in developing visual cortex. *Science* 282, 1504-8.

Hensch, T.K. (2005). Critical period plasticity in local cortical circuit. *Nat Rev Neurosci.* 6, 877-88.

Hobbs, S. S., Coffing, S. L., Le, A. T., Cameron, E. M., Williams, E. E., Andrew, M., Blommel, E.N., Hammer, R.P., Chang, H., and Riese, D.J. 2nd. (2002). Neuregulin isoforms exhibit distinct patterns of ErbB family receptor activation. *Oncogene* 21, 8442–8452.

Hoseini, M.S., Rakela, B., Flores-Ramirez, Q., Hasenstaub, A.R., Alvarez-Buylla, A., and Stryker, M.P. (2019). Transplanted cells are essential for the induction but not the expression of cortical plasticity. *J Neurosci.* 39, 7529-7538.

Hoy, J.L. and Niell, C.M. (2015). Layer-specific refinement of visual cortex function after eye opening in the awake mouse. *J Neurosci* 35, 3370–3383.

Huang, Y.Z., Won, S., Ali, D.W., Wang, Q., Tanowitz, M., Du, Q.S., Pelkey, K.A., Yang, D.J., Xiong, W.C., Salter, M.W. and Mei, L. (2000). Regulation of neuregulin signaling by PSD-95 interacting with ErbB4 at CNS synapses. *Neuron* 26, 443-55.

Huang, Z.J., Kirkwood, A., Pizzorusso, T., Porciatti, V., Morales, B., Bear, M.F., Maffei, L. and Tonegawa, S. (1999). BDNF regulates the maturation of inhibition and the critical period of plasticity in mouse visual cortex. *Cell* 98, 739-755.

Hubel, D.H. and Wiesel, T.N. (1970). The period of susceptibility to the physiological effects of unilateral eye closure in kittens. *J Physiol* 206, 419-36.

Huh, C. Y. L., Abdelaal, K., Salinas, K. J., Gu, D., Zeitoun, J., Figueroa Velez, D. X., Peach, J. P., Fowlkes, C. C., and Gandhi, S. P. (2020). Long-term monocular deprivation during juvenile critical period disrupts binocular integration in mouse visual thalamus. J Neurosci 40, 585–604.

Hunt, R. F., Girskis, K. M., Rubenstein, J. L., Alvarez-Buylla, A., and Baraban, S. C. (2013). GABA progenitors grafted into the adult epileptic brain control seizures and abnormal behavior. *Nat Neurosci.* 16, 692–697.

Inan, M., Welagen, J., and Anderson, S.A. (2012). Spatial and temporal bias in the mitotic origins of somatostatin- and parvalbumin-expressing interneuron subgroups and the chandelier subtype in the medial ganglionic eminence. *Cereb Cortex* 22, 820–827.

Jaepel, J., Hübener, M., Bonhoeffer, T., and Rose, T. (2017). Lateral geniculate neurons projecting to primary visual cortex show ocular dominance plasticity in adult mice. *Nat Neurosci* 854, 1708–1714.

Kalatsky, V. A. & Stryker, M. P. (2003). New paradigm for optical imaging: temporally encoded maps of intrinsic signal. *Neuron* 38, 529-45.

Kameyama, K., Sohya, K., Ebina, T., Fukuda, A., Yanagawa, Y. and Tsumoto, T. (2010). Difference in binocularity and ocular dominance plasticity between GABAergic and excitatory cortical neurons. *J Neurosci* 30, 1551-9.

Kerlin, A.M., Andermann, M.L., Berezovskii, V.K. and Reid, R.C. (2010). Broadly tuned response properties of diverse inhibitory neuron subtypes in mouse visual cortex. *Neuron* 67, 858–871.

Kuhlman, S.J., Tring, E. and Trachtenberg, J.T. (2011). Fast-spiking interneurons have an initial orientation bias that is lost with vision. *Nat Neurosci* 14, 1121-3.

Kuhlman, S.J., Olivas, N.D., Tring, E., Ikrar, T., Xu, X., Trachtenberg, J.T. (2013). A disinhibitory microcircuit initiates critical-period plasticity in the visual cortex. *Nature* 501, 543-6.

Larimer, P., Spatazza, J., Espinosa, J.S., Tang, Y., Kaneko, M., Hasenstaub, A.R., Stryker, M.P. and Alvarez-Buylla, A. (2016). Caudal ganglionic eminence precursor transplants disperse and integrate as lineage-specific interneurons but do not induce cortical plasticity. *Cell Report* 16, 1391-1404.

Larimer, P., Spatazza, J., Stryker, M.P., Alvarez-Buylla, A., Hasenstaub, A.R. (2017). Development and long-term integration of MGE-lineage cortical interneurons in the heterochronic environment. *J Neurophysiol*. 118, 131–139.

Lazarus, M.S. and Huang, Z.J. (2011). Distinct maturation profiles of perisomatic and dendritic targeting GABAergic interneurons in the mouse primary visual cortex during the critical period of ocular dominance plasticity. *J Neurophysiol* 106, 775-87.

Lehmann, K. and Löwel, S. (2008). Age-dependent ocular dominance plasticity in adult mice. *PLoS One* 3, e3120.

Letzkus, J.J., Wolff, S.B. and Lüthi, A. (2015). Disinhibition, a circuit mechanism for associative learning and memory. *Neuron* 88, 264-76.

Levelt, C.N. and Hübener, M. (2012). Critical-period plasticity in the visual cortex. *Annu Rev Neurosci* 35, 309-30.

Liu, X., Bates, R., Yin, D.M., Shen, C., Wang, F., Su, N., Kirov, S.A., Luo, Y., Wang, J.Z., Xiong, W.C. and Mei, L. (2011). Specific regulation of NRG1 isoform expression by neuronal activity. *J Neurosci* 31, 8491-501.

Lodovichi, C., Berardi, N., Pizzorusso, T. and Maffei, L. (2000). Effects of neurotrophins on cortical plasticity: same or different? *J. Neurosci* 20, 2155-2165.

Long, W., Wagner, K.U., Lloyd, K.C., Binart, N., Shillingford, J.M., Hennighausen, L., and Jones, F.E. (2003). Impaired differentiation and lactational failure of Erbb4-deficient mammary glands identify ERBB4 as an obligate mediator of STAT5. *Development* 130, 5257-5268.

Lu, J., Tucciarone, J., Lin, Y., and Huang Z. J. (2014). Input-specific maturation of synaptic dynamics of parvalbumin interneurons in primary visual cortex. *Proc Natl Acad Sci U S A* 111, 16895-16900.

Martinez-Losa, M., Tracy, T.E., Ma, K., Verret, L., Clemente-Perez, A., Khan, A.S., Cobos, I., Ho, K., Gan, L., Mucke, L., Alvarez-Dolado, M. and Palop, J.J. (2018). Nav1.1-overexpressing interneuron transplants restore brain rhythms and cognition in a mouse model of Alzheimer's disease. *Neuron* 98, 75-89.

McGee, A.W., Yang, Y., Fischer, Q.S., Daw, N.W. and Strittmatter, S.M. (2005). Experience-driven plasticity of visual cortex limited by myelin and Nogo receptor. *Science* 309, 2222-6.

Mei, L., and Nave, K.A. (2014). Neuregulin-ERBB signaling in the nervous system and neuropsychiatric diseases. *Neuron* 82, 27-49.

Mei, L., and Xiong, W. C. (2008). Neuregulin 1 in neural development, synaptic plasticity and schizophrenia. *Nat. Rev. Neurosci.* 9, 437-452.

Ming, G.L. and Song, H. (2011). Adult neurogenesis in the mammalian brain: significant answers and significant questions. *Neuron* 70, 687-702.

Oray, S., Majewska, A. and Sur, M. (2004). Dendritic spine dynamics are regulated by monocular deprivation and extracellular matrix degradation. *Neuron* 44, 1021-30.

Pelli, D. G. (1997). The video toolbox software for visual psychophysics: Transforming numbers into movies. *Spat Vis* 10, 437–442.

Pietrasanta, M., Restani, L., and Caleo, M. (2012). The Corpus Callosum and the Visual Cortex: Plasticity Is a Game for Two. Neural Plast. 2012, 838672.

Pizzorusso, T., Medini, P., Berardi, N., Chierzi, S., Fawcett, J.W. and Maffei, L. (2002). Reactivation of ocular dominance plasticity in the adult visual cortex. *Science* 298, 1248-51.

Priya, R., Rakela, B., Kaneko, M., Spatazza, J., Larimer, J., Hoseini, M.S., Hasenstaub, A.R., Alvarez-Buylla, A., and Stryker, M.P. (2019). Vesicular GABA transporter is necessary for transplant-induced critical period plasticity in mouse visual cortex. *J Neurosci.* 39, 2635-2648.

Renier, N., Adams, E.L., Kirst, C., Wu, Z., Azevedo, R., Kohl, J., Autry, A.E., Kadiri, L., Umadevi Venkataraju, K., Zhou, Y., Wang, V.X., Tang, C.Y., Olsen, O., Dulac, C., Osten, P., and Tessier-Lavigne, M. (2016). Mapping of brain activity by automated volume analysis of immediate early genes. *Cell* 165, 1789–1802.

Restani, L., Cerri, C., Pietrasanta, M., Gianfranceschi, L., Maffei, L., and Caleo, M. (2009). Functional masking of deprived eye responses by callosal input during ocular dominance plasticity. Neuron 64, 707–718.

Ruckh, J. M., Zhao, J. W., Shadrach, J. L., van Wijngaarden, P., Rao, T. N., Wagers, A. J. & Franklin, R.J. (2012) Rejuvenation of regeneration in the aging central nervous system. *Cell Stem Cell* 10, 96-103.

Sale, A., Maya Vetencourt, J.F., Medini, P., Cenni, M.C., Baroncelli, L., De Pasquale, R. and Maffei, L. (2007). Environmental enrichment in adulthood promotes amblyopia recovery through a reduction of intracortical inhibition. *Nat Neurosci* 10, 679-81.

Sale, A., Berardi, N., Spolidoro, M., Baroncelli, L. and Maffei, L. (2010). GABAergic inhibition in visual cortical plasticity. *Front Cell Neurosci* 4, 10.

Salinas, K. J., Figueroa Velez, D. X., Zeitoun, J. H., Kim, H. & Gandhi, S. P. (2017). Contralateral bias of high spatial frequency tuning and cardinal direction selectivity in mouse visual cortex. *J Neurosci.* 37,10125-10138.

Sato, M. and Stryker, M.P. (2008). Distinctive features of adult ocular dominance plasticity. *J Neurosci* 28, 10278-86.

Scheyltjens, I. and Arckens, L. (2016). The current status of somatostatin-interneurons in inhibitory control of brain function and plasticity. *Neural Plast* 2016, 8723623.

Seidler, B., Schmidt, A., Mayr, U., Nakhai, H., Schmid, R.M., Schneider, G., and Saur, D. (2008). A Cre-loxP-based mouse model for conditional somatic gene expression and knockdown in vivo by using avian retroviral vectors. *Proc Natl Acad Sci U S A* 105, 10137-42.

Sohya, K., Kameyama, K., Yanagawa, Y., Obata, K., and Tsumoto, T. (2007). GABAergic neurons are less selective to stimulus orientation than excitatory neurons in layer II/III of visual cortex, as revealed by in vivo functional Ca^{2+} imaging in transgenic mice. *J Neurosci* 27, 2145–2149.

Spatazza, J., Mancia Leon, W. R., and Alvarez-Buylla, A. (2016). Transplantation of GABAergic interneurons for cell-based therapy. Prog Brain Res. 231, 57–85.

Sommeijer, J-P., Ahmadlou, M., Saiepour, M. H., Seignette, K., Min, R., Heimel, J. A., and Levelt, C. N. (2017). Thalamic inhibition regulates critical-period plasticity in visual cortex and thalamus. Nat Neurosci 20, 1715–1721.

Southwell, D.G., Seifikar, H., Malik, R., Lavi, K., Vogt, D., Rubenstein, J.L. and Sohal, V.S. (2020). Interneuron transplantation rescues social behavior deficits without restoring wild-type physiology in a mouse model of autism with excessive synaptic inhibition. *J Neurosci* 40, 2215-2227.

Southwell, D. G., Froemke, R. C., Alvarez-Buylla, A., Stryker, M. P. & Gandhi, S. P. (2010). Cortical plasticity induced by inhibitory neuron transplantation. *Science* 327, 1145-8.

Southwell, D.G., Nicholas, C.R., Basbaum, A.I., Stryker, M.P., Kriegstein, A.R., Rubenstein, J.L., and Alvarez-Buylla, A. (2014). Interneurons from embryonic development to cell-based therapy. *Science* 344, 1240622.

Sun, Y., Nguyen, A.Q., Nguyen, J.P., Le, L., Saur, D., Choi, J., Callaway, E.M., and Xu, X. (2014). Cell-type-specific circuit connectivity of hippocampal CA1 revealed through Cre-dependent rabies tracing. *Cell Rep.* 7, 269-80.

Sun, Y., Ikrar, T., Davis, M.F., Gong, N., Zheng, X., Luo, Z.D., Lai, C., Mei, L., Holmes, T.C., Gandhi, S.P., and Xu, X. (2016). Neuregulin-1/ErbB4 signaling regulates visual cortical plasticity. *Neuron* 92,160-173.

Sun, Y., Jin, S., Lin, X., Chen, L., Qiao, X., Jiang, L., Zhou, P., Johnston, K., Golshani, P., Nie, Q., Holmes, T., Nitz, D., and Xu, X. (2019). CA1-projecting subiculum neurons facilitate object–place learning. Nature Neuroscience 22, 1857–1870.

Tang, Y., Stryker, M. P., Alvarez-Buylla, A. & Espinosa, J. S. (2014). Cortical plasticity induced by transplantation of embryonic somatostatin or parvalbumin interneurons. *Proc Natl Acad Sci U S A* 111,18339 –18344.

Taniguchi, H., Lu, J., and Huang, Z.J. (2013). The spatial and temporal origin of chandelier cells in mouse neocortex. *Science* 339, 70-74.

Trachtenberg, J.T. (2015). Competition, inhibition, and critical periods of cortical plasticity. *Curr Opin Neurobiol* 35, 44-8.

Tremblay R., Lee, S. and Rudy, B. (2016). GABAergic interneurons in the neocortex: from cellular properties to circuits. *Neuron* 91, 260-92.

Tyson, J. A. and Andersen, S. A. (2014). GABAergic interneuron transplants to study development and treat disease. Trends Neurosci. 37, 169-77.

Upadhya, D., Hattiangady, B., Castro, O.W., Shuai, B., Kodali, M., Attaluri, S., Bates, A., Dong, Y., Zhang, S.C., Prockop, D.J. and Shetty, A.K.. (2019). Human induced pluripotent stem cell-derived MGE cell grafting after status epilepticus attenuates chronic epilepsy and comorbidities via synaptic integration. *Proc Natl Acad Sci U S A* 116, 287-296.

Vullhorst, D., Neddens, J., Karavanova, I., Tricoire, L., Petralia, R.S., McBain, C.J., and Buonanno, A. (2009). Selective expression of ErbB4 in interneurons, but not pyramidal cells, of the rodent hippocampus. *J. Neurosci.* 29, 12255-12264.

Vullhorst, D., Ahamd, T., Karavanova, I., Keating, C. and Buonanno, A. (2017). Structural similarities between Neuregulin 1-3 isoforms determine their subcellular distribution and signaling mode in central neurons. *J Neurosci* 37, 5232-5249.

Wall, N. R., Wichersham, I. R., Cetin, A., De La Parra, M., and Callaway, E. M. (2010). Monosynaptic circuit tracing in vivo through Cre-dependent targeting and complementation of modified rabies virus. *Proc Natl Acad Sci U S A* 107, 21848-21853.

Wen, L., Lu, Y-S., Zhu, X-H., Li., X-M., Woo., R-S., Chen, Y-J., Y., D-M., Lai, C., Terry Jr., A.V., Vazdarjanova, A., Xiong, W-C., and Mei, L. (2010). Neuregulin 1 regulates pyramidal neuron activity via ErbB4 in parvalbumin-positive interneurons. *Proc Natl Acad Sci U S A* 107, 1211-1216.

Wiesel, T.N. and Hubel, D.H. (1963). Single-cell responses in striate cortex of kittens deprived of vision in one eye. *J Neurophysiol* 26, 1003-17.

Wonders, C.P. and Anderson, S.A. (2006). The origin and specification of cortical interneurons. *Nat Rev Neurosci* 7, 687-96.

Woo, R.S., Li, X.M., Tao, Y., Carpenter-Hyland, E., Huang, Y.Z., Weber, J., Neiswender, H., Dong X.P., Wu, J., Gassmann, M., Lai, C., Xiong, W.C., Gao, T.M. and Mei, L. (2007). Neureuglin-1 enhances depolarization-induced GABA release. *Neuron* 54, 599-610.

Yaeger, C.E., Ringach, D.L. and Trachtenberg, J.T. (2019). Neuromodulatory control of localized dendritic spiking in critical period cortex. *Nature* 567, 100-104.

Yang, W.Z., Liu, T.T., Cao, J.W., Chen, X.F., Liu, X., Wang, M., Su, X., Zhang, S.Q., Qiu, B.L., Hu, W.X., Liu, L.Y., Ma, L., and Yu, Y.C. (2016). Fear erasure facilitated by immature inhibitory neuron transplantation. *Neuron* 92, 1352–1367.

Yau, H.J., Wang, H.F., Lai, C. and Liu, F.C. (2003). Neural development of the neuregulin receptor ErbB4 in the cerebral cortex and the hippocampus: preferential expression by interneurons tangentially migrating from the ganglionic eminences. *Cereb Cortex* 13, 252-64.

Yazaki-Sugiyama, Y., Kang, S., Câteau, H., Fukai, T. and Hensch, T.K. (2009). Bidirectional plasticity in fast-spiking GABA circuit by visual experience. *Nature* 462, 218-21.

Zhu, B., Eom, J., and Hunt, R. (2019). Transplanted interneurons improve memory precision after traumatic brain injury. *Nat Commun* 10, 5156.